5-2015

Transformation of Swine Manure and Algal Consortia to Value-added Products

Mahmoud A. Sharara
University of Arkansas, Fayetteville

Transformation of Swine Manure and Algal Consortia to Value-added Products

Transformation of Swine Manure and Algal Consortia to Value-added Products

A dissertation is submitted in partial fulfillment
of the requirements for the degree of
Doctor of Philosophy in Biological Engineering

By
Mahmoud A. Sharara
Alexandria University
Bachelor of Science in Agricultural Engineering, 2003
University of Arkansas
Master of Science in Biological Engineering, 2010

May 2015
University of Arkansas

This dissertation is approved for recommendation to Graduate Council.

_____
Dr. Sammy Sadaka
Dissertation Director

_____   _____
Dr. Karl VanDevender   Dr. Thomas A. Costello
Committee member   Committee member

_____   _____
Dr. Danielle Julie Carrier   Dr. Greg Thoma
Committee member   Committee member

_____
Dr. Michael Popp
Committee member

Abstract

The swine production sector is projected to grow globally. In the past, this growth manifested itself in increased herd sizes and geographically concentrated production. Although economically sound, these trends had negative consequences on surrounding ecosystems. Over-application of manure resulted in water quality degradation, while long-term storage of manure slurries was found to promote release of potent GHG emissions. There is a need for innovative approaches for swine manure management that are compatible with current scales of production, and increasingly strict environmental regulations.

This study aims to investigate the potential for incorporating gasification as part of a novel swine manure management system which utilizes liquid-solid separation and periphytic algal consortia as a phycoremediation vector for the liquid slurry. The gasification of swine manure solids, and algal biomass solids generate both a gaseous fuel product (producer gas) in addition to a biochar co-product.

First, the decomposition kinetics for both feedstock, i.e., swine manure solids, and algal solids, were quantified using thermogravimetry at different heating rates ($1 \sim 40°C$ min^{-1}) under different atmospheres (nitrogen, and air). Pyrolysis kinetics were determined for manure solids from two farms with different manure management systems. Similarly, the pyrolysis kinetics were determined for phycoremediation algae grown on swine manure slurries. Modeling algal solids pyrolysis as first-order independent parallel reactions was sufficient to describe sample devolatilization. Combustion of swine manure solids blended with algal solids, at different ratios, showed no synergistic effects.

Gasification of phycoremediation algal biomass was studied using a bench-scale auger gasification system at temperatures between 760 and 960°C. The temperature profile suggested a

stratification of reaction zones common to fixed-bed reactors. The producer gas heating value ranged between 2.2 MJ m^{-3} at 760°C, and 3.6 MJ m^{-3} at 960°C.

Finally, life cycle assessment (LCA) was used to evaluate a proposed swine manure management system that includes a thermochemical conversion sub-system: drying, gasification, and producer-gas combustion (boiler). Liquid manure storage (uncovered tank) was the biggest contributor to GHG emissions. Liquid slurry management stages were credited with the highest fossil fuel use. Improvements to separation and drying technologies can improve this conversion scenario.

Acknowledgments

First and foremost, I want to thank my PhD advisor, Dr. Sammy Sadaka. It has been a privilege working under his guidance. His invaluable mentorship, encouragement, patience, and enthusiasm were my inspiration. I am also thankful to Dr. Karl VanDevender for many enlightening discussions that were crucial to this research. I am also grateful for the members of my committee, Professors Thomas A. Costello, Greg Thoma, Danielle Julie Carrier, and Michael Popp who were always generous with their time, attention, and resources to answer my scientific questions and also helped me find the answers on my own. Your mentorship and helpful career advice is greatly appreciated.

I'd like to thank Dr. Charles E. Wilson, Director of the Rice Research and Extension Center in Stuttgart, AR, for accommodating and providing resources for this research. I also would like to acknowledge and thank Dr. Marty Matlock, Heather Sandefur, Morgan Welch, Nathan Holeman, and Jerry Jackson for their invaluable assistance in growing, sampling and processing the algal biomass and the manure solids. I'd also like to thank Steve Balloun for giving us access to the waste management system on his farm to collect manure samples for this study. Thanks to Dr. Daesoo Kim and Jasmina Burek who offered me the opportunity to watch and learn from their knowledge and experience. I also would like to thank Andrew Wright, program technician at the bioenergy laboratory, for performing various tests and measurements that are essential to this work. His work ethic, dedication, and willingness to come through in time of need are greatly appreciated. I am also grateful to Linda Pate, Karen M. Withers, and Holly Beason for their great assistance and support in navigating the administrative world, which can be quite daunting.

Table of Contents

List of Tables

List of Figures

List of Papers

1. **Value-added Products from Swine Manure: Challenges and Opportunities**

2. **Thermogravimetric Analysis of Swine Manure Solids Obtained from Farrowing, and Growing-Finishing Farms**

Citation: Sharara, M. and Sadaka, S. 2014. Thermogravimetric Analysis of Swine Manure Solids Obtained from Farrowing, and Growing-Finishing Farms. *Journal of Sustainable Bioenergy Systems*, 4, 75-86. doi: 10.4236/jsbs.2014.41008

3. **Pyrolysis Kinetics of Algal Consortia Grown Using Swine Manure Wastewater**

Citation: Sharara, M. and Sadaka, S. 2014. Pyrolysis kinetics of algal consortia grown using swine manure wastewater. Bioresour Technol, 169: 653- 666

4. **Combustion Kinetics of Swine Manure and Algal Solids**

5. **Gasification of Phycoremediation Algal Biomass**

Citation: [a] Sharara, M. and Sadaka, S. 2012. Auger Gasification of Algal Blooms Produced in a Waste Water Treatment Facility. *In* ASABE Annual International Meeting. Dallas, Texas- July 2012

         [b] Sharara, M. and Sadaka, S. xxxx. Gasification of Phycoremediation Algal Biomass. *BioResources* [submitted December 2014, under review]

6. **Life Cycle Assessment of Swine Manure Management through Thermochemical Conversion**

Chapter 1 Introduction

Poor waste management practices trigger ecosystem imbalances on regional and global scales. Livestock production is an essential agricultural enterprise that is also responsible for large quantities of organic waste (manure). Livestock production practices changed drastically in during the past decades toward more integrated and concentrated systems. These changes yielded significant economic benefits to producers, aggregators, and consumers but also triggered severe ecological degradation. This degradation is caused by the concentration of animal operations and, in turn, the disposition of animal waste in relatively small regions. Traditional manure disposal methods, i.e. soil application and incorporation, are no longer sufficient to assimilate the huge quantities of manure. Manure over-application, i.e., beyond the soil assimilative capacity was shown to be responsible for numerous contamination problems; nitrates (NO_3-N) leaching from top soil to groundwater causing contaminations, and nitrogen (N) and phosphorous (P) runoff to rivers and lakes resulting in fertilized algal blooms, anoxic conditions and eutrophication of water bodies. Additionally, manure application beyond soil and crop needs alters the soil pH causing delayed plant emergence and reduced crop productivity. Volatilization of ammonia (NH_3-N) from over-application of manure to agricultural soils is malodorous, a respiratory nuisance, not to mention a precursor to the formation of particulate matter (PM), and acid rain.

Majority of aqueous manure wastes (dairy and swine manures) undergo a biological stabilization step, i.e., anaerobic decomposition prior to soil application. This step takes place in lagoons, which work to reduce the nutrient loading of the manure effluents prior to soil application in order to minimize nutrients runoff, leaching, and volatilization. This stage often results in the release of large quantities of methane (CH_4) and NH_3. Currently, few of these

lagoons are covered or equipped with gas collection or flaring capabilities. The lack of gas collection or flaring is responsible for a large contribution of the livestock sector to the agricultural global warming emissions either directly through increased CH_4 emissions, or indirectly through NH_3 emissions that contribute to the formation of PM.

This research aims at exploring the gasification of swine manure as a utilization approach that minimizes the impact of manure on the ecosystem. This conversion process, gasification, is an old technology that utilizes elevated temperature conditions, and controlled flow rate of a gasifying agent, to facilitate the conversion of organic solids to a gas fuel stream (producer gas) in addition to solid char (biochar). The feedstock under study here are: swine manure separated solids, and phycoremediation algal consortia. Algal biomass are grown using the liquid effluent from swine manure liquid-solid separation to reduce nutrients runoff and leaching. Both feedstocks were closely studied in a thermogravimetric analyzer (TGA) to understand the temperature-weight loss relationship under different atmospheres. These relationships are necessary to determine the conversion parameters, i.e., residence time and temperature levels suited for gasification. Additionally, the thermogravimetric study will be used to derive the various reaction kinetic parameters that are useful to modeling the conversion of swine manure solids, and the proper design of conversion equipment. The gasification system, used in this study, is an externally heated cylindrical batch reactor (auger reactor). Carbon fate will be investigated here to determine the amount of carbon sequestered, in biochar form, and the carbon released from burning producer gas.

Finally, a life cycle assessment (LCA) was conducted to investigate this utilization route: slurry storage>solid separation>drying> thermochemical conversion>utilization of producer gas to avoid natural gas fuel usage, to integrate the findings of this research into the manure

management systems (MMS) available to livestock producers. Furthermore, this study outlines the contributions of each step to the overall impacts, along with the potential areas for improvement.

As such, this document is divided into several chapters, each covering a specific point of investigation related to the review of literature, characterization, thermochemical conversion of manure solids and algal biomass, and the life cycle assessment of swine manure gasification.

Chapter 2 Value-added products from Swine Manure: Challenges and Opportunities

Chapter 3 Thermogravimetric Analysis of Swine Manure Solids Obtained From Farrowing, and Growing-Finishing Farms

Chapter 4 Pyrolysis Kinetics of Algal Consortia Grown Using Swine Manure Wastewater

Chapter 5 Combustion Kinetics of Swine Manure and Algal solids

Chapter 6 Gasification of Phycoremediation Algal Biomass

Chapter 7 Life Cycle Assessment of Swine Manure Management through Thermochemical Conversion

Chapter 2 Value-added products from Swine Manure: Challenges and Opportunities

1. **Abstract**

Swine production is projected to grow globally, and along with it the challenges associated with swine manure management. The environmental burden on production regions, due to consolidation and regional concentration in the swine sector, prompted stricter regulations on swine operations. This paper presents a critical assessment of the various technologies that target production of energy, fuels, and bio-products from swine manure using biological (composting, anaerobic digestion), and thermal (incineration, gasification, pyrolysis) techniques. Yields and quality of products, i.e., compost, biogas, syngas, bio-oil and biochar are discussed. Manure characteristics were shown to be a challenge to conversion technologies. Pretreatment steps, such as blending, solid-liquid separation, and drying are critical to the viability of any conversion technology. Biological processes were shown to necessitate blending with a carbon-rich source to adjust the carbon: nitrogen ratio, and thus facilitate biological activity. High levels of nitrogen in swine manure are inhibitory to biological conversion, and result in NO_x and NH_3 emissions under thermal conversion techniques. The high phosphorous levels in swine manure can be an added-advantage to the biochar produced from thermal conversion of swine manure solids acting as a fertilizer. The Dependence of end-product value on market prices and regional regulations influence the technology selection criteria. This review outlines several points worthy of further investigation to improve the applicability of these conversion processes.

2. **Introduction**

Livestock production has been an inseparable part of food production systems for millennia. Through hunting first, and then by domestication, man managed to secure a continuous supply of essential dietary components, i.e., protein and fat. The share of animal

4

protein and fat in the human diet, however, is not globally constant. In underdeveloped and

developing countries, carbohydrate-rich staples, such as grains, tubers or legumes are the main

sources of energy, with a smaller share of animal proteins and fats compared to diets in

developed and industrialized countries. Furthermore, as countries transition to a more developed

and industrialized stage, resulting in a corresponding increase in median incomes, diet

composition also changes to include more animal products [1]. Table 2-1 lists meat consumption

per capita in a sample of countries, representing different stages of industrial development, in the

years 1989, 1999, and 2009. In industrialized countries, advances made in the industries that

support livestock production, such as, feed production, transportation, and automation in

slaughterhouses and meat packing facilities pushed for an equally mechanized livestock

production model. This mechanization was realized through vertical integration of livestock

production with various upstream and downstream industries through contracts typically referred

to as "feeding contracts" [2].

Table 2-1 Meat Consumption (kg capita^{-1} year^{-1}) in various countries [3]

Country	1989	1999	2009
	Meat consumption (kg capita^{-1} year^{-1})		
United States	113.2	124.7	120
Brazil	48.7	76.5	85.3
China	24.2	47.4	58.2
Egypt	15.6	21.5	25.6
Nigeria	8.0	8.9	8.8
India	4.0	4.0	4.4

These contracts organized livestock production between an integrator that usually owns

both the feed and the livestock, and the grower who owns the production facility and is

responsible for growing livestock to market specifications and management of generated wastes.

These contracts entail a baseline rate, paid by the integrator to the grower, per unit animal

finished (usually per head of livestock) with additional incentives tied to the efficiency of production, i.e., animal weight, feed conversion efficiency and mortalities [4]. This approach, i.e., contracting, has essentially minimized price volatility and lowered risks to both growers and integrators which were relatively higher in the spot (negotiated) market. This trend also incentivized large investments by growers to expand growing facilities, to house a larger number of animals to maximize returns through the economies of scale. This consolidation pattern has been significant in the U.S. livestock sector since the 1970s, first with the poultry production sector, then increasingly with both feedlot cattle and swine production.

Along with the increase in animal inventory and production density, a corresponding increase in volumes of manure production followed. Based on the Department of Agriculture quarterly inventory for the end of 2012, the total number of pigs, cattle and calves, and layer hens was 66.3, 97.8 and 346 million head, respectively. The corresponding amounts of manure, for each type of animal, can be calculated using the following manure production rates for swine, cattle and layer hens: 4.67, 29.41 and 0.09 kg $hd^{-1} d^{-1}$, respectively [5]. Thus, the total amounts of manure generated daily by swine, cattle and layer hens are 0.30, 2.80 and 0.03 million metric tons (MMT) per day.

Swine sales in U.S. markets showed a drop in open market sales from 62% to 8.1% of total sales between the years 1994 and 2009 with an ancillary increase in the quality of pig sold by contract [6]. That trend is closely related to the intensification trend observed in Swine operations, during the same period [7]. Gradually, smaller, family-owned farms in the U.S. gave way to industrialized, large-scale operations clustered in the Midwest and the Southwest regions, close to feed production regions. The majority of the small- and medium -sized farms still in business today cater mostly to the niche organic and premium pork markets [8].

These structural changes brought significant improvements to the various elements of livestock production, namely, lowering the number of farm workers per unit livestock sold, improving feed rations leading to higher feed conversion efficiencies, and to advances in swine breeding. This led to higher numbers of pigs per litter, and a drop in mortality rates. Between the years 1992 and 2011, production volume in the swine sector (expressed in slaughtered pig weight) showed an increase by more than 30% [9] making the U.S. the biggest net exporter of pork meat globally [10].

Another facet of consolidation in the swine sector is the regional concentration of production [11]. The majority of swine production in the U.S., today, is centered in the Midwestern states: Iowa, Minnesota, Illinois, Indiana, Nebraska, and Kansas with the top-ten producing states contributing more than 85% of the national swine inventory [12]. Surveys put the total number of swine operations at 69,100 operations, 87% of which housing 2,000 head or more [9]. In 2011, Arkansas total swine inventory was roughly 0.16% of the total U.S. swine inventory with 107,000 head, divided between breeding swine inventory at 60,000 head and market inventory at 47,000 head [13]. In the following section, an overview of the swine production life cycle will be briefly presented with emphasis on the various types of swine farms, and the corresponding manure management approaches.

3. Swine production life cycle, feed, and housing

Swine production facilities could be classified into one of the following categories: *(1) Farrowing farms* which house pigs for the specific purpose of breeding and producing feeder piglets that are then sold, *(2) Feeder farms* in which pigs are raised from birth to 60 pounds (lbs.) and sold to grower-finisher farms, and *(3) Grower –Finisher farms* that raise small pigs to market weight (260 to 270 lbs.). Alternatively, production is accomplished in *Farrow-to-Finish*

farms in which the animal is raised from birth to slaughter weight on one farm. Figure 2-1 below shows the various stages in a pig life cycle with the typical terminology used.

Most swine farms today raise more than 2,000 head per farm, in confined animal houses using processed feed, while few farms still practice open feedlot grazing. Livestock housing can be generally categorized into: ventilated concrete structures, "houses", or open hoop structures "feedlots" that are roofed and fenced but not walled. Animals under hoop structures are kept over a bedding material (often corn stalks) that absorbs the manure initiating aerobic decomposition (composting). During gestation and nursery phases, however, all pigs are kept in confined (indoor) housing within separate stalls or pens for protection.

In concentrated production, animals are fed optimized rations composed mostly of a corn-soybean blend, to ensure supply of nominal protein and energy to the animal. Phosphorous (P) is added to feed rations in mineral form since pigs are incapable of digesting organically-bound P (phytate) that is already available in the feed [14]. Alternatively, a phytase enzyme can be added to the feed to facilitate biological-P digestion [15].

In confined, indoor production, animals are kept on concrete floors that are partially or fully slatted to facilitate cleaning and collection of manure (feces, and urine). Waste collects through the slatted floors, in pits below the houses before being emptied out for treatment or disposal. Deep pits (2.4 meters depth) act as a storage space, typically sized to hold a year's of production of manure, and as an anaerobic decomposition stage. This type of pit, however, was found to be harmful to the animal health due to the evolution of ammonia (NH_3), hydrogen sulfide (H_2S), and methane (CH_4) emissions [16].
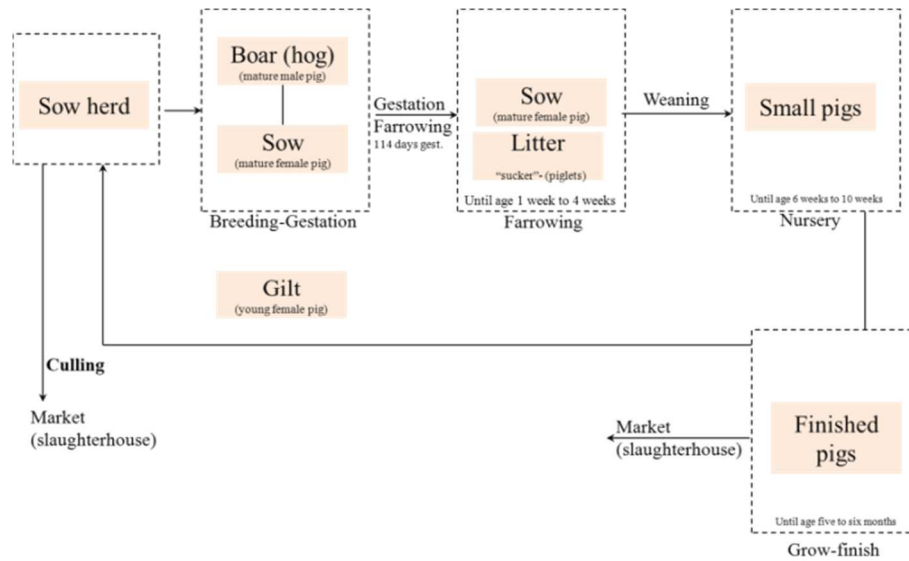
Figure 2-1 Production life cycle of pigs

A study on the agitation and removal of deep pit slurry indicates severe increases in concentrations of H_2S, CH_4, and NH_3 emissions, which are potentially harmful to animals and workers [17]. Several explosion incidents were reported in deep-pitted houses due to the flashing of these flammable gases [18]. Alternatively, the under-house pits can be shallow pits where manure is held for short intervals, typically 7 days, before being discharged to external storage. Discharging shallow pits can be accomplished via a pull-plug (drained) system, or a flushed system. Flushing is often accomplished by recirculating slurry liquids from the final manure holding pond to minimize the consumption of clean water. In addition to controlling the animal temperature, ventilation (natural, mechanical, or both) also work to remove the NH_3 and other volatile fatty acid (VFA) emissions from the houses. Emissions in swine houses can be further minimized using pit ventilation, wet scrubbers, or oil sprinklers [19, 20].

In confined swine houses, manure is managed in a slurry form, unlike in feedlot hoop structure production where manure undergoes partial aerobic decomposition (composting) and evaporation of liquids until seasonal scraping and soil application. Only 15% of swine

production takes place in farms that practice solid handling of the manure (north central Midwestern areas, mainly Iowa) while the remaining farms practice wet, slurry manure handling [21]. To gain a better understanding of manure as a problematic waste, and a potential feedstock for value-added products, characteristics and composition of manure were investigated. In the following section, a brief review of manure characteristics and composition is discussed.

4. Swine manure composition and characteristics

A survey of the literature shows large variability in swine manure composition data. This variability is attributable to the dependence of manure composition on animal feed, age, genetics, and the manure handling system, which alters the properties and composition of raw manure. Furthermore, manure composition data are often reported using different bases, i.e., as excreted, or as-removed basis. The latter option, as-removed basis, takes into account the influence of the handling method on the composition and the characteristics of the manure.

5. Biological Treatment of swine manure

Most swine farms utilize at least one type of biological treatment. In general, biological processes target elimination of pathogens, weed seeds, and parasites to alter the manure composition from a complex, malodorous effluent to an odor-free, plant-accessible one. Furthermore, biological treatments decrease the manure nutrient loading thus minimizing the risk of over application and nutrient runoff. Manure management in farms above 2,500 head falls under the purview of EPA's concentrated animal feeding operation (CAFO) rules [22]. Soil application in such cases is regulated through a permitting process. Application permits are tied to manure quality only from a nutrient loading perspective, unlike with municipal sludge in which permitting tracks both composition, and pathogen loading before permitting soil

application. Oversight also ensures that the targeted agricultural land is capable of assimilating the intended manure volumes through soil nutrients analysis.

Table 2-2 below lists the various characteristics of swine manure for the animals at different stages. It is clear that, regardless of age, the swine manure is predominantly water, with the total solids making up only 10% of the wet weight of the manure.

Generally speaking, maintaining the manure matrix within thermophilic conditions (above 50°C) for a few days is sufficient to kill off the pathogens. Modification of manure composition, however, is accomplished through a series of decomposition stages that break down the complex organic species in the manure (proteins, fibers, fat, organic acids… *etc*.) into simple, short-chain compounds while volatilizing a share of these nutrients in the form of gaseous emission; NH_3, CO_2, CH_4, and VFAs. This transformation, i.e., breakdown of complex organic species, is achievable through biological processes, namely, aerobic and anaerobic digestion.

Table 2-2 Weight of pigs at different stages and the corresponding characteristics of manure as-excreted [5]

Component	Units	Gestating sow	Lactating sow	Boar	Nursery	Grow-to-finish
Avg. animal weight	kg	200	192	200	12	70
Manure weight	kg hd^{-1} d^{-1}	4.99	11.32	3.79	1.098	4.54
Manure volume	L hd^{-1} d^{-1}	5.11	11.62	3.74	1.090	4.80
Manure moisture	(%)	90.0	90.0	90.0	90.0	90.0
Total solids (TS)	kg hd^{-1} d^{-1}	0.50	1.13	0.38	0.125	0.45
Volatile solids (VS)	kg hd^{-1} d^{-1}	0.46	1.04	0.34	0.110	0.38
Biological oxygen demand (BOD)	kg hd^{-1} d^{-1}	0.17	0.38	0.13	0.042	0.15
Nitrogen (N)	kg hd^{-1} d^{-1}	0.03	0.09	0.03	0.011	0.04
Phosphorous (P)	kg hd^{-1} d^{-1}	0.01	0.02	0.01	0.002	0.01
Potassium (K)	kg hd^{-1} d^{-1}	0.02	0.05	0.02	0.004	0.02

5.1. Aerobic decomposition (composting)

This process has been in practice as part of animal farming for centuries. Aerobic digestion functions as a treatment process that reduces odors and moisture, in addition to eliminating

pathogens and improving the manure characteristics as a soil conditioner. Aerobic decomposition is accomplished through a series of oxidation and mineralization stages carried out by aerobic microorganisms [mesophilic and thermophilic], which transform the biomass matrix into a stabilized, humus-like substance [23]. The following formula describes the composting process requirements, and outcomes [24]:

$$fresh\ organic\ waste + O_2 \xrightarrow{microbial\ metabolism} stabilized\ organic\ residue + CO_2 + H_2O + Heat \cdots$$

The elevated temperatures achieved during activation of thermophilic bacteria trigger increases in the rate of carbon and nitrogen mineralization. Partial aerobic digestion occurs naturally in the bedding mixture (crop residue, and animal manure) under hoop structure swine feeding. The bedding-manure mixture is often allowed to continue compositing, between herds, by scraping it into piles or windrows [25]. In wet-handling systems, where manure is flushed and collected in lagoons, a solid-separation step is necessary to increase the solid content in the matrix, and thus facilitate aerobic conditions.

The composting process is judged to be complete based on the levels of microbial activity and the phytotoxicity of the decomposed matrix [26]. The process can be divided, from a temperature standpoint, into three consecutives stages: heating phase, thermophilic phase, and cooling phase. The heating phase is typically the shortest and it starts immediately after mixing the biomass and setting the piles. This stage typically lasts 1 to 3 hours, during which the compost pile temperature increases rapidly from ambient to thermophilic levels, above 50°C. These temperatures are maintained throughout the thermophilic phase, the duration of which depends on the quality of the mixture, and the aeration levels. During this stage, mineralization and oxidation rates are at their highest, resulting in a volatilization of NH_3, CO_2, and moisture. This phase is instrumental in killing off pathogens, parasites, and weed seeds, which is why

recommendations maintain that for the compost to be deemed safe, it should remain in this stage, at 55°C, for at least three days [27]. The last stage, cooling and stabilization, is typically the longest and it ends with the material fully degraded and pathogen-free.

Proper management of the process parameters (aeration, C: N ratio, moisture, pH, and temperature) leads to a stabilized, pathogen-free compost within a suitable timeframe. C and N levels in manure (C: N ratio) are not sufficient to initiate and sustain composting by itself, Table 2-3. Therefore, the first step to initiate manure composting is to ensure a suitable C: N ratio, usually by introducing a carbon-rich source, i.e., wood chips, sawdust, or crop residue to adjust the C: N ratio to the recommended range: 25 to 35, and the moisture content between 50-60% w/w [28]. Excessively high temperatures (>60°C), or rapid drying of the pile were shown to result in rapid decomposition in the initial phase but also results in limited activity of bacterial communities, and consequently termination of the composting process [24]. Influence of aeration rates, both continuous and intermittent, on maintaining thermophilic conditions for a mixture of swine manure separated solids and peat moss in an in-vessel composting setup was investigated [29]. The C: N ratio dropped from between 15:1 and 18:1 to between 10:1 and 14: 1 within 15 days of composting. Similarly, the pH of the mixture decreased from near neutral to acidic range (5.2 to 6.9). Intermittent aeration regiment, at rates between 0.04 and 0.08 liters per minute per kg of volatile matter ($l\ min^{-1}\ kg_{VM}^{-1}$), was recommended to achieve pathogen-eradication (above 55°C for 3 days) and odor control without volatilizing the organic matter content in the mixture. Similarly, changes in C: N ratio during composting of household waste were found to be the smallest for both low and high initial C: N ratio, i.e., 11, and 39, respectively [30]. Changes in chemical composition during a 63-day composting experiment of pig manure mixed with sawdust in pile composting were investigated [31]. A rapid decline in organic-C from 45% to

36% within the first 14 days was observed, followed by a gradual decline for the remaining

duration, totaling a 10% drop throughout the process. As part of the decomposition and

mineralization stages, however, swine manure was found to lose up to 72% of its organic C and

60% of the total N through emissions [32]. Most of these losses are in the form of CO_2 and NH_3,

and much lower rates of CH_4 and N_2O. The various greenhouse gas (GHG) emissions from

turned and unturned compost piles of dairy manure and bedding material mixtures were

monitored over 80 days [33]. Higher GHG emissions from turned piles, 1.98 kg of CO_2

equivalent per kg of degraded volatile solids (kg $_{CO2\text{-}eq}$ kg $_{VS\ degraded}^{-1}$), were reported in

comparison to unturned ones, 1.55 kg $_{CO2\text{-}eq}$ kg $_{VS\ degraded}^{-1}$. CO_2 emissions accounted for 75-80%

of GHG emissions, followed by CH_4, at 18-21%, then finally N_2O at 2-4%. Close accounting of

this particular aspect of composting, GHG emissions, is necessary when selecting the most

environmentally sustainable approach to manure utilization.

Table 2-3 Typical composition of animal manure in mg kg⁻¹ fresh waste [32]

	Dry matter	Organic C	Total N	NH4-N	pH
Liquid manure/slurry (g kg⁻¹)					
Cattle	15-123	3.8-36	2.0-7.0	1.0-4.9	7.1-8.4
Pig	4.9-152	1.0-65	0.6-7.8	0.3-6.6	6.7-8.9
Poultry	10-367	11-112	2-21	1.9-9.4	7.9-8.8
Solid manure (g kg⁻¹)					
Cattle	140-300	65-126	4.2-8.1	0.3-2.0	8.6
Pig	150-330	42-132	3.5-11	0.5-6.0	8.1
Poultry	220-700	103-597	10-58	2.4-18	7.6

5.2. Anaerobic digestion (fermentation)

In large confined swine houses, anaerobic digestion takes place in the manure collection

pit under the swine houses, and in the final storage lagoons. This process requires anaerobic

conditions (oxygen-free) to activate certain bacterial and microbial communities that digest the

organic matter. The anaerobic bacteria convert complex manure substrate to an effluent of degraded humic acids, and a mixture of gases (CH_4, CO_2, NH_3, and N_2O). This process is practiced widely on U.S. swine farms in manure collection lagoons prior to the annual, or bi-annual, land application. Most of these lagoons, however, are not covered, which means the process only occurs within certain anaerobic zones of the lagoon. Furthermore, since most farms do not actively flare or collect volatilized gaseous species resulting from digestion, these gases become a prominent source of GHG emissions in agriculture. CH_4 and N_2O emissions between 1990 and 2011 from U.S. manure management were found to have increased from 31.5 to 52.0 Tg_{CO2-eq}, and from 14.4 Tg_{CO2-eq} to 18.0 Tg_{CO2-eq}, respectively [34]. These increases were attributed, in addition to expansion of size of production units, to the spread of liquid handling and storage in dairy and swine production. Few U.S. farms practice an active digestion process using a covered anaerobic digester where temperature, pH and organic matter loading are controlled, and where the resultant energy-positive gas (biogas) is burnt for heat, energy or both. Steady operation of these digesters is often challenging due to the complexity and the interdependencies in the process. The following section will outline the main factors that control this process.

5.2.1. Anaerobic digestion stages

Anaerobic digestion is a sequential process, as shown in Figure 2-2, with different groups of bacteria carrying out different tasks to fully digest the biological substrate. After the initial hydrolysis of soluble components (hydrolysis), acidogenic bacteria transform complex organic acids into volatile fatty acids (VFAs), which are transformed to acetate using acetogenic bacteria [35]. The VFAs were shown to be critical components that can decrease the pH of the mixture thus damaging the pH-sensitive acetogenic and methanogenic bacteria. Changes in the VFAs

concentration after inducing perturbation (changes in hydraulic retention time of substrate, temperature, and organic matter loading) to the anaerobic digestion of a cattle-swine manure mixture were monitored [36]. They concluded that tracking concentrations of individual VFAs, isobutyrate and butyrate, might be a good indicator of the stability of the digestion process, as opposed to tracking the overall concentration of VFAs. Ammonia (NH_3) is another product of the acidogenesis that was found to have an inhibitory effect on the digestion process. The anaerobic digestion literature indicates a wide range of ammonia concentrations, 1.7 to 14 g l^{-1} total ammonium nitrogen (TAN), which can reduce CH_4 production by 50% [37]. Swine manure, due to its high NH_4-N and sulfide contents, was proven to be challenging in anaerobic digestion studies [38, 39]. To overcome this challenge, a carbon-rich source such as crop residue, glucose or glycerol is added to the swine manure to adjust the starting C: N ratio. The influence of crop residue additives of wheat straw, corn stalks, or oat straw, and the C: N ratio (16, 20 and 25) on the gas yield from anaerobic digestion of swine waste was investigated [40]. Increasing the C: N ratio within this range showed increases in the yields of both the CH_4 and the total biogas. Wheat straw blends showed significantly lower CH_4 and biogas yields at all C: N levels when compared to corn stalks and oat straw blends. This was explained by the fact that wheat straw contained much higher lignin content. Lignin is inaccessible to most digestive bacteria, in comparison to the other crop residues.
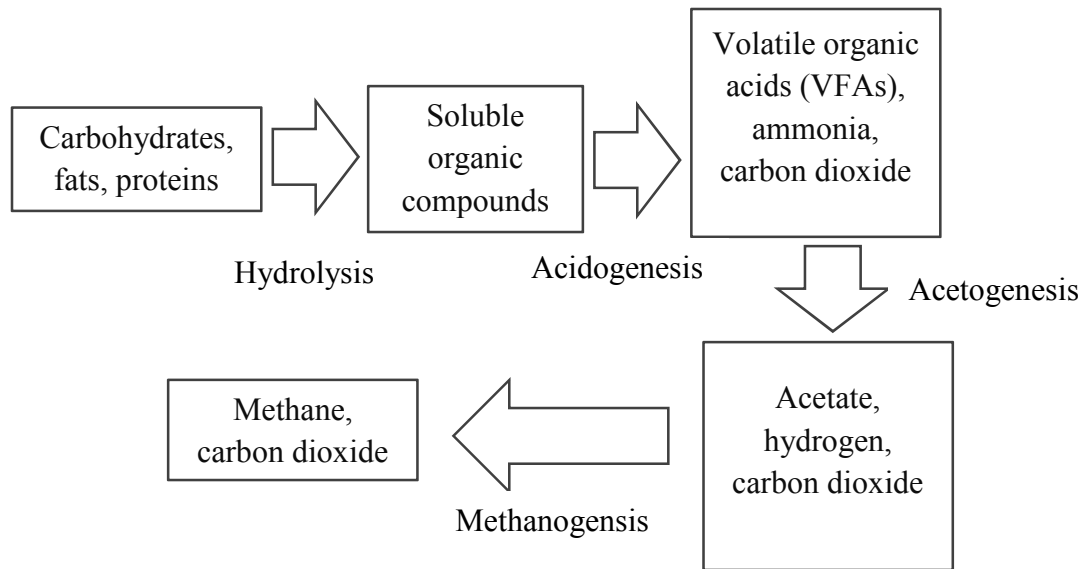
Figure 2-2 Biomass transformation with the various stages of anaerobic digestion [41]

5.2.2. Mesophilic and thermophilic digestion

Anaerobic digestion can be accomplished at two different temperature ranges; mesophilic (25°C -35°C), and thermophilic (50°C -55°C). Differences between mesophilic (37°C) and thermophilic (55°C) anaerobic digestion on the removal of chemical oxygen demand (COD), biogas production, and CH_4 production were studied [42]. Small differences in COD reduction, 63% versus 67%, and volatile solids (VS) reduction, 64% versus 65%, were observed between mesophilic and thermophilic conditions, respectively. CH_4 production was lower in thermophilic conditions when compared to mesophilic conditions, 3.3 versus 3.5 l l $_{reactor\ volume}^{-1}$ day^{-1}. Conversely, biogas yields, and CH_4 concentrations in the biogas under thermophilic conditions, 494 - 611 l kg$_{vs}^{-1}$ and 59.8-61.7%, were higher than under mesophilic conditions, 315 - 419 l kg$_{vs}^{-1}$ and 56.9-57.7%, for the anaerobic digestion of three different maize varieties [43]. High temperature fermentation (thermophilic) increases the metabolisms of bacterial communities but at the same time it results in accumulation of VFA and, in case of high-protein and urea substrates, results in an accumulation of NH_3 [44]. In a study of swine manure anaerobic

digestion, increases in free NH_3 concentration (0.75 to 2.6 g $_N$ l^{-1}), VFA accumulation (g $_{acetate}$ l^{-1}) and a decrease in methane yield (188 to 22 ml $_{CH4}$ g $_{VS}$ $^{-1}$) were observed with temperature increases [39].

Reluctance to adopt anaerobic digestion could be attributed to the complexity of the process, and its need for continual monitoring and control. Furthermore, digestion of nitrogen-rich sludge, such as swine manure, are more challenging due to the toxic effect of the liberated NH_3 [45]. According to data compiled by AgSTAR, an EPA program to promote CH_4 mitigation projects in the livestock sector, only 260 anaerobic digesters are operational on U.S. farms in 2014 with only 39 digesters operational in swine farms [46].

6. *Thermochemical conversion of manure*

This class of processes is the oldest known technologies to convert organic and biological residues to energy. Thermochemical conversion processes include: incineration, gasification, pyrolysis, hydrothermal gasification, and carbonization. Each of these processes utilizes elevated temperatures, a different range for each process, aided by an oxidative or an inert agent to facilitate chemical transformations. Thermochemical conversion of fossil fuels, wood and crop residues targets the production of heat and/or power, while the conversion of medical waste and municipal sludge targets the destruction and stabilization of hazardous waste. In this section, both common thermochemical routes such as combustion, gasification, and pyrolysis and also the less common routes such as hydrothermal conversion, and carbonization is discussed.

6.1. *Combustion*

Arguably the most important discovery in human history, fire enabled man to harness energy contained in organic matter for heating and cooking. The energy content in both fossilized organic residue (coal, petroleum and natural gas) and recent organic biomass (forest,

crop or livestock residue) is embedded in the hydrocarbon bonds which can be released under oxidative conditions using heat. This embedded energy can be directly correlated with the hydrogen (H), carbon (C), and oxygen (O) contents of the feedstock. Figure 2-3 below shows the dependency of heating value of common solid fuels on their atomic ratios of C, H and O. Biomass sulfur (S) and Nitrogen (N) have also been incorporated in heating value correlations [47]. The combustion process can be broken down into a set of sequential steps: *drying*, *pyrolysis* (devolatilization), *gasification*, *char combustion*, and *gas-phase oxidation*.

Under atmospheric pressure (101.3 kPa) and at temperatures above 100°C, the biomass moisture evaporates at rates dependent on the particle size, and the vapor pressure in the surrounding space. Then, pyrolysis of volatile organic species takes place at temperatures between 250°C and 500°C. This range varies according to the biomass type, and based on the size of biomass particles. At higher temperatures, 600°C to 1200°C, exothermic heterogeneous reactions (gas-solid gasification, and char combustion) and exothermic homogenous reactions (gasification, and gas combustion) take place. These reactions release thermal energy and flue gas (CO_2, H_2O, NO_2, and SO_2), in addition to an inert ash residue. The embedded energy in an organic molecule is the enthalpy of the complete oxidation of its hydrocarbons, into oxides and water. This enthalpy is typically measured as either the higher or lower heating value (HHV or LHV). Higher heating value (HHV) refers to the energy released upon oxidation of a unit mass of the feedstock taking into consideration the enthalpy of vaporization for the generated water. LHV, by contrast, accounts only the oxidation enthalpy. The following correlation [48] can be used to calculate one from the other, in units of MJ kg^{-1}:

$$HHV = LHV + 21.978*H$$, where H is the hydrogen weight fraction in the sample.

The heating value for a feedstock is the main characteristic that determines whether it could be logistically and economically used as an energy source.

Various models were developed to predict the heating value of biomass from the ultimate composition (C, H, N, O, and S), or proximate composition (volatile matter [VM], and fixed carbon [FC]), or alternatively using the chemical proximate composition (cellulose, hemicellulose, and lignin) [49]. Models based on ultimate analysis: C, H, and O were found to be the most accurate in predicting the higher heating values in biomass [50].

Adoption of biomass feedstock as fuel that replaces fossil fuels is problematic due to the low energy density of biomass, the large variability in biomass composition, and heating value. This complicates large-scale applications that utilize biomass from multiple sources. Animal waste, even more so than lignocellulosic biomass is problematic for thermochemical conversion due to its high moisture, minerals (ash), protein and its rapid degradation with handling and storage. Thermochemical processes, except for hydrothermal ones, require the biomass to be sufficiently dry, below 30% moisture content, wet basis, to avoid wasting the supplied heat energy on volatilizing biomass water. Liquid-solid separation of manure slurries can effectively reduce the manure water content from >90% to 60%. Mechanical, chemical, and gravitational separation technologies have all been employed to separate swine manure into solids-rich and liquids-rich fractions [51]. Similarly, dewatering swine manure and blending it with dry lignocellulosic feedstock can drastically improve the energetics of swine manure conversion. The energy requirements to produce 1 kg of char via pyrolysis from manure slurry, manure separated solids, and a manure-rye grass blend were calculated. A net energy requirement of 232 MJ for each kilogram of char produced from flushed manure, at 97 wt. % water, was reported, compared

to 12.5 MJ in dewatered manure (75 wt.% water), and 0.5 MJ in dewatered manure blended with rye grass [52].

The parameters that determine the combustion efficiency for animal waste were investigated [53]. Direct combustion was reported to be the most readily applicable technique, from both technological and economic perspectives. Nonetheless, the high mineral (ash) and S contents were mentioned as the main challenges facing all conversion routes. The presence of Si, Cl, and alkali elements in biomass ash was shown to cause fouling and slagging; both phenomena are damaging to incineration units [54]. These phenomena occur as a result of the formation of alkali silicates, and alkali sulfates which deposit on incinerator walls and grates. Table 2-4 below lists the typical higher heating values for both common fossil fuels, and different biomasses.
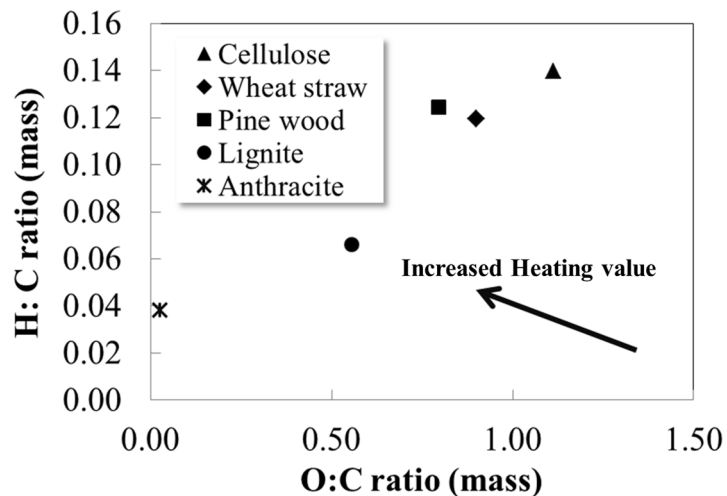
Figure 2-3 Compositional differences and the corresponding heating value (adapted from Van Krevelen diagram) [54, 55]

Table 2-4 Typical higher heating values (HHV, MJ kg^{-1}) for various hydrocarbon energy sources [54, 55]

Feedstock	HHV (MJ kg^{-1}) -dry basis
Bituminous coal	31.60
Peat	21.22
Cellulose	17.30
Lignin	26.70
Poplar wood chips	20.75
Oil shale	12.44
Wheat straw	17.55
Corn stover	18.10
Rice straw	15.95
Poultry litter	17.14
Cattle manure	17.36
Swine manure	19.70

Several slagging and fouling indices were developed to help relate composition and alkaline minerals in particular, to the biomass slagging and fouling tendency. One of the common measures to monitor slagging and fouling upon co-firing agricultural and biomass residue is to determine the weight of alkali oxides (potassium and sodium oxides) per unit energy (heat) in the fuels used. A study recommended setting an upper limit for alkali levels in fuel, 0.17 kg GJ^{-1}, pointing out that slagging is likely to occur at alkali levels of 0.34 kg GJ^{-1} or more [56]. Biomass Sulfur and chlorine were found to be instrumental in fouling and minerals deposition mainly due to the formation of alkali sulfates and chlorides that condenses on fly-ash, gas exits and downstream. The interaction of K and P with Si and Ca, on the other hand, is responsible for the formation of agglomerates in fluidized bed incinerators [57].

The most common incinerators that are used with biomass are grate, or fluidized-bed systems that are more flexible to the fuel type, followed by suspension burners which only allow for co-firing biomass at certain ratios (25% by energy share) with specific moisture, ash content and particle size requirements [58].

Manure ashes resulting from incineration at 700°C were investigated [59]. High pH (>10) along with increased concentration of P, K, and heavier metals such as zinc (Zn), copper (Cu)

and manganese (Mn) were observed for all ashes. No N was detectable in the manure. P concentration in ash residue, the highest in swine manure ashes, was around 10% - 12%. These P levels are similar to these found in phosphate rocks, which are used regularly as soil amendment. The ash-P, however, is not water –soluble therefore requires an acid digestion step in order to make it accessible to plants. Impact of incineration temperature of solids on plant-available P in the swine manure ash was investigated [60]. Temperatures of 700°C, or above, were found to result in the formation of an insoluble crystalline form of phosphorous (hydroxyapatite, $Ca_5(PO_4)_3(OH)$). Low-temperature incineration or gasification technologies (400°C -700°C) were recommended in order to retain the functionality of ash-bound P. In other words, there exists a trade-off during manure incineration between the energy yield and the phosphorous quality in the incineration residue.

6.2. Gasification

Gasification is a thermochemical process that takes place in a starved air environment (low oxygen) in which biomass particles undergo drying, devolatilization, solid-gas and gas-phase reactions that produce char, a producer gas, and a small fraction of condensables. This process takes place typically at temperatures, between 700°C and 1,000°C, lower than those associated with incineration. Exact gasification temperature depends on the type of feedstock used. Coal, for instance, has a low volatile matter content and low reactivity, which translate to higher reaction temperatures. Biomass, conversely, have a much higher volatile matter content (around 80% of dry weight) and a more reactive char due to the catalytic effect of the ash alkali minerals. Biomass is, therefore, typically gasified at temperatures between 600°C and 800°C.

The goal of this process is the production of an energy-rich blend of gases, "producer gas", which can be combusted in boilers, internal combustion (IC) engines or gas turbines. This

blend consists of carbon monoxide (CO), hydrogen (H_2), methane (CH_4), nitrogen (N_2), and carbon dioxide (CO_2), and trace gases. In addition to direct combustion in gas-burning systems, the producer gas can be purified and catalytically upgraded through the Fischer-Tropsch (F-T) process to produce liquid hydrocarbons [61]. The producer gas, however, must undergo a catalytic reforming step first to adjust the ratio of hydrogen to carbon monoxide above unity, $H_2/CO >1$, and also to convert all CH_4 and higher hydrocarbons to CO and H_2 [62]. The Fischer-Tropsch reaction, shown below, proceeds at a temperature between 200°C to 250°C, and between 25 to 60 bar pressure [63]. The output products are liquid long hydrocarbon chains, C5+, along with a byproduct gaseous fuel that is suitable for power production in gas turbines [64]. Adjusting the H_2/CO to values around 2 can be achieved through the water gas shift reaction:

$$CO + H_2O = CO_2 + H_2 \qquad\qquad -41MJ\ kmol^{-1}\ \text{(Water-gas shift reaction)}$$

$$CO + 2H_2 \longrightarrow -(CH_2)- +H_2O \qquad -165\ MJ\ kmol^{-1}\ \text{(Fischer-Tropsch reaction)}$$
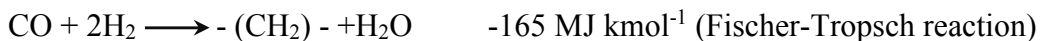
6.2.1. Gasification reactions

The gasification efficiency depends on numerous parameters, such as, the reaction temperature, the heating mode (auto-thermal or externally heated) the amount of oxidant present (typically oxygen) in the reaction volume per mole of biomass, the use of a catalyst, the physical and chemical characteristics of the biomass particles, and the type of gasification system used. The gasification reactions, shown below, commence after the biomass feedstock undergoes drying and devolatilization [65]. In addition to these reactions, volatile elements (N and S) are also devolatilized and released with the producer gas in the form of ammonia (NH_3), hydrogen sulfide (H_2S), hydrogen cyanide (HCN), and nitrous oxides (NOx).

1. Combustion reactions

    $$C + \tfrac{1}{2} O_2 = CO \qquad\qquad -111 \text{ MJ kmol}^{-1}$$

    $$CO + \tfrac{1}{2} O_2 = CO_2 \qquad\qquad -283 \text{ MJ kmol}^{-1}$$

2. The Boudouard reaction,

    $$C + CO_2 \longleftrightarrow 2\,CO \qquad\qquad +172 \text{ MJ kmol}^{-1}$$

3. The water gas reaction,

    $$C + H_2O \longleftrightarrow CO + H_2 \qquad +131 \text{ MJ kmol}^{-1}$$
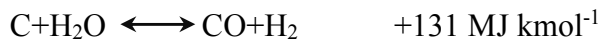
4. The methanation reaction,

    $$C + 2H_2 \longleftrightarrow CH_4 \qquad\qquad -75 \text{ MJ kmol}^{-1}$$

5. Methane steam reforming,

    $$CH_4 + H_2O \longleftrightarrow CO + 3H_2 \qquad +260 \text{ MJ kmol}^{-1}$$
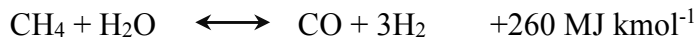
Aside from atmospheric air, the following agents: pure oxygen, steam, carbon dioxide or blends of these oxidants can be used as the gasifying agent [66, 67]. The thermodynamic efficiency of the conversion, however, suggests that energy-intensive oxidants such as pure oxygen or steam should only be used with high calorific value feedstock.

The amount of oxidant introduced during gasification is typically defined as the equivalence ratio (ER), which is the ratio of oxidant supplied during gasification to the amount of oxidant necessary for complete oxidation (combustion). This ratio, typically less than 1 for gasification, depends on whether the heat necessary for gasification is generated internally from exothermal reactions (auto-thermal mode) or an external heat source is utilized. Ideal ER values are typically higher when the gasification is in auto-thermal mode. Literature data on biomass gasification was used to evaluate the thermodynamic efficiencies (both first and second law of thermodynamics efficiencies) of auto-thermal gasification as a function of the ER [48]. The ideal

ER for wood chips, sawdust and rice husk autothermal gasification was found to fall between 0.36 and 0.40. Efficiency of biomass energy conversion varied between 52 % and 77%, whereas the exergy efficiencies (from the 2nd law of thermodynamics) ranged from 36% to 50%. In this context, exergy is the energy able to do work in a system.

Given that most biomasses contain O_2 as part of their structures, the gasification process can be accomplished possibly without supplying an external oxidant. This approach could be beneficial since the use of air as the gasifying agent also means the dilution of the product gas with air nitrogen (78.09 vol. %). An external source of heat, however, is necessary when no gasifying agent (oxidant) is supplied since all devolatilization reactions: the water-gas reaction, and the Boudouard reaction are endothermic. Supplying a gasifying agent, on the other hand, could eliminate the need for external heat beyond the startup (autothermal mode) since the exothermic reactions, full- or partial- oxidation reactions, can maintain the conversion. Supplying hydrogen and/or oxygen during gasification were shown to be necessary if the fuels are located above the solid carbon boundary, on a C-H-O ternary diagram, upon chemical equilibrium [68]. The solid carbon boundary (also known as carbon deposition boundary) is a function of the reaction temperature and it determines whether the original carbon will form solid carbon deposits, or react forming gaseous species at equilibrium [69]. Figure 2-4 plots a biomass waste; swine manure separated solids (SMSS), with the molecular formula $CH_{1.69}O_{0.5}$ on a C-H-O triangular (ternary) diagram. The area surrounded by dotted lines indicates an equilibrium state between gaseous species and solid carbon (i.e., gasification region). In the region above the gasification region, only solid carbon exists, while below it only fully-oxidized carbon gaseous species are present.

The type of oxidant used also determines the gaseous species generated. Similarly, the amount of oxidant supplied controls the process efficiency. Gasification efficiency is often expressed in terms of the ratio of chemical energy contained in the producer gas, discounting the sensible heat, to the calorific value of the original biomass. Generally speaking, ERs between 0.20 and 0.40 were found ideal to cross the carbon deposition boundary without oxidizing the generated valuable gas species [68, 70, 71]. Optimum value of ER, however, is a function of the composition of the biomass, and the type of gasification platform used.
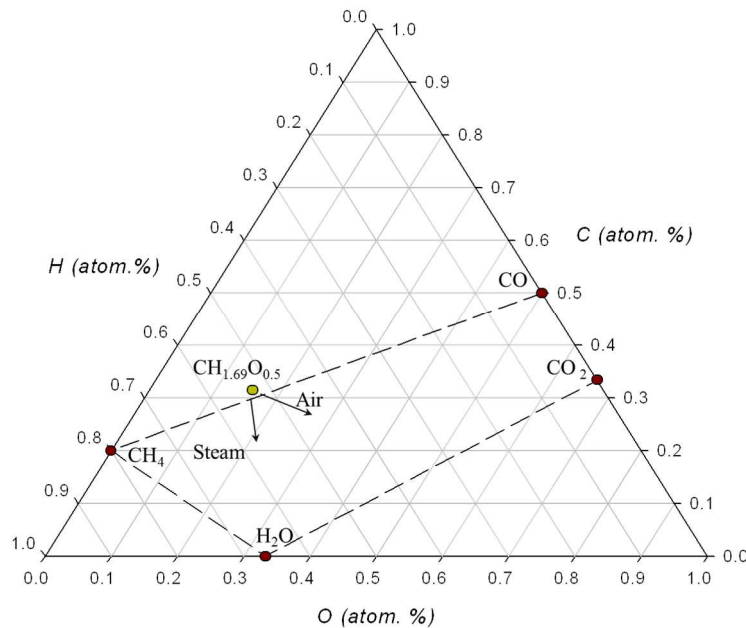
Figure 2-4 A ternary C-H-O plot illustrating biomass waste gasification using either air or steam as the gasification medium

6.2.2. Types of gasifier

a.　Fixed-bed gasifier

Biomass gasification has been investigated and adopted commercially in different gasifier configurations. Generally speaking, gasification platforms resemble combustion units in terms of the feeding mechanisms and reactor types. These systems are typically classified, according to

the interface between the feedstock and the gasifying agent, into: *fixed bed* and *moving bed* gasifiers. Biomass feed is introduced into fixed- bed gasifiers through a metered or gated entrance where it moves gradually, by gravity, across the various reaction zones. The feedstock is typically stacked within the gasifier and it is incrementally fed as part of the stack is reacted away into producer gas, char, and tars. Therefore, the stages of the gasification process; drying, devolatilization (pyrolysis), combustion and char gasification (Reduction) proceed within distinct stratified zones in the biomass stack. Correspondingly, the temperatures inside a fixed-bed gasifier are also stratified, and dependent on the thermodynamics of reaction taking place in each zone.

Fixed-bed gasifiers are classified into: downdraft, updraft, and cross draft systems, based on the relative movement of the producer gas with respect to the feedstock. Among fixed-bed systems, downdraft gasifiers are the most common due to their ease of operation, and the superior quality of producer gas (low tar and condensables) compared to other fixed gasification systems [72]. Tar and condensables are undesirable outcomes of the gasification process due to the fact that they are deposited on low-temperature surfaces, typically downstream, causing blockages and large pressure drops. Furthermore, in applications where the producer gas is directly fired, the tar content corrodes the combustion chamber and forms undesirable deposits.

A survey of commercial gasification systems showed that 75% of these systems are down-draft gasifiers while updraft type systems accounted for only 2.5% [73]. Agglomeration, formation of an ash-layer as well as condensation in upper parts of a countercurrent (updraft) laboratory-scale gasifier was reported with nutshells, and olive husks gasification [74].

The impact of the equivalence ratio (ER) on downdraft gasification of corn straw was studied [75]. A drop in the tar-to-producer gas ratio was reported when increasing the ER from

0.18 to 0.41, from 7.2 g Nm^{-3} to 4.6 g Nm^{-3} (Nm^3 is a cubic meter normalized to standard temperature and pressure conditions, 25°C and 101.3 kPa). Tar yields are generally higher in fixed bed gasifiers, representing between 12 wt. % and 20 wt. % of the carbon in the biomass, compared to tar in fluidized-bed systems, 4.3 wt. % of biomass carbon at 750°C [76]. The formation and cracking of tar in gasification systems will be discussed later in detail.

The stratification of the reactive zones in fixed-bed systems is a major drawback, especially with manure gasification, since it results in the formation of hot spots and agglomerations. The effects of blending cow manure with sawdust, at different mixing ratios, on gasification efficiency in a downdraft gasifier was investigated [77]. They reported drops in the reduction zone temperatures, the producer gas heating value, and the conversion efficiency with increasing the ratio of cow manure in the blends from 0% to 90%. The low conversion efficiency reported with cow manure was attributed to the fact that fixed carbon content in the manure was higher than in sawdust which translates to more endothermic char reduction reactions that cause a decrease in the temperatures and the conversion efficiency. Pelletized poultry litter was gasified in a commercial downdraft gasifier at temperatures between 825°C and 925°C [78]. Interruptions in gasification were reported due to the formation of clinkers (fused ash particles) in the reactor bed.

b.   Fluidized-bed gasifier

Compared to fixed-bed conversion, fluidized-bed gasification is a relatively newer mode of conversion. It was quickly established as rapid and efficient options that are also suitable for up-scaling. A fluidized gasification bed consists of an inert, thermally-stable media such as silica, olivine, or alumina particles, mixed at times with specialty catalysts for tar reforming. As the feedstock is fed into the reactor, this inert media serves as the heat-transfer medium that

facilitates conversion. The heat transfer is orders of magnitude higher than that achieved in fixed bed reactors due to the fluidization of the biomass-bed material mixture, which increases the contact between hot media and ambient biomass particles. Unlike in fixed-bed reactors, the fluidized bed does not have thermal stratification or distinct conversion zones (isothermal conditions), which helps achieve steady-state operation faster. In fluidized bed gasification, both the drying and the devolatilization stages occur nearly instantaneously once the biomass enters the reactor bed.

Fluidization of the bed material and biomass is achieved through purging continuous, uniformly-distributed, upward gas flow (often air-nitrogen mixtures). The velocity of this gas flow falls between the minimum fluidization velocity and the particle terminal velocity. This velocity, referred to as the fluidization velocity, ensures that both the bed media and the biomass particles remain suspended in the reactor without settling or entrainment in the gas flow. The ratio between reactor height and diameter in fluidized beds varies but is often around 10, as shown in Table 2-5. This is important to ensure that both biomass particles and devolatilized species are allowed sufficient time to react and to achieve equilibrium. Furthermore, fluidized bed reactors are designed so as to minimize the elutriation of partially-reacted chars or residual ashes with the producer gas, causing blockages and corrosion downstream.

The reactor bed is the lower segment of the reactor, with a height equivalent to 1 to 1.5 times the reactor diameter. This section is where the heat-transfer media is mostly located in a suspended mode (dense phase). The remainder of the reactor is referred to as the freeboard and it is occupied mainly by gaseous species (non-dense phase) with some partially-reacted solids that are elutriated in the gaseous phase (emulsion phase). Detailed models were developed to predict the quality of the producer gas from fluidized bed biomass gasification [79, 80]. In fluidized-bed

gasification, feedstock preparation, i.e., drying, and comminution is necessary to ensure uniform feeding and rapid devolatilization and to avoid carryover of loose, buoyant unreacted fragments into the gas stream.

In addition to the bubbling fluidized system described above, circulating fluidized bed conversion is also utilized in biomass conversion. This system, unlike a bubbling fluidized bed unit, consists of two reactors connected in-series to form a closed loop for the solids. The fluidization velocities are higher than in bubbling fluidization. Correspondingly, char particles are entrained out of the first reactor and are allowed to react in the secondary-bed with the residues collected and circulated back using gravity to the main reactor bed. In the following section, a brief survey of the main findings in the literature on fluidized bed gasification of biomass feedstock will be presented with an emphasis on manure gasification studies.

Table 2-5 . Survey of literature bed diameter and total height from fluidized bed systems studied in biomass gasification

Reactor diameter, D (mm)	Reactor total height, H (mm)	H/D (-)	Reference
40.0	1,400	3.5	[66]
229.0	1,728	7.5	[81]
150.0	1,200	8.0	[82]
300.0	2,500	8.3	[83]
150.0	1,400	9.3	[84]
53.5	530	9.9	[85]
100.0	1,000	10.0	[86]
30.0	400	13.3	[87]
200.0	6,000	30.0	[88]
100.0	6,500	65.0	[89]

The influence of temperature, between 900 K (627°C) and 1,000 K (727°C), on gasification of feedlot cattle manure in a fluidized bed system was evaluated [81]. Burner gas, generated from propane-air burning, was used as the fluidizing-gasifying agent. Yield and higher heating value of producer gas were 0.54 Nm^3 kg^{-1} and 19.53 MJ Nm^{-3}, respectively. The use of burner gas as gasifying agent has evidently enriched the producer gas with combustion

31

hydrocarbons. The yield of energy-rich gases, i.e., H_2, CO, and CH_4 were 38.7%, 26.1% and 14.7% of the dry produced gas composition.

Influence of gasification parameters, such as, ER, bed temperature, freeboard temperature, and the presence of a tar reforming catalyst (calcined dolomites: MgO. CaO) on quality of producer gas was evaluated [90]. The ER was shown to be the most influential factor in determining the quality of the producer gas and the amount of tars generated. ER values between 0.25 and 0.30 were recommended for optimal conversion. Increasing the H/ C ratio in the reactor was shown to be instrumental in improving the gas quality and minimizing the tar formation. Ideal H/C was found to be 2.2. Reactor bed temperature (> 800°C) and freeboard (> 600°C) were shown to be influential in improving carbon conversion, and tar destruction. However, temperatures above 800°C typically result in agglomeration, especially with high-ash feedstock, such as, manure. Quality of the producer gas under steam gasification of manure was studied as a function of bed media (Ni-Al_2O_3, or silica sand) and bed temperature [85]. Temperatures were varied between 540°C and 656°C which are lower than typical agglomeration or sintering temperatures. The use of catalyst, versus silica sand, resulted in a four-fold increase in H_2 yields and two-fold increases in CO and CO_2 yields.

6.2.3. Ash content and agglomeration

Ash reduction could be achieved by blending the high-ash manure with a low-ash feedstock, as well as using acid washing. Soaking biomass in diluted acid was shown to be an effective approach to eluting the ash minerals out of the biomass matrix. In a study of swine and hen manures, acid washing resulted in a drop in inorganic minerals (Fe, Ca, K, Zn, P and S), coupled with a similar drop in the char reactivity [91]. The reduced char reactivity was found to be closely related to low Ca concentration in acid-washed manures. Two approaches for ash

reduction: washing (soaking) and fractionation, i.e., removing <1 mm particle size fraction, were studied as pretreatment for peach stones gasification [92]. A drop in the ash content under both treatments was reported despite the formation of ash deposits with untreated as well as with the treated samples. Fractionation was shown to increase the ratio of potassium in the ash causing aggressive deposits when compared to untreated and soaked feedstock gasification. High-ash residues such as olive flesh and sugarcane trash were found to have a low agglomeration temperature making them a problematic feedstock for gasification. Wheat straw was also shown to agglomerate in gasification silica beds at 800°C, causing defluidization at a temperature well below nominal ash fusion temperatures for wheat straw, 1054°C [93]. Fusion tests on biomass feedstock samples were shown to overestimate agglomeration temperatures leading to unexpected operation interruptions [94]. Furnace testing of silica sand-wheat straw mixtures at varying ash ratios and furnace temperatures showed gradual increase in agglomeration and the bonding of the mixtures into hard brittle structures. Potassium oxide (K_2O), which has a melting point of 350°C, constituted 36.2% of the straw ash. Accordingly, potassium was cited as the reason behind the premature agglomeration occurrences. Controlled agglomeration testing showed that agglomeration in both biomass gasification and combustion commences by depositions on bed particles forming a homogenous sticky layer enriched in potassium and calcium silicates, followed by a thin outer layer of finer particles [95]. They showed that in gasification or combustion of sulfur-rich feedstock, a separate salt-melt phase initiated a glue-effect which bound bed particles causing large pressure drops in the reactor bed (defluidization). High K_2O and Cl contents in the agglomerated sand formed after fluidized-bed gasification of palm tree residues [96]. Two parameters were cited which could help predict sintering in fluidized bed biomass gasification:

1. $(K_2O+Na_2O)/SiO_2 > 1,$ and

2. $K_2O + Na_2O/HHV > 0.34$

In addition to biomass pretreatment or blending, various minerals have been studied and found to mitigate the adverse effects of ash when used as bed media or bed additive. Examples of these materials include limestone, calcite and high-melting point oxides (MgO, Fe_2O_3, CaO and Al_2O_3). Agglomeration and defluidization temperatures for three biomass types; Giant Reed, sweet sorghum bagasse, and olive bagasse with two different bed media; quartz and olivine were investigated [97]. Olivine showed slightly higher defluidization temperatures than those observed when using Quartz under all biomass types. Defluidization temperatures ranged between 785°C, and 830°C, except for olive bagasse in the olivine bed which did not show agglomeration even above 850°C. The high potassium content in tested biomass ashes; 30.0%, 31.6% and 25.8% for giant reed, sweet sorghum and olive bagasse, respectively, was cited as the cause behind sintering. The effect of bed media (calcined limestone, calcined waste concrete, and silica) on steam gasification of larch wood in a bubbling fluidized bed system was investigated [98]. Highest gas heating value, 10.98 MJ kg^{-1}, and cold gas efficiency, 56.5%, were reported with calcined limestone. However, calcined limestone showed breakage tendencies, which would instigate agglomeration, sintering and plugging of the reactor bed. Blending calcined concrete, which showed low wear resistance, with calcined limestone was recommended to improve the conversion efficiency while also minimizing plugging and agglomeration.

6.2.4. Tar formation

Another issue facing biomass gasification is the presence of tar in the producer gas. The term "tar" refers collectively to mixtures of phenolic, and aromatic hydrocarbons formed during the devolatilization (pyrolysis) stage of gasification that did not decompose sufficiently inside

the reactor to yield the targeted gases. This term, tar, extends to refer also to the secondary

hydrocarbon compounds formed under high reaction severity with higher molecular weights and

higher aromaticity (polyaromatic). Typically, the volatilized organics formed during the

pyrolysis stage are further decomposed by the elevated gasification temperatures and using either

the gasifying agent or the indigenous oxygen and moisture (steam) in the feedstock. Since most

tar decomposition reactions are endothermic, persistence of tar in the produced gas can be

attributed to the short residence time of the vapor phase in high-temperature regions, as is the

case with updraft gasifiers. Pyrolysis volatiles, in the absence of external oxidizing agents,

undergo secondary decomposition reactions at temperature above 650°C that increase yields of

permanent gases (H_2, CO, and CO_2) yields and decrease gravimetric tars [99]. Tars were

classified according to their molecular masses, using mass spectrometry, into primary,

secondary, and tertiary tars [100]. Close investigation showed tars to undergo both

decomposition and repolymarization with the increase in temperature. This phenomenon is

behind the transition of tars recovered in biomass conversion from primary tars under moderate

thermal conditions to secondary and tertiary tars under elevated gasification temperatures, as

shown in Table 2-6. Primary tars are more reactive and susceptible to thermal cracking than

polycyclic aromatic hydrocarbons (PAH), tertiary tars [101]. This is mainly because of the

presence of heteroatoms (O, N) and side-groups (OH, CH_3) in primary tars making them more

reactive than aromatic (ring) compounds. Free-radical reactions were cited as the primary

thermal cracking mechanism. These reactions initiate by breaking chemical bonds in a tar

compound, forming free radicals which undergo propagation, isomerization and termination

stages in which H_2 and CH_4 are released, and polyaromatic (tertiary) compounds are formed.

Table 2-6 Classes of tars formed during biomass gasification [100]

Tar class	Primary	Secondary	Tertiary (Alkyl)	Tertiary (Condensed)
Compounds	Levoglucosan, hydroxyacetaldehyde, furfurals, and methoxyphenols	Phenolics, and olefins	Methyl acenaphthylene, methylnaphthalene, toluene and indene	Benzene, naphthalene, acenaphthylene, pyrene
Temperature range	500°C- 800°C	500°C- 1,000°C	700°C- 1,000°C	700°C- >1,000°C

The transformation of the tar species as a function of the temperature is demonstrated in the following schematic [102], Figure 2-5.

Mixed Oxygenates, 400 °C → Phenolic Ethers, 500 °C → Alkyl Phenolics, 600 °C → Heterocyclic Ethers, 700 °C → PAH, 800 °C → Larger PAH, 900 °C
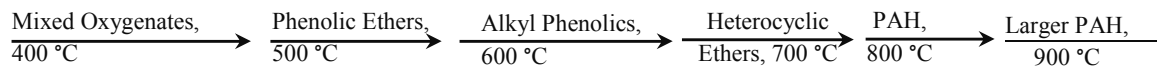
Figure 2-5 Tar species transformations with temperature increase

Tar presence is a nuisance only if the produced gas is transported over longer distances or if it is intended for use as feedstock for further chemical processing. If, on the other hand, the fuel gas is directly combusted in gas burners, or boilers then the tar will be burned along with the gases adding to the total calorific value without complications. Internal combustion (IC) engines, on the other hand, require tar content in producer gas to be below 100 mg Nm^{-3} in order to avoid problematic deposits that jam engine valves and corrode the cylinders [103]. Tar reduction is often achieved by employing thermal and/or catalytic cracking. Wet reforming, by Injecting steam (H_2O), or dry reforming, using carbon dioxide (CO_2), were shown to increase tar decomposition rates. Tar cracking, reforming and adsorption using air and steam as reforming agents was investigated with activated carbon, wood chips and synthetic cordierite as adsorption media [104]. Steam reforming was shown to increase yields of H_2 and CO and decrease CO_2,

C_2H_4 and C_2H_6 yields. Activated char was found to be more effective at adsorbing tars compared to activated carbon and synthetic cordierite. Steam reforming can be generally described using the following reaction:

$$C_nH_mO_k + (2n - k)H_2O = nCO_2 + \left(2n + \frac{m}{2} - k\right)H_2$$
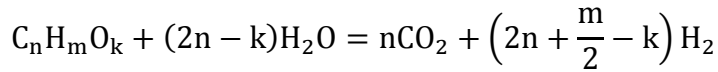
And for benzene (a tertiary tar compound):

$$C_6H_6 + 6H_2O \longrightarrow 6CO + 9H_2 \qquad \Delta H° (900°C) = +753 \text{ MJ.kmol}^{-1} \text{ [105]}$$

The reaction schemes for three tar compounds (toluene, benzene, and naphthalene) were derived in order to model tar products [106]. These model compounds were studied by varying temperature, residence time, the concentration of H_2 and H_2O injected. Hydrogen was shown to be highly effective in inhibiting the naphthalene conversion to solid carbon (soot) whereas steam was found to be marginally effective in the conversion of aromatics. Temperatures around 1,400°C were found necessary to convert both the soot and the aromatics to CO and H_2.

Most industrial tar reforming, however, is managed through the use of catalysts (catalytic reforming). Tar reforming catalysts are mixed with feedstock or incorporated in the primary gasification bed in fluidized-bed systems. Alternatively, catalysts could be added to dedicated (secondary) reactors. Tar cracking catalysts are generally classified into: dolomite catalysts ($CaCO_3$, $MgCO_3$), alkali metal catalysts (K_2CO_3, and Na_2CO_3), and nickel-based catalysts [107]. Incorporation of dolomites in the reactor bed was shown to cause attrition as well as deactivation due to carbon deposition on the catalyst active sites (coking). Nickel catalysts, on the other hand, were shown to be most effective when incorporated in fluidized gasification bed operated at 780°C. Indigenous alkali minerals in the biomass also act as catalysts reforming the produced tars and creating more permanent gases. Addition of ashes to the reactor bed was shown to be helpful in eliminating tar formation [108] yet problematic due to their agglomeration tendencies.

6.3. Pyrolysis

Pyrolysis, as discussed earlier, is a fundamental step to both the combustion and gasification of organic fuels. During the pyrolysis step, the solid biomass matrix undergoes thermal depolymerization causing the release of gaseous species, volatile organic compounds, and a restructuring of both the volatilized and solid phases. As a stand-alone process, however, biomass pyrolysis is optimized to generate condensable organic compounds resembling naturally-occurring crude oil (often referred to as bio-oil or bio-crude) in addition to char and gaseous products. Unlike combustion or gasification, pyrolysis does not require any oxidizing agent to facilitate the conversion. A sweeping inert gas, however, is necessary to rapidly remove the volatilized species from the reactor to the cold condensation unit. Rapid removal and cooling of pyrolysis vapors (quenching) is necessary to avoid further thermal decomposition of volatiles into permanent gases and also to minimize the solid-vapor reactions which facilitate char formation.

Pyrolysis can be classified, according to the process duration, to slow and fast (flash) pyrolysi*s*. Slow pyrolysis is characterized by low heat transfer rates, and longer residence times for both the solids and vapors, which lead to a high char yield. Fast or flash pyrolysis, on the other hand, has a high heating rate (10^3-10^{4}°C sec^{-1}), residence time of less than 2 seconds, and rapid cooling of the volatile species, all of which increase the condensable (bio-oil) yield [109]. Various types of reactors were investigated in the context of fast pyrolysis: *fluidized bed* (bubbling, and circulating), *ablative* (rotating cone, and vortex), and *vacuum reactors* [110]. Typical yields of fast pyrolysis products from lignocellulosic biomass (mainly wood) are: 60-75 wt. % bio-oil, 15-25 wt. % solid char, and 10-20 wt. % non-condensable gases [111]. The main product, i.e., bio-oil is an acidic mixture (pH between 2.5 and 3.5) of water (15 – 30 wt. %) with

a large number of oxygenated hydrocarbons of varying molecular weight. Bio-oils typically contain more than 200 chemical species including acids, alcohols, aldehydes, ketones, aromatics, phenols and sugars varying in concentration according to reaction conditions, and the composition of the original biomass [100, 112, 113]. Main pyrolysis reactions associated with the woody and lignocellulosic feedstock were grouped into cellulose, hemicellulose and lignin pyrolysis reactions [114].

Adding surplus water to the bio-oil was shown to facilitate phase separation of pyrolysis oil into water-rich and hydrocarbon-rich phases. Oxygen content of bio-oil is typically around 45-50 wt. % which, in combination with the water content in the bio-oil, result in low heating values, 18-26 MJ Kg^{-1}, when compared to petroleum liquid fuels.

In addition to its high water content, acidity and corrosiveness, biomass bio-oil was shown to be both thermally and temporally unstable. Various mechanisms were outlined in which reactions between various products, acids, alcohols and aldehydes cause the repolymarization and phase separation [115]. Bio-oil repolymarization and phase separation, shortly after production, complicates storage and transportation. These qualities deem the bio-oil unfit for most applications without an upgrading stage first. Bio-oil upgrading can be achieved through hydrodeoxygenation (HDO), and steam reforming often in the presence of catalysts. Bio-oil upgrading is often accomplished using one stage or two stage high pressures, catalytic hydro-treatment [116]. This process requires injecting hydrogen, elevated pressure (more than 100 bar) with temperatures between 250°C and 400°C in the presence of catalysts (sulfide CoMo or NiMo). A major challenge in bio-oil upgrading is the inhibition of repolymarization reactions, which are favored with increased reaction severity (pressure and temperature). Additionally, larger bio-oil compounds, where oxygen molecules are often difficult to dissociate, occupy

active sites on the catalyst resulting in plugging and coking (deactivation). Zeolite catalysts have been shown to facilitate bio-oil upgrading under atmospheric conditions without the need for additional hydrogen injection [117].

Catalytic steam reforming of bio-oil products has been modified to yield syngas products (CO, and H_2). This technique has been investigated on bio-oil and on model compounds such as phenol, acetone, and acetic acid as means to expand the usefulness of the pyrolysis products [118]. The amount of energy expended to facilitate hydrogen production from bio-oil was shown to be equal to that necessary to reform natural gas into syngas products [119]. Complications due to catalyst deactivation and coking, however, have been also reported with steam reforming of bio-oil [120].

Few studies have investigated animal manure as feedstock to pyrolysis conversion. Most of the available literature focuses on poultry litter pyrolysis. Pyrolysis of poultry litter yielded bio-oil 15-30 wt. % of the original feed with a HHV and dynamic viscosity within 26-29 MJ kg^{-1}, and 0.01-27.9 Pa s, respectively [121].A Multi-parameter study of pyrolysis of poultry litter-wood shaving mixtures, in a fluidized-bed reactor, showed the temperature to be the instrumental parameter impacting conversion, followed by biomass feed rate and then N_2 flow rate [122]. Highest bio-oil yield, 51 wt. %, and pH, 4.85, were achieved under 475°C. Swine compost, wood chips and sewage sludge were also investigated as feedstock for bio-oil production in a fluidized-bed pyrolysis unit [123]. The swine compost bio-oil was reported to have an H/C ratio of 1.63 and a higher heating value (HHV) of 31.2 MJ kg^{-1}, compared to 1.68 and 27.0 MJ kg^{-1} for sewage sludge, and 1.51 and 23.9 MJ.kg^{-1} for wood shavings. The high moisture and ash contents of animal waste are often cited as impediments for implementation of pyrolysis conversion and thermochemical conversion in general. The mineral and alkali salts, which are

available in varying quantities in manure, were shown to be influential in controlling the pyrolysis conversion pathways and the resulting oxygenates which further adds uncertainty to the bio-oil products generated.

An added advantage of thermochemical conversion of animal wastes, recently garnering attention, however, is the production of char. This term, char or "charcoal", refers to the solid residuals remaining after the devolatilization of volatile organics, and the partial reaction of biomass fixed carbon.

6.4. Biochar

Thermochemical conversion of carbonaceous biomass yields a solid byproduct, i.e., biochar. The characteristics of this char depend on the composition of the original biomass and also on the conversion severity. Complete combustion, for instance, yields only mineral oxides, with no carbon, collectively referred to as ash. Pyrolysis and gasification, on the other hand, generate a carbon-rich solid component (char) that also contains the ash minerals. Char can also be produced in a dedicated process at temperatures between 250°C and 400°C in the absence of air or oxygen, a process less severe than pyrolysis or gasification. The dedicated char production process is typically referred to as slow-pyrolysis, carbonization or torrefaction. The latter, i.e., torrefaction is a mild thermal treatment that takes places at lower temperatures (200°C -300°C) in which the biomass matrix remains largely unchanged except for the easily devolatilized fraction (hemicellulose). Torrefaction improves friability and energy density of the biomass, which facilitate co-firing with coal, or stand-alone conversion [124]. Char can be utilized in a variety of applications from soil quality improvement, to use as filtration and adsorption media [125], to incineration as a blend-in with fossil coal or as a stand-alone solid fuel. The term

biochar is commonly used to indicate that the specific end-use of the produced char is as a soil amendment[126].

Biochar production dates back thousands of years. Dark soils in the Amazonian basin (*terra preta*) are considered earliest example of a char-fortified soil. Studying these soils revealed numerous advantages to the incorporation of biochar in the soil. The aromatic carbon structures, in the biochar, provide a stable carbon form that facilitates nutrients retention. Furthermore, the biochar porous structures improve the soil porosity and facilitate the growth of microbial microorganisms. The increased alkalinity of the soil due to biochar addition also helps increase the soil cation exchange capacity (CEC). The impact of biochar application rates (10, 50 and 100 t ha^{-1}) and origin (cotton trash, grass clippings and prunings) were studied on yields of a radish crop in an Alfisol type soil [127]. Nitrogen fertilization was shown to be necessary even with the highest rate of biochar application given that C: N for biochar is quite high, i.e., 200. The interaction between N fertilization and biochar, however, was shown to significantly improve radish dry matter production with increasing biochar application rates. The soil quality was also shown to improve, i.e., increases in pH, exchangeable alkali ions (Na, K and Ca) and a decrease in the soil tensile strength, with the addition of biochar. Recent studies have pointed out that incorporation of biochar in the soil not only improves soil properties and immobilizes heavy metals, but it also helps mitigate carbon emissions by sequestering carbon in a stable form.

Biochar quality from wood and grasses, expressed in terms of aromaticity and crystallinity, was investigated as a function of the charring temperature between 100°C to 700°C [128]. Biomass was shown to undergo progressive structural transformation with temperature increase, which was classified into four stages: transition char, amorphous char, composite char, and lastly, turbostratic char. They concluded that the level of char transformation correlates

strongly with its persistence (stability) in the soil, with more aromatic char produced at higher temperatures exhibiting more stable characteristics. Similarly, pyrolysis temperatures were shown to correlate inversely with the biochar degradation in the soil [129]. The residual cellulose and hemicellulose in the biochar matrix under low-severity conversion are easily degraded and lost in the soil compared to aromatic biochar produced under elevated temperatures (525°C to 575°C). Higher temperatures for pyrolysis/biochar production, however, reduce the recoverable biochar mass. The influence of air injection during corn stover pyrolysis on the quality of biochar as a soil amendment was investigated [130]. Chars produced at 0% and 10% air injection showed higher organic carbon content until week 6 of the study where differences became insignificant. This observation was explained by the presence of more biologically available carbon in the 0% and 10% chars that was utilized during the first few weeks by the soil microorganisms. Inversely, extractable P started to increase in week 4, which was explained by the increased microbial activity that facilitated char decomposition and P demineralization.

Interest in using manure solids as biochar feedstock can be attributed to their high macro- and micro-nutrient contents, both of which are necessary for plant growth. The characteristics of biochar produced at 380°C from various biomass feedstocks were studied [131]. Cattle sludge biochar exhibited the highest electrical conductivity, 2.90 mS cm^{-1}, water retention capacity, 294%, organic N, 0.25 mg kg^{-1}, and phosphate, 0.76 mg kg^{-1}. Swine manure and woodchip biochars were soil incorporated to monitor the carbon emissions [132]. Biochar-treated soils maintained the soil organic C with CO_2 emissions equal to those from control soil. Furthermore, biochar application facilitated a reduction in carbon emissions with the application of manure digestate when compared with biochar-free soils. The largest drop in Olsen P levels

was reported for soils amended with both manure digestate and manure biochar but they still maintained more than 50 mg $_{Olsen\ P}$ kg^{-1}.

The influence of temperature on the quality of biochar produced from swine manure solids was studied [133]. A decrease in char yields from 62.3% to 36.4% of original mass was reported with the increase of charring temperature from 350°C to 700°C. A transformation of the char carbon was also reported. It resulted from the loss of alcoholic, paraffinic, and carboxylate carbon and a corresponding increase in aromatic and carbonyl carbon. Biochar from manure gasification in a circulating fluidized bed (at 730°C), and acid-treated ash produced from manure combustion were studied comparatively as phosphorous (P) fertilizers [134]. No discernible differences were observed between the two types of thermal residue (ashes and chars) on P availability in the soil. Results also indicated that gasification char can be used as a phosphate fertilizer to maintain soil P levels but not as a starter P fertilizer.

Physical characteristics of biochar generated from swine manure solids at different temperatures, 400°C to 800°C, at slow pyrolysis conditions (no air) were investigated [135]. The yields of biochar ranged from 39 wt. % at 400°C to 34 wt. % at 800°C. The pH of the biochar solution (5 g biochar in 10 mL deionized water) increased from 7.5 to 11.4 with the increase in pyrolysis temperature from 400°C to 800°C. Increasing pyrolysis temperature to 800°C was found to increase biochar P content, porosity, and surface area to reach 7.7 wt. %, 0.13, and 63 m^2 g^{-1}, respectively.

Most biochar literature report adopting torrefaction, slow pyrolysis (carbonization), or flash pyrolysis as the conversion technology. Few studies, however, have investigated the quality of gasification char as a potential biochar despite the maturity of gasification as a conversion technology [136]. Additionally, although pyrolysis-derived biochar contains more char carbon in

44

principal, studies showed that a fraction of this carbon is raw unconverted cellulosic carbon that is readily degraded by microorganisms upon soil application. This, in consequence, results in a rapid carbon loss from the biochar reducing its sequestration potential. Given also that bio-oil studies point to the challenges of storage, transportation, pretreatment and upgrading, the energetics and economics of biochar production via pyrolysis would be further constrained.

7. Conclusions

- Increases in scale and aggregation of swine production farms, while economically advantageous, have resulted in manure accumulation problems in high production regions.

- Various manure management technologies, i.e., biological, and thermal, are in practice to utilize swine manure while mitigating its negative impacts on surrounding ecosystems.

- Thermochemical conversion technologies are mature, stable and modular but, so far, underutilized in manure management.

- Gasification of swine manure solids, although under investigation, can overcome the challenges associated with high-ash feedstock, and can also generate a biochar stream.

- A need for studies of the conversion kinetics of swine manure solids, namely thermal decomposition kinetics, was recognized and addressed in the following studies (Chapters 2, 3, and 4).

- There is a need for more comprehensive assessments of environmental impacts of thermochemical conversion as a manure management strategy (Chapter 6).

8. References

[1] Popkin BM. Urbanization, Lifestyle Changes and the Nutrition Transition. World Dev 1999; 27: 1905-16.

[2] Honeyman M. Sustainability issues of US swine production. J Anim Sci 1996; 74: 1410-7.

[3] FAO. Food and Agriculture Organization Statistical Database (FAOSTAT), Online at: http://faostat.fao.org/site/368/DesktopDefault.aspx?PageID=368#ancor [Last accessed: January 27, 2015].

[4] Gillespie JM, Davis CG, Rahelizatovo NC. An evaluation of US hog producer preferences toward autonomy. J. Agr. Appl. Econ. 2004; 36: 575-90.

[5] American Society of Agricultural and Biological Engineers (ASABE). Standard D3843.2-Manure Production and Characteristics 2005.

[6] Grimes G, Plain RL. US hog marketing contract study. Agricultural Economics publications (MU) 2009.

[7] USDA-NASS. Overview of the U.S. Hog Industry 2009.

[8] Honeyman MS, Pirog R, Huber G, Lammers P, Hermann J. The United States pork niche market phenomenon. J Anim Sci 2006; 84: 2269-75.

[9] USDA- NASS. Quarterly Hogs and Pigs December 2012; 1949-1921.

[10] OECD, Food and Agriculture Organization of the United Nations. OECD-FAO Agricultural Outlook 2011: Organisation for Economic Co-operation and Development; 2011.

[11] Tilman D, Cassman KG, Matson PA, Naylor R, Polasky S. Agricultural sustainability and intensive production practices. Nature 2002; 418: 671-7.

[12] USDA- NASS. Overview of the U.S. Hog Industry October 2009; Hg 9 (10-09).

[13] USDA- NASS. Arkansas Hog and Pig Report December 2011.

[14] Jongbloed A, Mroz Z, Kemme P. The effect of supplementary Aspergillus niger phytase in diets for pigs on concentration and apparent digestibility of dry matter, total phosphorus, and phytic acid in different sections of the alimentary tract. J Anim Sci 1992; 70: 1159-68.

[15] Traylor S, Cromwell G, Lindemann M, Knabe D. Effects of level of supplemental phytase on ileal digestibility of amino acids, calcium, and phosphorus in dehulled soybean meal for growing pigs. J Anim Sci 2001; 79: 2634-42.

[16] Wing S, Cole D, Grant G. Environmental injustice in North Carolina's hog industry. Environ Health Perspect 2000; 108: 225.

[17] Hoff SJ, Bundy DS, Nelson MA, Zelle BC, Jacobson LD, Heber AJ, et al. Emissions of ammonia, hydrogen sulfide, and odor before, during, and after slurry removal from a deep-pit swine finisher. J Air Waste Manage Assoc 2006; 56: 581-90.

[18] Moody L, Burns R, Muhlbauer R. Literature Review: Deep Pit Swine Facility Fires and Explosions: Sources, Occurences, Factors, and Management. Report to National Pork Board, 2009, online at: http://old.pork.org/filelibrary/researchdocuments/09-252-burns-isu.pdf [Last accessed: January 27, 2015].

[19] Huang H, Miller GY, Ellis M, Funk T, Zhang Y, Hollis G, and Heber A. Odor management in swine finishing operations: cost effectiveness. JFAE 2004; 2: 130-5.

[20] Buiter JJ, Hoff SJ. Ammonia distribution in a pit-ventilated confinement building: one-half scale model study. Trans ASAE 1998; 41: 1817.

[21] Hatfield J, Brumm M, Melvin S. Swine manure management. Agricultural utilization of municipal, animal, and industrial waste.USDA-ARS, Washington, DC 1993: 40-57.

[22] Sweeten J, Miner R, Tengman C. Fact sheet# 1 A Brief History and Background of the EPA CAFO Rule 2003. MidWest Plan Service, Iowa State University, Ames, Iowa 50011-3080.

[23] Bernal MP, Sánchez-Monedero MA, Paredes C, Roig A. Carbon mineralization from organic wastes at different composting stages during their incubation with soil. Agric Ecosyst Environ 1998; 69: 175-89.

[24] Finstein M, Miller F, Strom P. Monitoring and evaluating composting process performance. Journal (Water Pollution Control Federation) 1986: 272-8.

[25] Tiquia S, Richard T, Honeyman M. Effect of windrow turning and seasonal temperatures on composting of hog manure from hoop structures. Environ Technol 2000; 21: 1037-46.

[26] Sadaka SS, Richard TL, Loecke TD, Liebman M. Determination of Compost Respiration Rates Using Pressure Sensors. Compost Sci Util 2006; 14: 124-31.

[27] Gamroth MJ. . Composting: an alternative for livestock manure management and disposal of dead animals 2012. Oregon State University Extension Service, online at: http://ir.library.oregonstate.edu/xmlui/bitstream/handle/1957/29173/em8825.pdf [Last updated: January 27, 2015].

[28] Gajalakshmi S, Abbasi SA. Solid Waste Management by Composting: State of the Art. Critical Reviews in Environmental Science & Technology 2008; 38: 311-400.

[29] Lau AK, Lo KV, Liao PH, Yu JC. Aeration experiments for swine waste composting. Bioresour Technol 1992; 41: 145-52.

[30] Sadaka S, El-Taweel A. Effects of aeration and C: N ratio on household waste composting in Egypt. Compost Sci Util 2003; 11: 36-40.

[31] Huang G, Wu Q, Wong J, Nagar B. Transformation of organic matter during co-composting of pig manure with sawdust. Bioresource Technol 2006; 97: 1834-42.

[32] Bernal M, Alburquerque J, Moral R. Composting of animal manures and chemical criteria for compost maturity assessment. A review. Bioresource Technol 2009; 100: 5444-53.

[33] Ahn HK, Mulbry W, White J, Kondrad S. Pile mixing increases greenhouse gas emissions during composting of dairy manure. Bioresource Technol 2011; 102: 2904-9.

[34] U.S. Environmental Protection Agency (EPA). Inventory of U.S. Greenhouse Gas Emissions and Sinks: 1990- 2011 April 2013; EPA 430-R-13-001. Online at: http://www.epa.gov/climatechange/Downloads/ghgemissions/US-GHG-Inventory-2013-Main-Text.pdf [Last accessed: January 27, 2015].

[35] Wang Q, Kuninobu M, Ogawa HI, Kato Y. Degradation of volatile fatty acids in highly efficient anaerobic digestion. Biomass Bioenerg 1999; 16: 407-16.

[36] Ahring BK, Sandberg M, Angelidaki I. Volatile fatty acids as indicators of process imbalance in anaerobic digestors. Appl Microbiol Biotechnol 1995; 43: 559-65.

[37] Chen Hanping, Li Bin, Yang Haiping, Yang Guolai, Zhang Shihong. Experimental investigation of biomass gasification in a fluidized bed reactor. Energy Fuels 2008; 22: 3493-8.

[38] Angelidaki I, Ahring B. Thermophilic anaerobic digestion of livestock waste: the effect of ammonia. Appl Microbiol and Biotechnol 1993; 38: 560-4.

[39] Hansen KH, Angelidaki I, Ahring BK. Anaerobic digestion of swine manure: inhibition by ammonia. Water Res 1998; 32: 5-12.

[40] Wu X, Yao W, Zhu J, Miller C. Biogas and CH_4 productivity by co-digesting swine manure with three crop residues as an external carbon source. Bioresour Technol 2010; 101: 4042-7.

[41] Lyberatos G, Skiadas I. Modelling of anaerobic digestion–a review. Global Nest Int J 1999; 1: 63-76.

[42] Gallert C, Winter J. Mesophilic and thermophilic anaerobic digestion of source-sorted organic wastes: effect of ammonia on glucose degradation and methane production. Appl Microbiol Biotechnol 1997; 48: 405-10.

[43] Vindis P, Mursec B, Janzekovic M, Cus F. The impact of mesophilic and thermophilic anaerobic digestion on biogas production. JAMME 2009; 36: 192-8.

[44] Chen Y, Cheng JJ, Creamer KS. Inhibition of anaerobic digestion process: a review. Bioresour Technol 2008; 99: 4044-64.

[45] Rajagopal R, Massé DI, Singh G. A critical review on inhibition of anaerobic digestion process by excess ammonia. Bioresour Technol 2013; 143: 632-41.

[46] U.S. Environmental Protection Agency (EPA), AgStar Program. Operating Anaerobic Digester Projects, last updated: Novemeber 2014 http://www.epa.gov/agstar/projects/index.html#database [last accessed: January 27, 2015].

[47] Mason DM, Gandhi KN. Formulas for calculating the calorific value of coal and coal chars: Development, tests, and uses. Fuel Process Technol 1983; 7: 11-22.

[48] Zhang Y, Li B, Li H, Liu H. Thermodynamic evaluation of biomass gasification with air in autothermal gasifiers. Thermochimica Acta 2011; 519: 65-71.

[49] Cordero T, Marquez F, Rodriguez-Mirasol J, Rodriguez J. Predicting heating values of lignocellulosics and carbonaceous materials from proximate analysis. Fuel 2001; 80: 1567-71.

[50] Sheng C, Azevedo J. Estimating the higher heating value of biomass fuels from basic analysis data. Biomass Bioenerg 2005; 28: 499-507.

[51] Hjorth M, Christensen KV, Christensen ML, Sommer SG. Solid–liquid separation of animal slurry in theory and practice. A review. Agron Sustain Dev 2010; 30: 153-80.

[52] Ro KS, Cantrell KB, Hunt PG. High-temperature pyrolysis of blended animal manures for producing renewable energy and value-added biochar. Ind Eng Chem Res 2010; 49: 10125-31.

[53] Sweeten JM, Korenberg J, LePori WA, Annamalai K, Parnell CB. Combustion of cattle feedlot manure for energy production. Energy Agric 1986; 5: 55-72.

[54] Jenkins B, Baxter L, Miles Jr T, Miles T. Combustion properties of biomass. Fuel Process Technol 1998; 54: 17-46.

[55] Energie Centrum Nederland (ECN), 2007. Phyllis, The composition of biomass and waste. Available online at: www.ecn.nl/phyllis2 [Last accessed: January 27, 2015].

[56] Miles TR, Miles Jr TR, Baxter LL, Bryers RW, Jenkins BM, Oden LL. Boiler deposits from firing biomass fuels. Biomass Bioenerg 1996; 10: 125-38.

[57] Saidur R, Abdelaziz E, Demirbas A, Hossain M, Mekhilef S. A review on biomass as a fuel for boilers. Renewable and Sustainable Energy Reviews 2011; 15: 2262-89.

[58] Yin C, Rosendahl LA, Kær SK. Grate-firing of biomass for heat and power production. Prog Energy Combust Sci 2008; 34: 725-54.

[59] Komiyama T, Kobayashi A, Yahagi M. The chemical characteristics of ashes from cattle, swine and poultry manure. J Mater Cycles Waste Manage 2013; 15: 106-10.

[60] Thygesen A, Wernberg O, Skou E, Sommer SG. Effect of incineration temperature on phosphorus availability in bio-ash from manure. Environ Technol 2011; 32: 633-8.

[61] Petrus L, Noordermeer MA. Biomass to biofuels, a chemical perspective. Green Chem 2006; 8: 861-7.

[62] Yung MM, Jablonski WS, Magrini-Bair KA. Review of catalytic conditioning of biomass-derived syngas. Energy Fuels 2009; 23: 1874-87.

[63] Boerrigter H, den Uil H, Calis H. Green diesel from biomass via Fischer-Tropsch synthesis: new insights in gas cleaning and process design. Paper presented at: Pyrolysis and gasification of Biomass and waste, Expert Meeting, 30 September – 1 October 2002: 371-83.

[64] Tijmensen MJ, Faaij AP, Hamelinck CN, van Hardeveld MR. Exploration of the possibilities for production of Fischer Tropsch liquids and power via biomass gasification. Biomass Bioenerg 2002; 23: 129-52.

[65] Higman C, Van der Burgt M. Gasification: Gulf Professional Publishing; 2003.

[66] Lv P, Xiong Z, Chang J, Wu C, Chen Y, Zhu J. An experimental study on biomass air–steam gasification in a fluidized bed. Bioresour Technol 2004; 95: 95-101.

[67] González J, Román S, Bragado D, Calderón M. Investigation on the reactions influencing biomass air and air/steam gasification for hydrogen production. Fuel Process Technol 2008; 89: 764-72.

[68] J Prins M, J Ptasinski K, JJG Janssen F. Thermodynamics of gas-char reactions: first and second law analysis. Chem Eng Sci 2003; 58: 1003-11.

[69] Cairns E, Tevebaugh A. CHO Gas Phase Compositions in Equilibrium with Carbon, and Carbon Deposition Boundaries at One Atmosphere. J Chem Eng Data 1964; 9: 453-62.

[70] Zainal Z, Rifau A, Quadir G, Seetharamu K. Experimental investigation of a downdraft biomass gasifier. Biomass Bioenerg 2002; 23: 283-9.

[71] Mevissen N, Schulzke T, Unger CA. Thermodynamics of autothermal wood gasification. Environ prog sustain energy 2009; 28: 347-54.

[72] Reed T, Reed TB, Das A, Das A. Handbook of biomass downdraft gasifier engine systems: Biomass Energy Foundation; 1988.

[73] Balat M, Balat M, Kırtay E, Balat H. Main routes for the thermo-conversion of biomass into fuels and chemicals. Part 2: Gasification systems. Energy convers manage 2009; 50: 3158-68.

[74] Di Blasi C, Signorelli G, Portoricco G. Countercurrent fixed-bed gasification of biomass at laboratory scale. Ind Eng Chem Res 1999; 38: 2571-81.

[75] Gai C, Dong Y. Experimental study on non-woody biomass gasification in a downdraft gasifier. Int J Hydrogen Energy 2012; 37: 4935-44.

[76] Baker E, Brown M, Elliott D, Mudge L. Characterization and treatment of tars from biomass gasifiers 1988. Denver, CO: AIChE 1988 Summer National Meeting; 1–11.

[77] Roy PC, Datta A, Chakraborty N. Assessment of cow dung as a supplementary fuel in a downdraft biomass gasifier. Renew Energ 2010; 35: 379-86.

[78] Gautam G, Adhikari S, Brodbeck C, Bhavnani S, Fasina O, Taylor S. Gasification of wood chips, agricultural residues, and waste in a commercial downdraft gasifier. Trans ASABE 2011; 54: 1801-7.

[79] Sadaka SS, Ghaly A, Sabbah M. Two phase biomass air-steam gasification model for fluidized bed reactors: Part I—model development. Biomass Bioenerg 2002; 22: 439-62.

[80] Gómez-Barea A, Leckner B. Modeling of biomass gasification in fluidized bed. Prog Energy Combust Sci 2010; 36: 444-509.

[81] Raman KP, Walawender WP, Fan L. Gasification of feedlot manure in a fluidized bed reactor. The effect of temperature. Ind Eng Chem Proc DD 1980; 19: 623-9.

[82] Herguido J, Corella J, Gonzalez-Saiz J. Steam gasification of lignocellulosic residues in a fluidized bed at a small pilot scale. Effect of the type of feedstock. Ind Eng Chem Res 1992; 31: 1274-82.

[83] Kaewluan S, Pipatmanomai S. Potential of synthesis gas production from rubber wood chip gasification in a bubbling fluidised bed gasifier. Energy convers manage 2011; 52: 75-84.

[84] Campoy M, Gómez-Barea A, Villanueva AL, Ollero P. Air− Steam Gasification of Biomass in a Fluidized Bed under Simulated Autothermal and Adiabatic Conditions. Ind Eng Chem Res 2008; 47: 5957-65.

[85] Xiao X, Le DD, Li L, Meng X, Cao J, Morishita K, et al. Catalytic steam gasification of biomass in fluidized bed at low temperature: Conversion from livestock manure compost to hydrogen-rich syngas. Biomass Bioenerg 2010; 34: 1505-12.

[86] Abanades JC, Anthony EJ, Lu DY, Salvador C, Alvarez D. Capture of CO2 from combustion gases in a fluidized bed of CaO. AIChE J 2004; 50: 1614-22.

[87] Zhang H, Xiao R, Huang H, Xiao G. Comparison of non-catalytic and catalytic fast pyrolysis of corncob in a fluidized bed reactor. Bioresour Technol 2009; 100: 1428-34.

[88] Van der Drift A, Van Doorn J, Vermeulen J. Ten residual biomass fuels for circulating fluidized-bed gasification. Biomass Bioenerg 2001; 20: 45-56.

[89] Li XT, Grace JR, Lim CJ, Watkinson AP, Chen HP, Kim JR. Biomass gasification in a circulating fluidized bed. Biomass Bioenerg 2004; 26: 171-93.

[90] Narvaez I, Orio A, Aznar MP, Corella J. Biomass gasification with air in an atmospheric bubbling fluidized bed. Effect of six operational variables on the quality of the produced raw gas. Ind Eng Chem Res 1996; 35: 2110-20.

[91] Zhang S, Cao J, Takarada T. Effect of pretreatment with different washing methods on the reactivity of manure char. Bioresour Technol 2010; 101: 6130-5.

[92] Arvelakis S, Gehrmann H, Beckmann M, Koukios EG. Preliminary results on the ash behavior of peach stones during fluidized bed gasification: evaluation of fractionation and leaching as pre-treatments. Biomass Bioenerg 2005; 28: 331-8.

[93] Ergudenler A, Ghaly A. Agglomeration of silica sand in a fluidized bed gasifier operating on wheat straw. Biomass Bioenerg 1993; 4: 135-47.

[94] Natarajan E, Öhman M, Gabra M, Nordin A, Liliedahl T, Rao A. Experimental determination of bed agglomeration tendencies of some common agricultural residues in fluidized bed combustion and gasification. Biomass Bioenerg 1998; 15: 163-9.

[95] Öhman M, Pommer L, Nordin A. Bed agglomeration characteristics and mechanisms during gasification and combustion of biomass fuels. Energy Fuels 2005; 19: 1742-8.

[96] Lahijani P, Zainal ZA. Gasification of palm empty fruit bunch in a bubbling fluidized bed: A performance and agglomeration study. Bioresour Technol 2011; 102: 2068-76.

[97] Fryda LE, Panopoulos KD, Kakaras E. Agglomeration in fluidised bed gasification of biomass. Powder Technol 2008; 181: 307-20.

[98] Weerachanchai P, Horio M, Tangsathitkulchai C. Effects of gasifying conditions and bed materials on fluidized bed steam gasification of wood biomass. Bioresour Technol 2009; 100: 1419-27.

[99] Morf P, Hasler P, Nussbaumer T. Mechanisms and kinetics of homogeneous secondary reactions of tar from continuous pyrolysis of wood chips. Fuel 2002; 81: 843-53.

[100] Evans RJ, Milne TA. Molecular characterization of the pyrolysis of biomass. Energy Fuels 1987; 1: 123-37.

[101] Vreugdenhil B, Zwart R, Neeft JPA. Tar formation in pyrolysis and gasification: Energieonderzoek Centrum Nederland (ECN); 2009. Online at: https://www.ecn.nl/publications/ECN-E--08-087 [Last accessed: January 27, 2015].

[102] Elliott DC. Relation of reaction time and temperature to chemical composition of pyrolysis oils, in Pyrolysis Oils from Biomass: Producing, Analyzing, and Upgrading. American Chemical Society (ACS) 1988.

[103] Basu P. Biomass gasification, pyrolysis and torrefaction: practical design and theory: Academic press; 2013.

[104] Phuphuakrat T, Namioka T, Yoshikawa K. Tar removal from biomass pyrolysis gas in two-step function of decomposition and adsorption. Appl Energ 2010; 87: 2203-11.

[105] Simell PA, Hirvensalo EK, Smolander VT, Krause AOI. Steam reforming of gasification gas tar over dolomite with benzene as a model compound. Ind Eng Chem Res 1999; 38: 1250-7.

[106] Jess A. Mechanisms and kinetics of thermal reactions of aromatic hydrocarbons from pyrolysis of solid fuels. Fuel 1996; 75: 1441-8.

[107] Sutton D, Kelleher B, Ross JRH. Review of literature on catalysts for biomass gasification. Fuel Process Technol 2001; 73: 155-73.

[108] Wang Q, Endo T, Aparu P, Kurogawa H, Wang Q. Study on biomass tar reduction by ash and fluidizing medium in a heterogeneous reaction. International Journal of Sustainable Development and Planning 2014; 9: 669-79.

[109] Bridgwater A, Meier D, Radlein D. An overview of fast pyrolysis of biomass. Org Geochem 1999; 30: 1479-93.

[110] Meier D, Faix O. State of the art of applied fast pyrolysis of lignocellulosic materials—a review. Bioresour Technol 1999; 68: 71-7.

[111] Mohan D, Pittman CU, Steele PH. Pyrolysis of wood/biomass for bio-oil: a critical review. Energy Fuels 2006; 20: 848-89.

[112] Mullen CA, Boateng AA. Chemical Composition of Bio-oils Produced by Fast Pyrolysis of Two Energy Crops. Energy Fuels 2008; 22: 2104-9.

[113] Maggi R, Delmon B. Comparison between 'slow'and 'flash'pyrolysis oils from biomass. Fuel 1994; 73: 671-7.

[114] Demirbaş A. Mechanisms of liquefaction and pyrolysis reactions of biomass. Energy convers manage 2000; 41: 633-46.

[115] Diebold JP. A review of the chemical and physical mechanisms of the storage stability of fast pyrolysis bio-oils: National Renewable Energy Laboratory (NREL), Golden, CO; 2000.

[116] Elliott DC. Historical developments in hydroprocessing bio-oils. Energy Fuels 2007; 21: 1792-815.

[117] Huber GW, Iborra S, Corma A. Synthesis of transportation fuels from biomass: chemistry, catalysts, and engineering. Chem Rev 2006; 106: 4044-98.

[118] Rioche C, Kulkarni S, Meunier FC, Breen JP, Burch R. Steam reforming of model compounds and fast pyrolysis bio-oil on supported noble metal catalysts. Appl Catal, B 2005; 61: 130-9.

[119] Vagia EC, Lemonidou AA. Thermodynamic analysis of hydrogen production via steam reforming of selected components of aqueous bio-oil fraction. Int J Hydrogen Energy 2007; 32: 212-23.

[120] Takanabe K, Aika K, Seshan K, Lefferts L. Sustainable hydrogen from bio-oil—Steam reforming of acetic acid as a model oxygenate. J Catal 2004; 227: 101-8.

[121] Kim S, Agblevor FA, Lim J. Fast pyrolysis of chicken litter and turkey litter in a fluidized bed reactor. J Ind Eng Chem 2009; 15: 247-52.

[122] Mante OD, Agblevor FA. Parametric study on the pyrolysis of manure and wood shavings. Biomass Bioenerg 2011; 35: 4417-25.

[123] Cao J, Xiao X, Zhang S, Zhao X, Sato K, Ogawa Y, et al. Preparation and characterization of bio-oils from internally circulating fluidized-bed pyrolyses of municipal, livestock, and wood waste. Bioresour Technol 2011; 102: 2009-15.

[124] Bergman PC, Patrick CA, and Kiel JH. Torrefaction for biomass upgrading. Proc. 14th European Biomass Conference, Paris, France. 2005: 17-21.

[125] Qiu Y, Zheng Z, Zhou Z, Sheng GD. Effectiveness and mechanisms of dye adsorption on a straw-based biochar. Bioresour Technol 2009; 100: 5348-51.

[126] Sohi S, Krull E, Lopez-Capel E, Bol R. A review of biochar and its use and function in soil. Adv Agron 2010; 105: 47-82.

[127] Chan K, Van Zwieten L, Meszaros I, Downie A, Joseph S. Agronomic values of greenwaste biochar as a soil amendment. Soil Research 2008; 45: 629-34.

[128] Keiluweit M, Nico PS, Johnson MG, Kleber M. Dynamic molecular structure of plant biomass-derived black carbon (biochar). Environ Sci Technol 2010; 44: 1247-53.

[129] Bruun EW, Hauggaard-Nielsen H, Ibrahim N, Egsgaard H, Ambus P, Jensen PA, et al. Influence of fast pyrolysis temperature on biochar labile fraction and short-term carbon loss in a loamy soil. Biomass Bioenerg 2011; 35: 1182-9.

[130] Unger R, Killorn R. Effect of Three Different Qualities of Biochar on Selected Soil Properties. Communnications in Soil Science and Plant Analysis 2011; 42: 2274-83.

[131] Shinogi Y, Yoshida H, Koizumi T, Yamaoka M, Saito T. Basic characteristics of low-temperature carbon products from waste sludge. Advances in Environmental Research 2003; 7: 661-5.

[132] Marchetti R, Castelli F, Orsi A, Sghedoni L, Bochicchio D. Biochar from swine manure solids: influence on carbon sequestration and Olsen phosphorus and mineral nitrogen dynamics in soil with and without digestate incorporation. Italian Journal of Agronomy 2012; 7: e26.

[133] Cantrell KB, Martin JH. Stochastic state-space temperature regulation of biochar production. Part II: Application to manure processing via pyrolysis. Journal of the Science of Food and Agriculture 2012; 92: 490-5.

[134] Kuligowski K, Poulsen TG, Rubæk GH, Sørensen P. Plant-availability to barley of phosphorus in ash from thermally treated animal manure in comparison to other manure based materials and commercial fertilizer. Eur J Agron 2010; 33: 293-303.

[135] Tsai W, Liu S, Chen H, Chang Y, Tsai Y. Textural and chemical properties of swine-manure-derived biochar pertinent to its potential use as a soil amendment. Chemosphere 2012; 89: 198-203.

[136] Meyer S, Glaser B, Quicker P. Technical, economical, and climate-related aspects of biochar production technologies: a literature review. Environmental Science & Technology 2011; 45: 9473-83.

Chapter 3 Thermogravimetric Analysis of Swine Manure Solids Obtained From Farrowing, and Growing-Finishing Farms

Citation

1. Abstract

The modern trend of increasing the number of pigs at production sites led to a noticeable surplus of manure. Separation of manure solids provides an avenue for utilizing them via thermochemical conversion techniques. Therefore, the goal of this paper was to assess the physical and thermal properties of solid separated swine manure obtained from two different farms, i.e., farrowing, and growing-finishing, and to determine their pyrolysis kinetic parameters. Swine manure solids were dried and milled prior to assessing their properties. Differential and integral isoconversional methods (Friedman, and Flynn-Wall-Ozawa (FWO)) were used to determine the apparent activation energy as a function of the conversion ratio. Significant differences were observed in the proximate and ultimate composition between both manure types. The higher heating value (HHV) for the manure solids from farrowing, and growing-finishing farms reached 16.6 MJ kg^{-1} and 19.4 MJ kg^{-1}, respectively. The apparent activation energy computed using Friedman and FWO methods increased with the increase in the degree of conversion. Between 10% and 40% degrees of conversion, the average activation energies, using Friedman method, were 103 and 116 kJ mol^{-1} for the farrowing and growing-finishing manure

solids, respectively. The average activation energies calculated using FWO method between the same degrees of conversion (10% ~ 40%) were 98 and 104 kJ mol^{-1} for manure solids obtained from farrowing and growing-finishing farms, respectively. The findings in this study will assist in the effort to optimize thermochemical conversion processes to accommodate swine waste. This could, in turn, minimize swine production impacts on the surrounding ecologies and provide sustainable energy and biochar streams.

2. Introduction

Swine production is increasingly becoming the world's largest meat production enterprise. Global consumption of pork meat, currently at 110 million metric tons per year, exceeds beef and chicken meat consumption, 67 and 104 million metric tons, respectively [1]. The latest inventory puts the total number of U.S. hogs at 68.3 million head, 62.5 million of which are market hogs and 5.8 million head are breeding hogs [2]. Most swine production in the U.S., however, is clustered around feed production, i.e., corn growing regions, in few Midwestern states. Moreover, intensive livestock production replaced conventional farming which lead to increased productivity and a drop in the number of livestock operations [3]. Unintended consequence of these changes, however, is the large volumes of generated manure, which surpass the assimilative capacity of nearby fields. Using an estimate of daily manure productivity for growing-finishing hogs, i.e., 4.54 kg manure per head [4], shows that the inventory of market hogs alone produce 0.28 million metric tons of manure daily. Separating the nutrient-rich manure solids can offer an opportunity to utilize or transport the manure nutrients in a sustainable, environmentally safe manner.

In this process, the manure slurry is separated into a solids-rich fraction (containing 80% of the total solids) and a low-solids effluent, i.e., low in nutrients, which can be safely recycled to

clean the stalls, or applied to nearby fields. Separation systems include stationary and vibrating screens, belt presses, and screw presses [5]. The separated solids were shown to be a more suitable feedstock for anaerobic digestion than raw, diluted slurries [6]. Alternatively, the separated solids can be further dried and blended with coal or wood and converted to bioenergy sources via thermochemical processes [7, 8].

Thermochemical processes offer rapid disposal capabilities while generating a continuous stream of heat and/or gaseous and liquid fuels. The solids separation method applied was found to influence the energy content of the manure solids [9]. Mechanically separated solids were shown to be more favorable, in terms of energy content, when compared to chemically separated solids. The high energy density of swine manure, 17.9 to 19.3

MJ kg^{-1} (dry-basis) compared to dry poultry litter, 12.0 to 14.8 MJ kg^{-1} [10], or dry cattle manures: 6.3 to 16.6 MJ kg^{-1} [11], makes it a more suitable candidate for energy conversion. Despite its high energy density, however, swine manure solids contain ash minerals, typically between 10% and 20% of the dry weight, more than other biomass feedstocks with similar calorific value, i.e., wood or switchgrass. These ash residues were shown to be problematic to thermochemical conversion, especially at elevated temperatures, since they form oxides with low-melting temperatures that cause slagging and agglomeration [12]. In poultry litter and pinewood-bedding mixtures, separation of the fine particles was found to improve the litter fuel properties [13]. Additionally, low-temperature gasification and pyrolysis typically minimize the problematic qualities of the manure minerals.

Despite the variety of swine manure handling and separation strategies, only few studies looked into the decomposition kinetics of swine manure solids [14, 15]. Studying decomposition kinetics via thermogravimetric analysis offers insight into the behavior of the feedstock under

thermochemical conversion conditions. Several methods, i.e., model-fitting methods and isoconversional methods were developed to formulate the mathematical expression describing feedstock decomposition. Isoconversional methods (model-free methods) were shown to be more robust and reliable compared to model-fitting methods [16]. Oxidation kinetics for swine manure solids was determined using isoconversional methods, i.e., Vyazovkin method, and Flynn-Wall-Ozawa method [15]. No studies were found in the literature that used isoconversional methods to determine the pyrolysis kinetics of swine manure solids.

The goal of this study was to determine the pyrolysis kinetics of swine manure solids obtained from two different farms using two different isoconversional methods.

3. Materials and Methods

3.1. Swine manure collection

Swine manure solids were collected from two different hog farms in Arkansas. The first is a commercial breeding farm (farrowing) (2,450 head) in Yell County, whereas the second is a growing-finishing farm (818 head), in Washington County, that is part of the Dale Bumpers College of Agricultural, Food & Life Sciences at the University of Arkansas. The farrowing farm employs a two-step solids separation system, i.e., a mechanical screw press to separate the larger solids then a chemical separation step using flocculants to facilitate aggregation and sedimentation of finer solids. This separation system was installed in order to reduce the phosphorous loading of the aqueous effluent. Such measures are necessary in regions where the soil phosphorous levels are elevated. The surplus manure phosphorous, therefore, has to be moved off-farm. In this research, the manure studied was sampled from the solids separated in the first step, i.e., mechanically separated solids. In the growing-finishing farm, the effluent from the hog houses is pumped directly to a settling pond before it collects in a storage lagoon. No

mechanical or chemical separation is practiced in this farm. For the purpose of this study, the solids were collected directly from the settling pond using a sample collection bag. The sampling bag is made from fine-pored fabric fitted on a triangular metal frame. The settled solids were sampled from different parts of the pond, and then later mixed, to ensure representative sampling.

The swine manure solids were first oven-dried (72°C for 48 hours) to prepare the feedstock for subsequent steps, i.e., size-reduction (milling) and the various tests and analyses. The dried solids were ground using a cutting mill (Thomas Wiley Mill No.2, Swedesboro, NJ) fitted with a 1-mm (1,000 micron) mesh size screen.

3.2. Swine manure collection

The swine manure solids were first oven-dried (72°C for 48 hours) to prepare the feedstock for subsequent steps, i.e., size-reduction (milling) and the various tests and analyses. The dried solids were ground using a cutting mill (Thomas Wiley Mill No.2, Swedesboro, NJ) fitted with a 1-mm (1,000 micron) mesh size screen.

3.3. Swine manure characterization

All tests were done on triplicates except for the chemical composition, which was determined in one composite sample from each manure source in an analytical laboratory (Huffman laboratories, 4630 Indiana Street Golden, CO). The ash content was determined as the percentage of remaining weight after completely burning off dry samples at 750ºC [17] whereas the volatile matter content is the weight loss lost after holding the sample at 800ºC in an oxygen-free environment for 10 minutes. The calorific values were determined using oxygen bomb calorimetry (Parr instruments, Model 1341) according to standard [18].

3.4. Thermogravimetric analyses

A programmable thermogravimetric analyzer (Model TGA 4000, PerkinElmer, Inc. Waltham, MA) was used in this study to examine the decomposition behavior of the manure solids from both farms. Specifications of this analyzer are shown in Table 3-1. Before running the thermogravimetric analyses, weight and temperature calibrations were conducted according to the manufacturer instructions. Each manure source was analyzed at three different heating rates: 20, 30 and 40ºC min^{-1} with nitrogen as the purge gas (30 ml/min) in order to simulate pyrolysis conditions. The thermogravimetric analysis program ran according to the following steps:

1. Heating from 30ºC to 105°C in a nitrogen environment

2. Isothermal stage at a 105°C for 10 minutes

3. Heating from 105°C to 800°C at the specified heating rate

4. Isothermal stage at 800°C in an oxygen environment for 10 minutes

Step 2 was added to ensure samples were completely dry before pyrolysis. In each analysis, temperature and sample weight were continuously recorded at 1-second intervals. TGA sample size was kept at approximately 20 ± 2mg (mg=10^{-3} g) to avoid introducing diffusion-based variability. After each analysis, the sample holder (crucible) was thoroughly cleaned with methanol then completely burnt (purging oxygen at 800°C for 10 minutes) to eliminate any residues. The following section outlines the theory behind the methods used to extract the pyrolysis kinetics.

Table 3-1 . Specifications of thermogravimetric analyzer used

Temperature range (°C)	Room temperature to 1,000
Temperature accuracy (°C)	+/- 1
Temperature precision (°C)	+/- 0.8
Heating rate (°C min^{-1})	0.1-200

Max. sample weight (g)	1.5
Scale resolution (μg)	0.2
Scale accuracy(μg)	+/- 0.02%
Scale precision (μg)	+/- 0.01%

3.5. Theory

The degree of conversion (α) is defined as follows:

$$\alpha = \frac{W_o - W_t}{W_o - W_\infty} \qquad (1)$$

Where W_o, W_t, and W_∞ are the initial sample weight, the sample weight at time t, and the final

sample weight, respectively. The rate of conversion is expressed as follows:

$$\frac{d\alpha}{dt} = k\, f(\alpha) \qquad (2)$$

Where k is the decomposition rate constant, and $f(\alpha)$ is the reaction model, which expresses the

dependence of conversion rate on the conversion ratio. Using the Arrhenius formulation, the

rate constant can be expanded:

$$\frac{d\alpha}{dt} = A \exp\left(\frac{-E_a}{RT}\right) f(\alpha) \qquad (3)$$

Where A, E_a, and R are the frequency factor (pre-exponential coefficient), the activation energy,

and the universal gas constant, respectively. Under non-isothermal conditions, where the

heating rate is known, the sample temperature can be related to time using the following

relation:

$$T_t = T_o + \beta * t \qquad (4)$$

Where T_o is the initial temperature, and β is the heating rate. Using equation 4, the

conversion rate can be transformed into a temperature-derivative:

$$\frac{d\alpha}{dT} = \frac{A}{\beta} \exp\left(\frac{-E_a}{RT}\right) f(\alpha) \tag{5}$$

Rearranging equation 5 to separate the variables α and T, then integrating:

$$\int_0^\alpha \frac{d\alpha}{f(\alpha)} = \int_{T_o}^T \frac{A}{\beta} \exp\left(\frac{-E_a}{RT}\right) \cdot dT \tag{6}$$

Since $\int_0^{T_o} \frac{A}{\beta} \exp\left(\frac{-E_a}{RT}\right) \cdot dT = 0$, then

$$g(\alpha) = \int_0^T \frac{A}{\beta} \exp\left(\frac{-E_a}{RT}\right) \cdot dT \tag{7}$$

Thermogravimetric analysis methods target the determination of the kinetics triplicate, i.e., A, E_a, and $f(\alpha)$ or $g(\alpha)$. The methods that use equation (5) are referred to as differential methods whereas those using equation (7) are known as integral methods [19]. Some studies reported the use of a single analysis, one thermogravimetric experiment, to derive the reaction kinetics. A prerequisite to using this approach (model-fitting methods) is assuming a reaction model: $f(\alpha)$, or $g(\alpha)$ in order to extract the activation energy, and the frequency factor. This approach was found to produce erroneous activation energy values that are highly dependent on the assumed reaction model [20]. An alternative approach is the use of multiple thermogravimetric analyses performed at different heating rates, i.e., isoconversional methods, to determine the kinetic parameters.

3.6. Isoconversional methods

These methods are also known as "model-free methods" because they bypass the need for a specific reaction model in order to compute the decomposition parameters. The underlying basis in these methods is that, at any given conversion ratio (α), the rate of conversion is a function of the temperature alone. Therefore, under isoconversional methods, the activation

energy is in fact a range of values that are functions of corresponding conversion ratios (α) [21]. Two different methods were used to analyze the thermogravimetric data, one is differential, i.e., Friedman method [22] while the other is integral, Ozawa-Flynn-Wall method [23, 24]. Details of each method are shown below:

Friedman method

Starting with a re-arrangement of equation 6:

$$\beta \left(\frac{d\alpha}{dT} \right) = A \exp \left(-\frac{E_a}{RT} \right) f(\alpha) \qquad (8)$$

Then, taking the natural logarithm for both sides of equation (8) yields

$$ln \left(\beta \frac{d\alpha}{dT} \right) = \ln[Af(\alpha)] - \frac{E_a}{RT} \qquad (9)$$

For every analysis performed at a given heating rate, a set of $ln\ (\beta\ (d\alpha/dT))$ and 1/T pairs that correspond to different α values, i.e., $\alpha = 0.05, 0.10\ldots 0.85$ was collected. For each manure type, three data points, i.e., $ln(\beta(d\alpha/dT))$ and 1/T pairs, representing the same degree of conversion (α) under the studied heating rates were plotted and fitted to a straight line. The result is a family of straight lines, for each manure type, that represent the kinetics of decomposition at different degrees of conversion. The slope of each straight line, ($-E_a$/R), was used to compute the apparent activation energy E_a, while each intercept, $ln(A, f(\alpha))$ was a combined expression of frequency factor A and the reaction model $f(\alpha)$ at each degree of conversion.

The raw data of each analysis, i.e., sample weights and temperatures, was retrieved through the equipment software (Pyris™ Software-Version 11.0.0.0449, Perkin Elmer, Inc. Waltham, MA) then imported into MATLAB® R2013b (MathWorks, Inc. Natick, MA) where the differentiation, data filtering, and sampling was performed. Plotting $ln(\beta(d\alpha/dT))$ and 1/T pairs, and the determination of slope and intercept were carried out using Microsoft® Excel® 2010 (Microsoft Corp., Redmond, WA).

Ozawa-Flynn-Wall method

In this method, equation (7) was integrated then the Doyle's approximation [25] was applied

to the temperature integral. The resulting equation is:

$$\ln \beta = ln \left[\frac{AE_a}{Rg(\alpha)}\right] - 5.3305 - 1.052 \left(\frac{E_a}{RT}\right) \quad (10)$$

Alternately,

$$\ln \beta = ln \left[\frac{0.0048*AE_a}{Rg(\alpha)}\right] - 1.052 \left(\frac{E_a}{RT}\right) \quad\quad (11)$$

At each degree of conversion, i.e., α= 0.05, 0.10… 0.85, the three pairs of *ln β* and 1/T data

points, obtained from the three heating rates, were plotted and fitted to a straight line. The slope,

(-1.052 (E_a/R)), represents the apparent activation energy term, while the intercept is a coupled

expression of the reaction model in the integral form, *g(α)*, the apparent activation energy E_a, and

the frequency factor, *A*. The same software tools were used to analyze the thermogravimetric

data for this method.

4. Results and Discussions

4.1. Proximate and ultimate analyses

Table 3-2 lists the proximate and ultimate analyses of the two types of swine manure

solids. The volatile matter in the growing-finishing manure solids were noticeably higher, 7.9%

more, than in the farrowing farm solids. The ash content in both farms was slightly below values

reported in the literature, i.e., 18% to 25% dry basis [7] but close to reported ash content under

mechanical separation, i.e., 9% [9]. The nitrogen content in the farrowing manure was more than

6 times that in the growing-finishing manure. This elevated nitrogen content, 12%, could be

explained by the high amounts of animal hair observable in the solids recovered after screw press

separation. Keratin, the main ingredient of animal hair, is a polymer of various amino acids. The

percentage of nitrogen in amino acids typically varies between 13.4% and 19.3%, by weight, based on the type of amino acid [26].

Table 3-2 Characteristics of swine manure solids by source

	Farrowing Farm	Growing-finishing Farm
*Proximate analysis, %db**		
Volatile solids	63.04 (0.63)	70.95 (0.47)
Fixed carbon**	22.99 (0.96)	18.15 (0.66)
Ash content	13.97 (0.73)	10.90 (0.46)
Ultimate analysis, %db		
C	43.8	46.4
H	5.5	6.9
O*	23.7	33.4
N	12.0	1.8
S	1.0	0.6
HHV, MJ/kg	16.62 (0.32)	19.39 (0.05)
Stoichiometry	$CH_{1.50}O_{0.24}N_{0.41}S_{0.01}$	$CH_{1.78}O_{0.56}N_{0.03}S_{0.01}$

* Dry, weight basis
** By difference

Screw press separators are generally known to be more effective in separating out larger solids from the manure slurry [5], which explains the increased amount of animal hair in the mechanically separated solids. On the other hand, the nitrogen content of growing-finishing manure solids, 1.8% by weight, was slightly below the reported values of nitrogen content in manure solids, i.e., between 2% to 5% by weight. No animal hair was observed in the solids collected from the growing-finishing farm. Carbon and hydrogen contents in growing-finishing manure solids were higher than that of farrowing manure solids by 2.6 and 1.3 points, respectively. Both manure solids, however, exhibited levels of carbon comparable to reported values in the literature.

The calorific content of manure solids collected from the growing-finishing farm was noticeably higher than the farrowing farm manure solids. This difference could be attributed to

the differences in carbon and hydrogen contents between manure types. A correlation to predict

biomass calorific value using the elemental composition [27] was implemented using the

elemental composition for both farms listed in Table 3-2. The predicted heating value for the

growing-finishing and the farrowing manure solids were 18.9 MJ kg^{-1}, and 16.5 MJ kg^{-1},

respectively. The presence of keratin in the farrowing farm manure solids might be responsible

for the noticeably low calorific value observed.

4.2. Thermogravimetric analysis

Figure 3-1 details the weight loss profiles for manure solids from both farms, in an inert

atmosphere, as influenced by sample temperature and heating rate. The focus in this study was

pyrolytic decomposition, which takes place above 100°C. As a result, the drying step was not

included in the kinetic analysis. Increasing the sample-heating rate shifted the decomposition

temperatures higher, which is in agreement with most thermogravimetry studies. The weight loss

in all samples appeared to proceed in three consecutive steps. In the first step, which took place

between 100°C and 250°C, the sample mostly heated up and only marginal weight loss occurred.

The second stage (280°C - 420°C) is the active pyrolysis as the easily degradable organic

components are devolatilized in sequence. The final stage, known as the passive pyrolysis stage,

from 420°C to 800°C, is a slow-decomposition phase in which the remaining sample that was

carbonized into stable and complex organic species in the active pyrolysis step, partially

devolatilized. At the end of the pyrolysis test, the remaining weight represented the combined

ash and fixed carbon contents.

The weight loss in the growing-finishing manure solids proceeded faster than in the farrowing

farm solids as evidenced by the temperatures at which the sample weight reached 50% of the

starting weight, 381°C and 427°C, respectively. In all samples, most of the weight loss occurred

between 280°C and 380°C, the temperature range typically associated with both hemicellulose

(220°C - 315°C) and cellulose (315°C - 400°C) decomposition [28]. From a compositional

standpoint, however, swine manure solids contain less structural carbohydrates (cellulose) than

lignocellulosic materials such as wood or grasses. In addition, swine manure solids contain

higher amounts of protein and lipids [29]. These structural differences yielded decomposition

temperatures and decomposition rates that are different from those observed in

thermogravimetric tests of typical biomass.
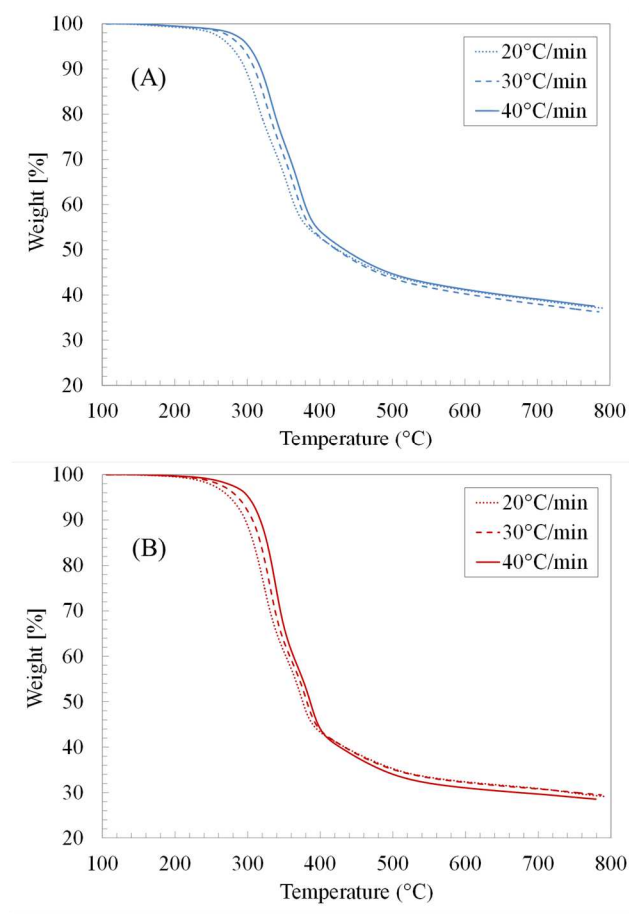
Figure 3-1 Weight loss during thermogravimetric analysis (TGA) for swine manure solids from (A) farrowing farm, and (B) growing-finishing farm in nitrogen environment

Another point of difference is the ratio of cellulose to hemicellulose in wood and grasses versus that in manure solids, and how this difference influenced decomposition rate curves. In wood and cellulosic material weight-loss derivative curves, one prominent peak is usually observed which corresponds to cellulose decomposition. The cellulose peak is usually preceded by a smaller unseparated peak representing hemicellulose decomposition (typically referred to as the hemicellulose shoulder). The cellulose-to-hemicellulose ratios in wood, typically around 1.56 [30], confirm the DTA observations. In swine manure solids, however, cellulose/hemicellulose ratios were much lower, reportedly ranged between 0.25 and 0.81 depending on the manure collection and solids separation strategy [31]. In all DTA curves (Figure 3-2), two overlapping peaks were noticeable between 300°C and 400°C. In the growing-finishing farm samples, the height of the first peak was significantly more than the second peak. This first peak is attributable to hemicellulose decomposition as well as the decomposition of both protein (keratin) and lipids [32, 33]. In the farrowing farm manure solids, the maximum decomposition rate occurred between 318°C and 335°C, a temperature range associated with the hemicellulose and keratin decomposition. The maximum decomposition rates in the manure solids from the farrowing and the growing-finishing farms are 0.55 and 0.83% °C^{-1}, respectively. These distinct differences in the DTA curves for swine manure solids from different farms further confirm the earlier observations that various compositional ingredients: starch, keratin, lipids, and cellulose are not uniform. These observations can help in customizing the feedstock to suit the thermochemical conversion conditions.
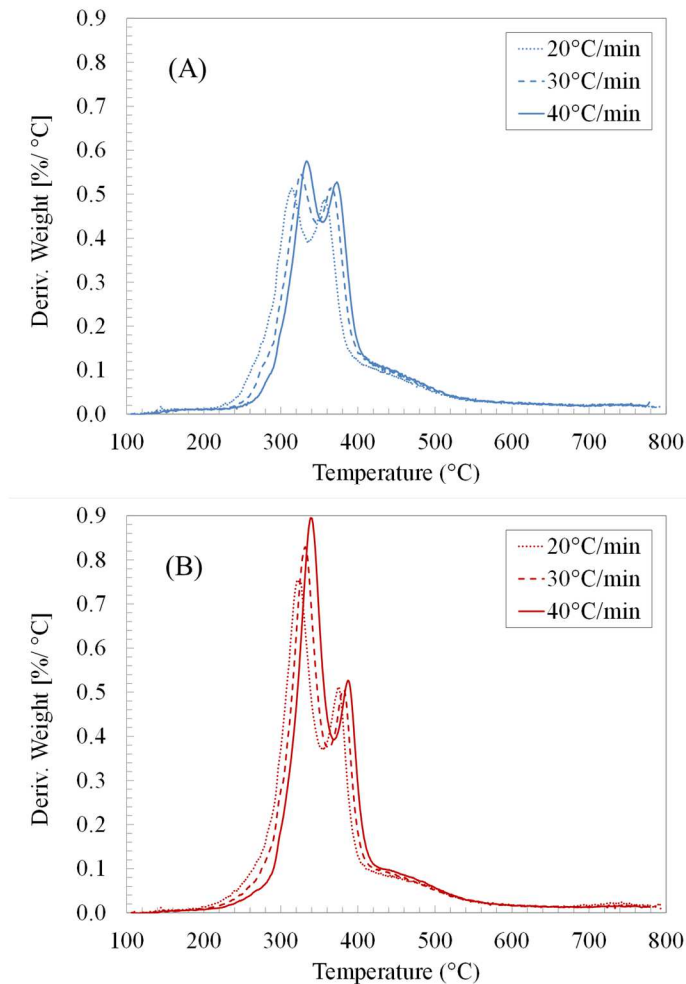
Figure 3-2 Derivative of thermogravimetric analysis (DTA) curves for manure solids from (A) farrowing farm, and (B) growing-finishing farm in nitrogen environment

4.3. Pyrolysis kinetics

Decomposition kinetics during active pyrolysis stage (T ≤ 420°C) were determined using two isoconversional methods, i.e., Friedman and Flynn-Wall-Ozawa (FWO) at degrees of conversion (α) ranging from 0.05 to 0.85. The isoconversional lines used in both methods are shown in Figure 3-3. The slopes of these lines, $(-E_a/R)$ in the Friedman method and -1.052 (E_a/R) in the FWO method, were used to extract the apparent activation energy (E_a) as shown in Table 3-3 and Table 3-4.

Figure 3-3 (A) shows the transition in the slopes of isoconversional lines that corresponded to the sequential devolatilization of sample components. The apparent activation energy computed using Friedman and FWO methods increased with the increase in the degree of conversion. Between 10% and 40% degrees of conversion, the average activation energy, using Friedman method, was 103 kJ mol^{-1} and 116 kJ mol^{-1} for the farrowing and growing-finishing manure solids, respectively. These values represent activation energies associated with the first decomposition peak (hemicellulose, and lipids pyrolysis). On the other hand, the average apparent activation energies during the cellulose decomposition, taken to be the weight loss between $\alpha = 60\%$ and 80%, was 177 and 199 kJ mol^{-1} for the farrowing and the growing-finishing farms, respectively.

Similarly, the slopes of the isoconversional lines, Figure 3-3 (B), show the apparent activation energies using FWO method at the same degrees of conversion. The average apparent activation energies of manure solids obtained from farrowing farm reached 98 kJ/mol between $\alpha = 10\%$ and 40%. Whereas the growing-finishing manure solids had an average apparent activation energy of 104 kJ/mol. Similar to the observations in Friedman method, average apparent activation energies using FWO method corresponding to the second decomposition stage ($\alpha = 60\% - 80\%$), increased to 173 kJ/mol for the farrowing manure solids, and 188 kJ mol^{-1} in the growing-finishing manure solids. These observations are similar to findings in other studies where average activation energies for hemicellulose and cellulose pyrolysis, using FWO and Friedman methods, were found to be 110 kJ mol^{-1} and 185 kJ mol^{-1}, respectively [34]. Similarly, Otero et al. [15] reported activation energies between 129 and 213 kJ mol^{-1} during the pyrolysis of raw and digested cattle manure while using FWO method. In another pyrolysis study, the average

activation energy of the microalgae *Dunaliella tertiolecta* using Flynn-Wall-Ozawa method was reported to be 146.4 kJ mol^{-1} [35].
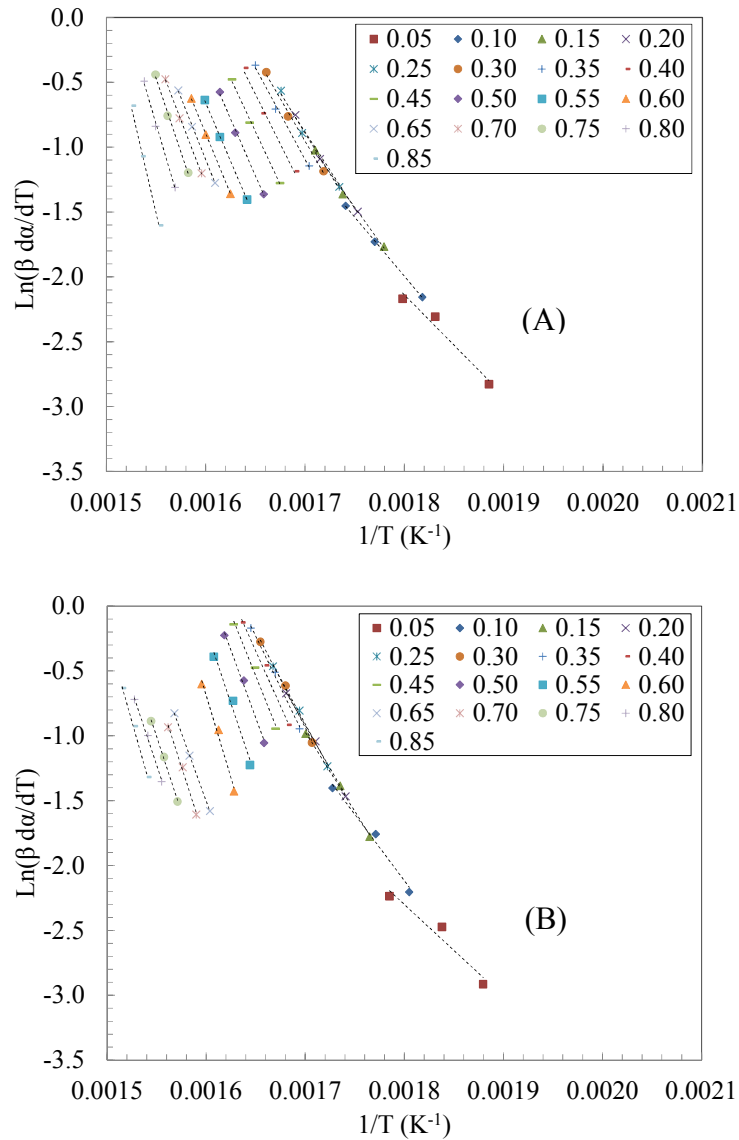
Figure 3-3 Plots of ln(β*dα/dT) versus 1/T at three heating rate: 20, 30 and 40 °C/min for manure solids from (A) farrowing farm and (B) growing-finishing farm

Table 3-3 The activation energies (E_a, kJ mol^{-1}) using Friedman method at different degrees of conversion (α) for swine manure solids by source

Degrees of conversion (α)	Farrowing farm		Growing-finishing farm	
	Ea (kJ/mol)	R^2	Ea (kJ/mol)	R^2
0.05	64.5	0.966	58.8	0.942
0.10	75.8	0.999	85.0	0.980
0.15	88.3	0.996	101.8	0.998
0.20	97.9	0.995	109.9	0.998
0.25	103.4	0.993	116.9	0.997
0.30	109.0	0.994	124.0	0.997
0.35	117.6	0.995	131.4	0.995
0.40	127.4	0.989	141.4	0.989
0.45	136.0	0.997	158.2	0.988
0.50	146.4	0.997	173.3	0.994
0.55	149.2	0.999	189.2	0.981
0.60	154.9	0.999	210.5	0.989
0.65	159.4	0.999	202.7	0.983
0.70	165.3	0.999	197.2	0.993
0.75	188.7	0.996	193.2	0.997
0.80	215.8	0.995	191.8	0.996
0.85	273.7	0.993	223.9	0.998

Analysis of the correlations between the activation energies computed using both methods showed that the values of the FWO activation energy were around 5% lower than those calculated using the Friedman method. However, the activation energies calculated using both methods were correlated for each swine manure type. It is worth noting when comparing both methods that while the differential methods, Friedman method in this case, provide actual values of the activation parameter, the integral isoconversional methods, e.g., Flynn-Wall-Ozawa,

provide averaged values of that parameter [36]. Correlating these values, however, provide a useful approach to predict the actual values of the activation energy from the averages, or vice versa.

Table 3-4 The activation energies (E_a, kJ mol^{-1}) using Flynn- Wall- Ozawa method at different degrees of conversion (α) for swine manure solids by source

.Degree of conversion (α)	Farrowing farm		Growing-Finishing farm	
	Ea (kJ/mol)	R^2	Ea (kJ/mol)	R^2
0.05	61.3	0.966	55.9	0.942
0.10	72.0	0.999	80.8	0.980
0.15	84.0	0.996	96.8	0.998
0.20	92.6	0.995	104.4	0.998
0.25	98.3	0.993	119.1	0.997
0.30	103.6	0.994	117.9	0.997
0.35	111.8	0.995	124.9	0.995
0.40	121.1	0.989	134.4	0.989
0.45	129.3	0.997	150.4	0.988
0.50	139.2	0.997	164.8	0.994
0.55	141.8	0.999	179.9	0.981
0.60	147.2	0.999	200.1	0.989
0.65	151.6	0.999	192.7	0.983
0.70	157.1	0.999	187.5	0.993
0.75	179.4	0.996	183.7	0.998
0.80	205.2	0.995	182.3	0.997
0.85	260.2	0.993	212.8	0.998

5. Conclusions

Swine manure solids from two farms, i.e., farrowing and growing-finishing, were successfully characterized. The main findings are:

1. The type of farm influenced the composition and the higher heating value (HHV) of swine manure solids.

2. Keratin in the manure solids, from animal hair, increased the nitrogen content and might be responsible for the low HHV.

3. Compositional differences between the two swine manure types translated to variability in the weight loss rates, and the shape of decomposition peaks.

4. The activation energy during pyrolysis of swine manure solids (T ≤420°C) showed a gradual increase corresponding with the devolatilization of the sample ingredients (hemicellulose, cellulose, in addition to the keratin and lipid).

5. These findings shed more light on the behavior of swine manure solids under thermochemical conversion conditions.

6. References

[1] J. McGlone. 2013. The Future of Pork Production in the World: Towards Sustainable, Welfare-Positive Systems. Animals; 3:401-15.

[2] NASS-USDA. 2013. Quarterly Hogs and Pigs September 27, 2013; 1949-1921.

[3] D. Tilman, K. Cassman, P. Matson, R. Naylor, and S. Polasky. 2002. Agricultural sustainability and intensive production practices. Nature. 418: 671-7.

[4] American Society of Agricultural and Biological Engineers (ASABE). 2005. Standard D3843.2-Manure Production and Characteristics.

[5] C. Burton. 2007. The potential contribution of separation technologies to the management of livestock manure. Livestock Science. 112: 208-16.

[6] H. Møller, J. Hansen, and C. Sørensen. 2007. Nutrient recovery by solid-liquid separation and methane productivity of solids. Transactions of ASABE. 50: 193-200.

[7] K. Ro, K. Cantrell, and P. Hunt. 2010. High-temperature pyrolysis of blended animal manures for producing renewable energy and value-added biochar. Ind Eng Chem Res. 49: 10125-31.

[8] M. Park, S. Kumar, and R. ChangSix. 2012. Solid Waste from Swine Wastewater as a Fuel Source for Heat Production. Asian - Australasian Journal of Animal Sciences. 25: 1627-32.

[9] R. Wnetrzak, W. Kwapinski, K. Peters, S. Sommer, L. Jensen, and J. Leahy. 2013. The influence of the pig manure separation system on the energy production potentials. Bioresour Technol. 136: 502-8.

[10] C. Font-Palma. 2012. Characterisation, kinetics and modelling of gasification of poultry manure and litter: an overview. Energy convers manage. 53: 92-8.

[11] J. Sweeten, K. Heflin, B. Auvermann, K. Annamalai, and F. McCollum. 2013. Combustion fuel properties of manure and compost from paved and unpaved cattle feedlots as modified by annual precipitation. Transactions of the ASABE. 56: 279-94.

[12] B. Jenkins, L. Baxter, T. Miles Jr, and T. Miles. 1998. Combustion properties of biomass. Fuel Process Technol. 54: 17-46.

[13] K. Singh, M. Risse, J. Worley, K. Das, and S. Thompson. 2008. Effect of fractionation on fuel properties of poultry litter. Appl Eng Agric. 24: 383-8.

[14] K. Ro, K. Cantrell, P. Hunt, T. Ducey, M. Vanotti, and A. Szogi. 2009. Thermochemical conversion of livestock wastes: Carbonization of swine solids. Bioresour Technol. 100: 5466-71.

[15] M. Otero, M. Sánchez, and X. Gómez. Co-firing of coal and manure biomass: A TG–MS approach. 2011. Bioresour Technol. 102: 8304-9.

[16] S. Vyazovkin, and C. Wight. 1999. Model-free and model-fitting approaches to kinetic analysis of isothermal and nonisothermal data. Thermochimica Acta. 340–341: 53-68.

[17] ASTM Standard D 2974. 2007. Standard Test Methods for Moisture, Ash, and Organic Matter of Peat and Other Organic Soils. ASTM D2974-07a.

[18] ASTM Standard D5865. 2012. Standard Test Method for Gross Calorific Value of Coal and Coke. D5865-12.

[19] A. Galwey, M. Brown. 1998. Handbook of thermal analysis and calorimetry. Chapter 3 Kinetic Background to Thermal Analysis and Calorimetry. 1: 147-224.

 [20] D. Zhou, and D. Grant. 2004. Model dependence of the activation energy derived from nonisothermal kinetic data. The Journal of Physical Chemistry. 108: 4239-46.

[21] J. Cai, and L. Bi. 2009. Kinetic analysis of wheat straw pyrolysis using isoconversional methods. J therm anal calorim 98: 325-30.

[22] H. Friedman. 1965. Kinetics of thermal degradation of char-foaming plastics from thermogravimetry: application to a phenolic resin. Journal of Polymer Science. 6: 183-95.

[23] Flynn J,H., Wall L,A. General Treatment of the Thermogravimetry of Polymers. Journal of Research of National Bureau of Standards- A. Physics and Chemistry 1966; 70Z: 487-523.

[24] T. Ozawa. 1965. A New Method of Analyzing Thermogravimetric Data. Bull Chem Soc Jpn. 38: 1881-6.

[25] C. Doyle. 1962. Estimating isothermal life from thermogravimetric data. J Appl Polym Sci. 6: 639-42.

[26] F. Mariotti, D. Tomé, and P. Mirand. 2008. Converting nitrogen into protein—beyond 6.25 and Jones' factors. Crit Rev Food Sci Nutr. 48: 177-84.

[27] A. Demirbaş.1997. Calculation of higher heating values of biomass fuels. Fuel. 76: 431-4.

[28] H. Yang, R. Yan, H. Chen, C. Zheng, D. Lee, and D. Liang. 2006. In-depth investigation of biomass pyrolysis based on three major components: hemicellulose, cellulose and lignin. Energy Fuels. 20: 388-93.

[29] H. Møller, S. Sommer, and B. Ahring. 2004. Methane productivity of manure, straw and solid fractions of manure. Biomass Bioenerg. 26: 485-95.

[30] F. Yao, Q. Wu, Y. Lei, W. Guo, and Y. Xu. 2008. Thermal decomposition kinetics of natural fibers: activation energy with dynamic thermogravimetric analysis. Polym Degrad Stab. 93: 90-8.

[31] S. Xiu, Y. Zhang, A. Shahbazi. 2009. Swine manure solids separation and thermochemical conversion to heavy oil. BioResources. 4: 458-70.

[32] M. Brebu, I. Spiridon. 2011. Thermal degradation of keratin waste. J Anal Appl Pyrolysis. 91: 288-95.

[33] B. Maddi, S. Viamajala, and S. Varanasi. 2011. Comparative study of pyrolysis of algal biomass from natural lake blooms with lignocellulosic biomass. Bioresour Technol. 102: 11018-26.

[34] S. Draman, R. Daik, F. Latif, and S. El-Sheikh. 2013. Characterization and Thermal Decomposition Kinetics of Kapok (Ceiba pentandra L.)–Based Cellulose. BioResources. 9: 8-23.

[35] Z. Shuping, W. Yulong, Y. Mingde, L. Chun, and T. Junmao. 2010. Pyrolysis characteristics and kinetics of the marine microalgae. Dunaliella tertiolecta using thermogravimetric analyzer. Bioresour Technol.101: 359-65.

[36] P. Šimon. 2004. Isoconversional methods. Journal of Thermal Analysis and Calorimetry. 76: 123-32.

Chapter 4 Pyrolysis Kinetics of Algal Consortia Grown Using Swine Manure Wastewater

Citation

1. Abstract

In this study, pyrolysis kinetics of periphytic microalgae consortia grown using swine manure slurry in two seasonal climatic patterns in northwest Arkansas were investigated. Four heating rates (5, 10, 20 and 40ºC min^{-1}) were used to determine the pyrolysis kinetics. Differences in proximate, ultimate, and heating value analyses reflected variability in growing substrate conditions, i.e., flocculant use, manure slurry dilution, and differences in diurnal solar radiation and air temperature regimes. Peak decomposition temperature in algal harvests varied with changing the heating rate. Analyzing pyrolysis kinetics using differential and integral isoconversional methods (Friedman, Flynn-Wall-Ozawa, and Kissinger-Akahira-Sunose) showed strong dependency of apparent activation energy on the degree of conversion suggesting parallel reaction scheme. Consequently, the weight loss data in each thermogravimetric test was modeled using Independent Parallel Reactions (IPR). The quality of fit (QOF) for the model ranged between 2.09% and 3.31% indicating a good agreement with the experimental data.

2. Introduction

Thermogravimetry is a powerful and versatile tool in understanding and modeling biomass reactions. It is also a quick and reliable approach to determine the moisture, organic matter, and ash contents in biomass [11]. Other uses of thermogravimetric analysis (TGA)

include quantification of the hemicellulose and α-cellulose contents in wood [3], as well as evaluation of digestate stability during anaerobic digestion [13]. The predominant use of TGA, however, is to determine the rate of thermal decomposition for various feedstocks. A survey of the literature shows the importance of this analysis to the determination of decomposition kinetics of woody biomass [12], crop residue [20], animal manures [28], and municipal solid waste [27]. However, the recent interest in aquatic biomass, as a biofuel and bioenergy crop, brought to light the dearth of thermogravimetric studies on this class of biomass.

Historically, microalgae mass-production was mostly accomplished to support aquaculture systems [23] as well as to extract important bioactive compounds [29]. Recently, however, interest in sustainable biofuel sources brought attention to microalgae due to the high lipid content in certain species, which can be converted via "transesterification" to biodiesel. The oil content in microalgae species such as *Schizochytrium* sp. can exceed 75% on a dry-weight basis [6]. A vital ecological service that microalgae could provide is treatment of nutrient-rich wastewater effluents, i.e., phycoremediation. This particular service is becoming increasingly crucial with the increase in global urbanization, industrialization, and intensive cropping activities [14].

Contamination of surface and ground water with nitrogen (N), phosphorous (P), polycyclic aromatic hydrocarbons (PAH), and heavy metals is the primary cause behind hypoxic conditions, eutrophication, and poisoning of aquatic habitats in rivers and lakes [4]. Uptake and biosorption of these contaminants by algal species has been investigated on a variety of wastewater substrates, i.e., municipal, industrial, and agricultural wastewater streams [26]. Adopting phycoremediation in livestock wastewater management can offer an added-advantage by minimizing phosphorus loss. Algal species were successfully grown on raw swine manure

effluents, 9 g m^{-2} day^{-1}, but growth rates were found to be sensitive to the loading rates of N and P [18].

The harvested phycoremediation algae can be directed to a variety of uses such as composting, anaerobic digestion, and the extraction of lipids and sugars for biodiesel and ethanol production. Alternatively, the algal biomass can be utilized through thermochemical conversion processes. The end-use for a specific algae harvest is highly dependent on its composition. Algae used in water remediation are typically indigenous species grown in open systems that results in a diverse species consortium in the collected biomass. Thermogravimetric analyses can assist in the effort to characterize the harvested microalgae and to direct them to the optimal end-uses. For instance, TGA decomposition rate curves were proven effective in detecting and quantifying the lipid contents in *Chlorella* sp. [24]. Understanding the decomposition kinetics of microalgae in various atmospheres, in addition to providing insight into the proximate composition, is essential to the design and optimization of thermochemical conversion processes. There is a need in research for studies covering the thermal decomposition kinetics of mixed algae consortia grown for water remediation purposes, especially as part of sustainable livestock production scenarios. The goal of this research is to evaluate the thermal decomposition of indigenous periphytic microalgae grown in an open water-remediation system for a swine production facility under nitrogen environment using thermogravimetric analysis (TGA).

3. Materials and Methods

3.1. Swine wastewater treatment system

Algal biomass was produced using open channel raceways lined with a growth medium for periphyton attachment and irrigated by circulation of swine-manure based wastewater. Algae consortia produced using two systems were investigated in this study. System 1 was a small

system with 8 raceways that were each 15 cm wide by 3.0 m long. It was sited outdoors adjacent to the University of Arkansas Biological and Agricultural Engineering Research Lab, Fayetteville, Arkansas. System 2 was a larger pilot system with 4 raceways that were each 1.5 m wide by 61 m long. It was constructed at the University of Arkansas Swine Research Grower Facility, near Savoy Arkansas. The raceways in both systems were lined with specialty fibrous carpeting (proprietary fiber selection and layout intended to optimize periphyton growth, provided by Interface, Inc.) to maximize algae attachment during water circulation. System 1 was operated during the summer of 2013 (June-July) on swine manure slurries at different degrees of dilution to vary targeted starting ammonia (NH_3) concentrations between 5 mg L^{-1} to 40 mg L^{-1} (mg=10^{-6} kg). Details of the NH_3 loading influence will be discussed in a separate publication. System 1 was seeded with mixed consortia which were collected from a local stream in Fayetteville, AR whereas System 2 was seeded from the mixed consortia harvested from System 1. Wastewater used in System 2 was pumped from swine slurry storage lagoon, then treated with alum (aluminum sulfate 14-hydrate granules, $Al_2(SO_4)_3 \cdot 14\ H_2O$, addition rate 2 g L^{-1}) to flocculate solids. After a 24 h settling period, the undiluted supernatant was removed for circulation in the raceway. System 2 was operated during the fall of 2013 (November-December). Both systems were open during production without any control over the growing algal species.

3.2. Algae collection and preparation methods

Harvest of algae was accomplished manually, in 5-day cycles, using a rubber-bladed squeegee for removal and collection of attached algae. Harvested algae were dried immediately or else stored at 4°C for 24 h before drying. Subsamples of fresh algae were stored for analysis and species identification. One composite sample was collected from each algae consortium for

the thermogravimetric analysis (TGA). Composite algae samples were dried at 105°C for 24 h before grinding to 1 mm (Thomas Wiley® cutting mill- Model 3383L10, Swedesboro, NJ). A second grinding step, using a cutting mill (Polymix PX-MFC 90 D, Kinematica AG, Switzerland), was added to homogenize the dried samples and minimize mass transport resistance during thermogravimetric analysis. The algal solids used in the following tests and analyses all passed through a 200 μm sieve (μm=10^{-6} m).

3.3. Proximate, ultimate, heating value and pH analyses

The remaining moisture was determined, in triplet samples, as the weight loss after drying at 105°C, ASTM E871 – 82 (2006). Standard methods were also used to determine the volatile matter, ASTM E872 – 82 (2006), and ash content, ASTM D2974-87 (2007), while the fixed carbon (%) was determined by difference. Complete elemental analyses of representative samples from each algae harvest were performed in a specialized diagnostic laboratory (Huffman laboratories, Golden, CO, USA). The heating values were determined on sample triplets, according to standard ASTM D5865-12 (2012), using bomb calorimetry (Parr instruments, Model 1341, Moline, IL, USA). The pH of algal biomass was determined using a pH electrode (SB70P, SympHony, VWR, Radnor, PA, USA) after the dry, ground samples were diluted with deionized water, 10 mL per 1 g of sample, then vigorously stirred and allowed to stand for 1 h before measurement.

3.4. Thermogravimetric analysis methodology

A thermogravimetric analyzer (Model TGA 4000, PerkinElmer, Inc. Waltham, MA, USA) was used to study the decomposition behavior of the two algal harvests. Prior to the algae decomposition tests, a curie-point temperature calibration was performed using three reference materials, i.e., alumel, perkalloy, and Iron, according to the manufacturer's guidelines. Similarly,

a weight calibration was performed, before tests, using the manufacturer supplied reference

weight. Pyrolysis of each of two algae biomasses was studied under four different heating rates

(5, 10, 20, and 40°C min⁻¹) from 30°C to 800°C. Nitrogen gas was used to purge the sample (30

mL min⁻¹) to simulate pyrolysis conditions. The sample size was consistently kept at 5 ± 0.5 mg

to minimize deviation (lag) between measured and actual sample temperatures, and to also

ensure that the decomposition reactions were not transport-limited. For each sample, blank, clean

crucibles were tested using the same thermal decomposition programs in order to adjust the

weight baseline by compensating for the drag force acting on the crucible.

3.5. Decomposition kinetics

The decomposition is often expressed in terms of the conversion (α) which describes the change

in sample weight, in a dimensionless form.

$$\alpha = \frac{W_o - W_t}{W_o - W_\infty} \tag{1}$$

W_o, W_t, and W_∞ are the sample weights at the beginning, at time t, and at the end of the

decomposition stage, respectively. The rate of conversion ($d\alpha/dt$) is often expressed using an

Arrhenius type expression.

$$\frac{d\alpha}{dt} = A \exp\left(\frac{-E_a}{RT}\right) f(\alpha) \tag{2}$$

A, E_a, R, and T are the pre-exponential coefficient (frequency factor), the activation

energy, the universal gas constant, and the sample absolute temperature, respectively. $f(\alpha)$

represents the kinetic model that describes the rate of conversion dependence on the conversion,

e.g., an n-order reaction model: $f(\alpha) = (1 - \alpha)^n$.

Under a constant heating-rate ($\beta = dT/dt$), the time-dependence of the conversion rate can be transformed to a temperature-dependence which can be used to rewrite the differential form (equation 3) or the integral form (equation 4) of the decomposition kinetic expression.

$$\frac{d\alpha}{dT} = \frac{A}{\beta} \exp\left(\frac{-E_a}{RT}\right) f(\alpha) \tag{3}$$

$$g(\alpha) = \int_0^T \frac{A}{\beta} \exp\left(\frac{-E_a}{RT}\right) dT \tag{4}$$

The following sections will detail the different model-free (isoconversional) methods used to determine the apparent activation energies for algae pyrolysis.

3.6. Model-free (isoconversional) methods

Isoconversional methods overcome the requirement of determining the reaction model, $f(\alpha)$, in order to determine the activation energy, E_a. This is accomplished by simultaneously analyzing decomposition curves generated under different heating rates to extract the apparent kinetics data, i.e., E_a and $\ln A$, corresponding to each degree of conversion (α). Isoconversional methods are popular in biomass decomposition studies due to the fact that biomass, a natural biopolymer, undergoes a series of overlapping reactions, during pyrolysis or oxidation, which cannot be described accurately by one-step, global reaction model. The downside in isoconversional methods, however, is the inability to straightforwardly determine an exact model expression, $f(\alpha)$ or $g(\alpha)$, to describe the entire decomposition.

In this research, one differential isoconversional method, Friedman method [9], and three integral isoconversional methods: Kissinger's [2], Flynn-Wall-Ozawa's [8, 25], and Kissinger-Akahira-Sunose's [30] were used to determine the pyrolysis kinetics of the two algae harvests under study. Below is a brief description of each the methods.

Friedman method

Re-arranging equation (3), then linearizing it by taking the natural log of both sides of the equation

$$ln\left(\beta \frac{d\alpha}{dT}\right) = \ln\left(A f(\alpha)\right) - \frac{E_a}{RT} \tag{5}$$

At each α, the above equation describes the linear relationship between $1/T$ and $ln(\beta\ d\alpha/dT)$ with each point representing a tested heating rate. The slope of this line represents the activation energy term, E_a/RT, at this conversion degree whereas the intercept represents an expression combining the reaction model and the pre-exponential factor, $ln(A\ f(\alpha))$. Calculating the slopes and intercepts at different α values, between 0.05 and 0.90, describe the kinetics of decomposition as a function of the conversion degree.

Kissinger method

This method determines the activation energy (E_a) and the pre-exponential factor (A) using the temperatures, T_{max} values, that correspond to peak decomposition rates, $(d\alpha/dt)_{max}$ in thermogravimetric tests under different heating rates (β). The temperature integral in equation (4) doesn't yield an analytical, closed-form solution. Therefore, it is alternatively presented as follows (Starink, 2003)

$$g(\alpha) = \frac{AE_a}{\beta R}p(x) \tag{6}$$

Where $x = E_a/RT$, and the function $p(x)$ represents

$$p(x) = \int_x^\infty \frac{e^{-x}}{x^2}dx \tag{7}$$

Many approximations were derived to determine $p(x)$ numerically. In the Kissinger method, the Murray and White approximation (Starink, 2003), $p(x) \cong e^{-x}/x^2$, is used. The underlying assumption in this method is that the decomposition follows a first-order reaction model, i.e., $f(\alpha) = (1-\alpha)$. Equation (8) details the relationship between T_{max}, β, and E_a and A.

$$\ln\left(\frac{\beta}{T_{max}^2}\right) = ln\left(\frac{AR}{E_a}\right) - \frac{E_a}{RT_{max}} \tag{8}$$

By plotting $ln\ (\beta/T_{max}^2)$ against $(1/\ T_{max})$, the activation energy (E_a/R) and the pre-exponential factor, $ln\ (AR/E_a)$, terms can be determined, respectively, as the slope and the intercept of the resulting straight-line.

Kissinger-Akahira-Sunose (KAS) method

A modified form of Kissinger's method that was described earlier, KAS method dispenses with the kinetic model assumption, and the use of only the peak decomposition data. Instead, KAS is an integral method that relies on the different (α) values instead of the single value corresponding to peak decomposition $(d\alpha/dt)$. Equation (8) can then be rearranged and linearized

$$\ln\left(\frac{\beta}{T^2}\right) = ln\left[\frac{AR}{E_a}\right] - \ln(g(\alpha)) - \frac{E_a}{RT} \tag{9}$$

The slope of the straight lines formed by plotting $\ln\ (\beta/T^2)$ against $1/T$ at each degree of conversion (α), with the points corresponding to the different β values, yields the activation energy, E_a, corresponding to that conversion degree.

Flynn-Wall-Ozawa (FWO) method

In this method, the Doyle's approximation (Doyle, 1962) to the temperature integral, $p(x)$, is applied: $p(x) \cong -5.33 - 1.05x$. The linearized form of equation (4) becomes:

$$\ln \beta = \ln\left[\frac{AE_a}{Rg(\alpha)}\right] - 5.33 - 1.052\left(\frac{E_a}{RT}\right) \tag{10}$$

At each degree of conversion (α), $\ln \beta$ and $1/T$ corresponding to each heating rate are fitted into a straight line. The slope, ($-1.052\ E_a/R$), represents the apparent activation energy term, while the intercept is a coupled expression of the reaction model in the integral form, $g(\alpha)$, the apparent activation energy E_a, and the frequency factor, A.

3.7. Kinetic modeling of algae pyrolysis

In order to investigate the pyrolysis of the two algae consortia, the weight loss was modeled as a series of overlapping independent, parallel reactions taking place between 100°C and 700°C. This approach was presented elsewhere as a deconvolution step necessary to understand the devolatilization of a biopolymer by modeling the various pseudo-components contributing to its overall decomposition. In this study, algae pyrolysis was modeled as 4 independent, 1st order reactions. The rate of conversion ($d\alpha/dt$) for pseudo-component (N) is:

$$\frac{d\alpha_N}{dt} = A_N \exp\left(\frac{-E_{a\,N}}{RT}\right)(1 - \alpha_N), \qquad \text{where } N=1\ldots 4 \tag{11}$$

Consequently, the total rate of conversion ($d\alpha_{Total}/dt$) can be determined from the individual pseudo-components using the following expression:

$$\frac{d\alpha_{Total}}{dt} = \sum_{i=1}^{N} w_i \frac{d\alpha_N}{dt}, \quad \text{and} \quad \sum_{i=1}^{N} w_i = 1 \tag{12}$$

The quantity, w_i, represents the contribution of each individual pseudo-component to the overall sample conversion. The conversion rate can be converted to the mass loss rate using the following relation:

$$\frac{dm_{calc}}{dt} = -(m_o - m_f)\frac{d\alpha_{Total}}{dt} \tag{13}$$

m_o and m_f represent the initial and final sample weights. Numerical integration between the temperatures of interest, i.e., 100°C to 700°C in this study, yields the computed overall weight, m_{calc}. The parameters of each reaction, i.e., A, E_a, and w were determined by nonlinear minimization of an objective function (O.F.) which represents the sum of squared differences between observed sample mass loss rate, dm_{obs}/dt, and the calculated mass loss rate, dm_{calc}/dt:

$$O.F. = \sum_{i=1}^{Np}(\frac{dm_{calc}}{dt} - \frac{dm_{obs}}{dt})^2 \tag{14}$$

In this study, the total number of points, N_p, used in reaction modeling for each thermogram was 300 points. The quality of fit, QOF (%), for the weight loss derivative (DTG) and the weight loss (TG) were determined using the following expressions:

$$QOF_{DTG}(\%) = 100\left(\frac{\sqrt{\frac{\sum_{i=1}^{Np}\left(\frac{dm_{calc}}{dt}-\frac{dm_{obs}}{dt}\right)^2}{Np}}}{}\right) / \left|\frac{dm_{obs}}{dt}\right|_{max} \tag{15}$$

$$QOF_{TG}(\%) = 100\left(\frac{\sqrt{\frac{\sum_{i=1}^{Np}(m_{calc}-m_{obs})^2}{Np}}}{}\right) / (m_{obs})_{max} \tag{16}$$

Numerical integration was performed using a numerical integrator for stiff-equations, (ODE15s) while the constrained nonlinear minimization was performed using the (fmincon) function, both of which are part of the MATLAB software package (MATLAB R2013b, The Mathworks, Inc., Natick, MA, USA).

4. Results and Discussions

4.1. Species indentification

The harvested microalgae species were inspected non-quantitatively using optical microscopy. The microalgae consortium in each harvest, i.e., Algae 1 and Algae 2, consisted

mostly of filamentous microalgae mixtures in addition to diatoms. The most common

filamentous genus identified in Algae 1 was *Mougeotia*, while the genus *Cladophora* dominated

Algae 2 harvest. Both genera are common fresh-water microalgae, which were reported to be

tolerant of a wide range of growing conditions [15, 22]. In a study of algal growths in Lake Mead

(Nevada-Arizona, USA), predominance of *Mougeotia* species was reported in certain

monitoring stations during the summer months (June-July) which then changed to *Cladophora*

and *Stigeoclonium* dominance during the months of October and November.

4.2. Proximate analysis

Table 4-1 shows the results of proximate analysis of the two algae. The low moisture

content in both harvests, around 5% wet-basis, represents the moisture absorbed after drying and

during sample preparation. Comparison of proximate analysis results for the two algae harvests

showed significant differences (*t*-test, $p < 0.01$) in volatile matter, fixed carbon, and ash contents.

The ash contents observed in both algae consortia: 20% in Algae 1 and 32% in Algae 2 are

noticeably high in comparison to the ash contents of terrestrial biomass (wood, grasses, and crop

residue) which are below 10 *wt.*%. This is explained by algae's high potential for mineral

biosorption and due to their simple cellular structures. The ash content in aquatic biomass vary

drastically from less than 10% [10] to more than 50% [35], according to type of alga and growth

conditions. Algae grown on wastewater or high-mineral effluents in open ponds/raceways are

expected to contain higher ash than algae produced in a closed-system on low-minerals water.

The difference in ash contents, 12 percentage points, in this study could be attributed to use of

the alum flocculant, $Al_2(SO_4)_3 \cdot 14 H_2O$, on the swine manure slurries used to grow Algae 2. The

high percentages of Al_2O_3 and SO_3 found in Algae 2 ash residue, 19.86% and 10.25%, compared

to Algae 1, 1.93% and 4.54%, respectively, supports this hypothesis (Table 4-1). This difference

in the ash contents also explains the relatively low volatile matter and fixed carbon contents observed in Algae 2 when compared to Algae 1.

4.3. Elemental composition and higher heating value

Percentages of the main organic elements: carbon (C), hydrogen (H), nitrogen (N), and oxygen (O), in both algae are shown in Table 4-1. Algae 1 sample showed higher content of organic elements when compared to Algae 2 sample, except for N. These differences are attributable, as discussed earlier, to the use of metal salt to precipitate the suspended solids in the manure slurry used in Algae 2 production. By contrast, the higher N content in Algae 2 is due to the elimination of slurry dilution, which was employed in growing the Algae 1 consortia. N loading was reported to influence the lipid and protein in the algal biomass [33]. In lipid production from microalgae, a nutrient stress is typically imposed by reducing N-loading to induce lipid production and storage in algae cells. In phycoremediation, by contrast, algae are grown on N-rich substrates, which increase the protein content in the cells. From their N contents, the protein content in Algae 1 and 2 can be estimated using Jones' factor of 6.25 [17] to be 33.8% and 39.7%, respectively. Unlike terrestrial biomasses, which consist primarily of cellulose, hemicellulose, and lignin, microalgae are single cell organisms that consist of carbohydrates, proteins, and lipids. This structural difference can be observed in the stoichiometric expressions for Algae 1: $CH_{1.62}N_{0.11}O_{0.49}$ and Algae 2: $CH_{1.68}N_{0.16}O_{0.47}$, as compared to that for hybrid poplar wood [16]: $CH_{1.45}N_{0.01}O_{0.60}$.

Table 4-1 Proximate, ultimate, ash, calorific value, and pH analyses for the two algae consortia studied

	Algae 1	Algae 2
Proximate analysis (wt%*)		
Moisture	5.14	5.09
Volatile matter	64.49	56.30
Fixed carbon**	10.41	6.32
Ash	19.96	32.29
Ultimate analysis (wt%)		
C	41.51	33.79
H	5.59	4.73
N	5.40	6.35
S	0.51	1.57
O**	27.03	21.27
Ash	19.96	32.29
Ash analysis (wt %)		
Al_2O_3	1.93	19.86
SiO_2	14.57	16.44
P_2O_5	15.69	15.27
K_2O	6.57	12.09
SO_3	4.54	10.25
CaO	37.15	9.85
Na_2O	3.08	4.88
MgO	4.46	4.06
Fe_2O_3	1.42	3.50
MnO	0.08	0.17
TiO_2	0.06	0.15
HHV*** (kJ g^{-1})	16.63	14.53
pH	6.88	7.69

*Weight-basis percentage

**By difference

The difference observed in the higher heating values (HHV) between the studied algae harvests, 16.6 kJ g^{-1} in Algae 1, and 14.5 kJ g^{-1} in Algae 2, could be attributed to the difference in the ash contents. Calculating the dry, ash-free HHV (DAF), using the ash contents and the dry-basis HHVs in Table 4-1, shows both algae to have similar energy contents, i.e., 21 kJ g^{-1}$_{DAF}$.

4.4. Thermogravimetric analysis

With the temperature increase, the samples underwent a series of endothermic and exothermic reactions, which involved varying degrees of weight-loss (devolatilization) and structural change to the sample matrix. In both algae consortia, decomposition temperatures increased with increasing the heating rate (β). Doubling β led to an increase between 7 and 9°C for the entire weight loss curve. Similarly, the rate of weight loss was observed to double with each doubling of the heating rate. In Algae 1, the pyrolysis resulted in a weight loss of 69 – 72% of initial weight whereas in Algae 2 the weight loss ranged between 62 and 67% over the entire temperature range, 30 – 800°C. The difference in ash contents between the two algal consortia was reflected in difference between overall weight-loss.

During algae pyrolysis, the weight loss can be divided into three consecutive stages: *drying*, *active pyrolysis*, and *passive pyrolysis*. Drying, which typically takes place below 110°C, is the first step in algae pyrolysis and it involves the evaporation of both free and hygroscopic water in the sample matrix. In this step the initial weight dropped around 5% with the corresponding DTG peak at around 100°C. After drying, the samples underwent a brief induction period, between 110 and 150°C, in which the weight loss was minimal.

In pyrolysis, most of the weight loss takes place, between 150°C and 550°C, during the active pyrolysis stage. This weight loss represents the thermal depolymarization and

volatilization of various organic matter (volatile matter) components. Algae 1 lost 58% of total

weight during the active pyrolysis step compared to only 50% weight-loss in Algae 2. Despite

the similarity in peak decomposition temperatures in the two consortia (Table 4-2), the maximum

decomposition rates for Algae 1 samples, 0.44 – 0.48% °C^{-1}, were consistently higher than those

observed for Algae 2, 0.33 – 0.37 % °C^{-1}.

Table 4-2 Pyrolysis temperature (°C) and weight loss (%) corresponding to peak decomposition rate (% °C-1) in both algae consortia

Heating rate	Algae 1			Algae 2		
	$-(dW/dT)_p$	T_p	WL_p	$-(dW/dT)_p$	T_p	WL_p
(°C min^{-1})	(% °C^{-1})	(°C)	(%)	(% °C^{-1})	(°C)	(%)
5	0.48	298.58	28.4	0.36	302.16	24.4
10	0.47	308.01	28.2	0.37	309.30	23.9
20	0.44	315.72	27.3	0.33	317.28	23.9
40	0.45	328.31	27.6	0.33	328.64	24.3

In biopolymers such as microalgae, the thermal decomposition represents the summation of

decomposition profiles for the individual components. Given the wide variability between

microalgae species, in terms of main ingredients' concentration and composition, the

decomposition profiles under pyrolysis can vary greatly. Maddi, Viamajala and Varanasi (2011)

compared pyrolysis thermograms of *Lyngbya sp.* and *Cladophora sp.*, and attributed the

dissimilarity to differences in protein compositions [19]. In this study, the seasonal variability

between consortia induced differences in algal community compositions, which were reflected in

the respective decomposition profiles. In both consortia, however, the main decomposition peak

took place in the range associated with carbohydrates and proteins indicating a similarity in the

main composition. Furthermore, the peak associated with lipids decomposition (above 390°C) [24] was only a small shoulder in both consortia, indicating low lipid contents.

During passive-pyrolysis ($T > 550°C$), both algae harvests showed minimal weight-loss, which is characteristic of char pyrolysis. A minor decomposition peak (0.06 % °C) which was observed in Algae 1 between 650 and 700°C was not observed in Algae 2. In studying the pyrolysis of *Chlorella vulgaris*, Agrawal and Chakraborty (2013) attributed a similar high temperature weight-loss peak (at 700°C) to a char gasification step, which was explained as CO_2 loss [1]. Maddi, Viamajala and Varanasi (2011) also reported a high temperature peak during the decomposition of *Cladophora sp.* but could not identify the component associated with it [19]. The kinetics of decomposition for both algae consortia during the active pyrolysis stage, 150-550°C, will be discussed in the following section.

4.5. Pyrolysis kinetics

The temperature-conversion data in each algae sample (

Figure 4-1) was used to determine the decomposition kinetics during the active pyrolysis stage (150-550°C). The conversion profile for each algae consortium approximates a sigmoidal function, which is typically associated with the autocatalytic reactions involved in pyrolysis [21].

The kinetics determined using isoconversional methods, i.e., activation energy and pre-exponential term, are detailed in Table 4-3. Both isoconversional and integral methods showed strong correlation coefficients (*r*) and high significance (*p*-value<0.01). In each algae consortium, the KAS and FWO activation energy values were very close, within 2%, at each conversion degree. Activation energies determined using Friedman method, on the other hand, were consistently higher than KAS and FWO, at times by 12%, as shown in Figure 4-2. This

difference in the activation energies, between the differential and integral methods, could be attributed to the numerical differentiation step necessary to determine the kinetics in Friedman method.
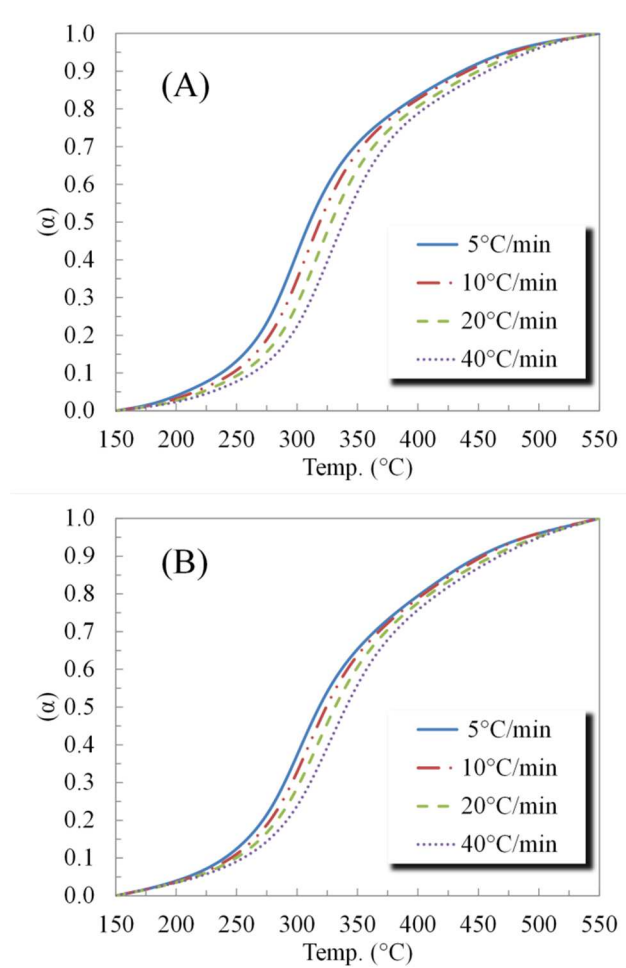
Figure 4-1 Conversion-temperature (α-T) curves for (A) algae 1, and (B) algae 2 under different heating rates: β= 5, 10, 20, and 40°C min^{-1}
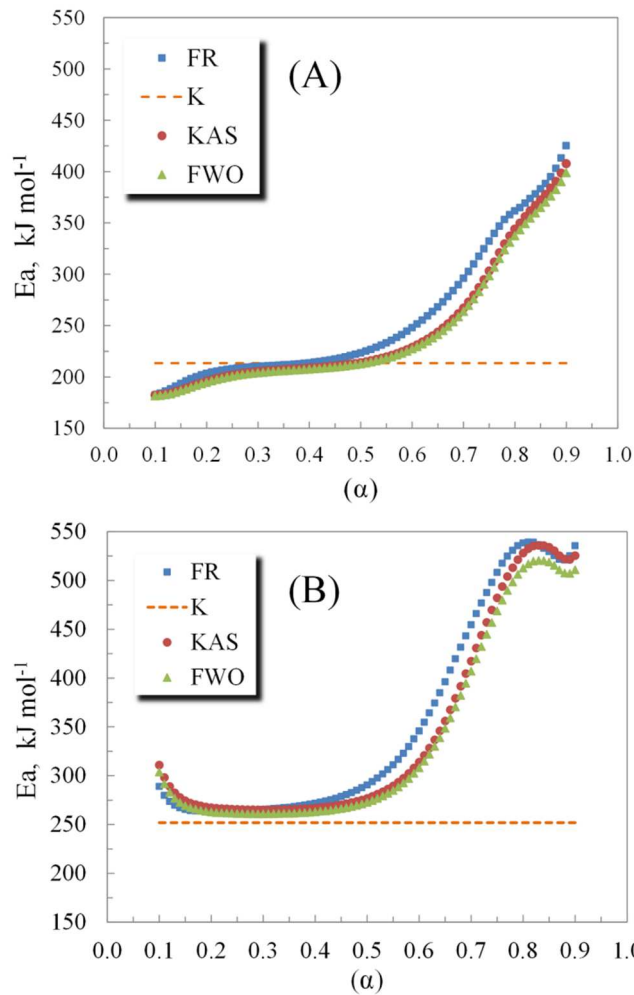
Figure 4-2 The activation energy (Ea) corresponding to degrees of conversion (α) during pyrolysis of (A) Algae 1, and (B) Algae 2 using: Friedman (FR), Kissinger (K), Kissinger-Akahira-Sunose (KAS), and Flynn-Wall-Ozawa (FWO) methods

Table 4-3 The pyrolysis activation energy (Ea), and intercept term (ln z) corresponding to different degrees of conversion (α) for Algae 1 and Algae 2 using Friedman, Kissinger-Akahira-Sunose (KAS), Flynn-Wall-Ozawa (FWO), and Kissinger methods

	(α)	Friedman method E_a (kJ mol^{-1})	Friedman method ln z (s^{-1})	Friedman method r	KAS method E_a (kJ mol^{-1})	KAS method ln z (s^{-1})	KAS method r	FWO method E_a (kJ mol^{-1})	FWO method ln z (s^{-1})	FWO method r
Algae 1	0.2	203.3	37.319	1.000	195.7	32.461	1.000	194.7	47.098	1.000
	0.3	210.1	37.856	0.999	205.1	33.158	1.000	204.0	47.855	1.000
	0.4	213.7	37.738	0.999	208.6	32.874	1.000	207.5	47.617	1.000
	0.5	223.4	38.709	0.999	213.9	32.984	1.000	212.8	47.770	1.000
	0.6	247.8	42.195	0.998	228.8	34.835	0.999	227.2	49.670	0.999
	0.7	296.0	49.348	0.995	267.0	40.565	0.996	263.8	55.467	0.996
	0.8	361.7	57.759	0.991	343.9	51.735	0.990	337.5	66.742	0.990
Kissinger method		213.4	39.815*	0.998						
Algae 2	0.2	263.1	50.229	0.997	267.2	48.025	0.997	262.7	62.662	0.998
	0.3	265.3	49.248	0.997	264.9	45.597	0.998	260.9	60.300	0.998
	0.4	271.6	49.269	0.997	266.8	44.580	0.997	262.9	59.334	0.997
	0.5	290.4	51.609	0.996	276.7	45.197	0.996	272.6	60.000	0.997
	0.6	345.6	60.407	0.994	313.8	50.767	0.994	308.1	65.628	0.995
	0.7	454.5	77.656	0.991	417.3	67.603	0.990	406.9	82.544	0.990
	0.8	538.3	87.512	0.984	527.9	82.781	0.984	512.6	97.834	0.985
Kissinger method		247.8	46.886*	0.999						

*ln A (s^{-1})

Although Friedman method does not rely on the integral approximation which is crucial to the integral methods, the numerical differentiation used in this method magnifies the instrument noise which necessitates data smoothing prior to analysis thus introducing a degree of uncertainty. The activation energies calculated using Kissinger method were 213.4 and 247.8 kJ mol^{-1} for Algae 1 and Algae 2, respectively. These values were constant over the entire range of conversion since they represent one data point, $\alpha - T$ pair, from each thermogram. By contrast, the activation energies computed using Friedman, KAS and FWO methods showed a strong dependence on the degree of conversion (α) in each algae consortium. This dependence, however, can be divided into three stages: $\alpha < 0.20$ where the activation energies fluctuated strongly with the conversion, $0.20 \leq \alpha \leq 0.60$ where the activation energies were not strongly dependent on the conversion degree, and finally, $0.60 < \alpha$ where the activation energies increased dramatically with the progress of decomposition. The increased $E_a - \alpha$ dependence in polymers was associated with parallel reactions, each having different activation energy [32]. Yao et al. (2008) suggested that multistep decomposition mechanisms are the cause for increases E_a at $\alpha > 0.7$ during the pyrolysis of natural fibers [34]. It is worth noting, however, that the activation energy estimated using Kissinger method closely represents the mean activation energy value using Friedman, KAS and FWO during constant activation energy zone, i.e., $0.20 \leq \alpha \leq 0.60$.

Results of pyrolysis modeling using independent parallel reactions (IPR) are detailed in Table 4-4 as well as in Figure 4-3, and Figure 4-4. The IPR model closely captured the weight loss profiles observed during active and passive pyrolysis stages for both algae harvests as shown in Figure 4-3. The quality of fit (QOF $_{DTG}$ %) ranged between 2.09 and 3.31% indicating only minor deviations between calculated and observed weight loss data.
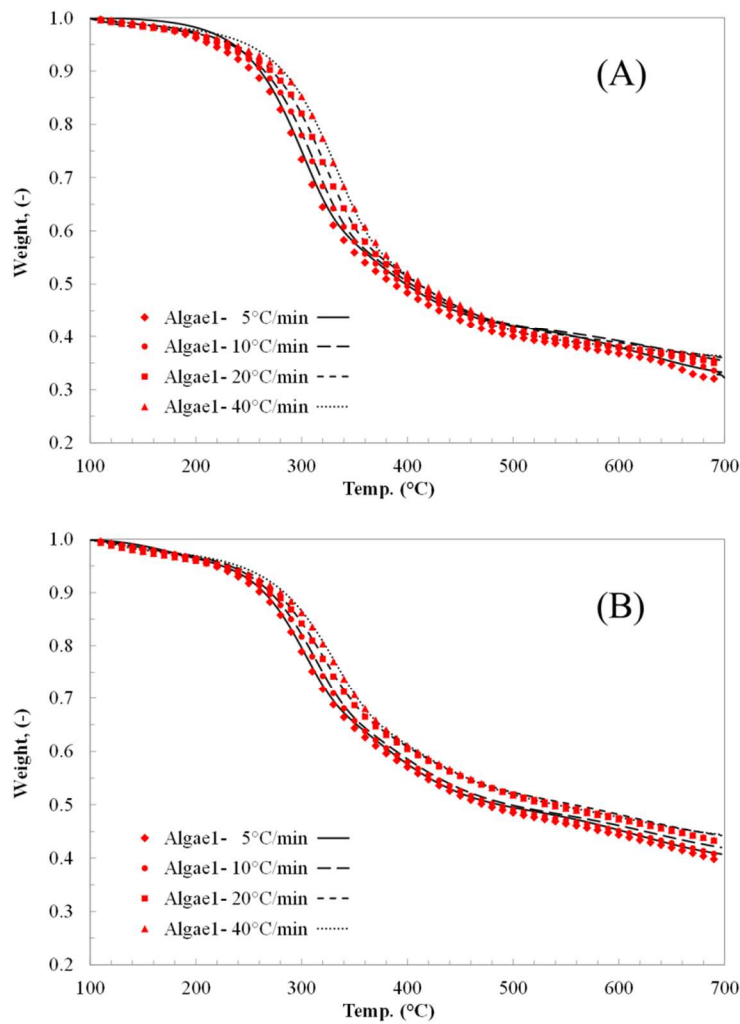
Figure 4-3 Comparison between observed weight loss (markers) and calculated weight loss (lines) using independent parallel reactions (IPR) model for Algae 1 (A) and Algae 2 (B)

First-order reaction model appears to be capable of describing microalgae pyrolysis reactions satisfactorily. Earlier studies used this model to describe the pyrolysis kinetics of various biomass residues such as cardoon stems and leaves, and rice hulls [31, 5].

The apparent activation energies for Algae 1 pyrolysis reactions ranged from 33.26 to 97.66 kJ mol^{-1} while the apparent activation energies for Algae 2 pyrolysis reactions varied

between 33.87 and 97.36 kJ mol^{-1}. Contribution of the modeled pseudo-components to the overall decomposition rate is detailed in Figure 4-4.

In both consortia, the peak devolatilization of each pseudo-component took place at a different temperature, starting at 100° to 120°C for pseudo-component 1(47.00 ~ 49.65 kJ mol^{-1}) which represents the devolatilization of moisture and light hydrocarbons. Between 300°C and 400°C, both pseudo-components 2 and 3 (Table 4-4) showed overlapping peak devolatilization representing the bulk of the total weight loss (between 72% and 92% of total weight loss). Decomposition peak for reaction 2, as shown in Figure 4-4, coincided with the overall peak decomposition observed in both algae as listed in Table 4-2. The two overlapping peaks: reactions 2 and 3 in both consortia appear to represent the decomposition of the main algae ingredients, *i.e.*, protein and starch. The decomposition peaks of individual starch and protein model substances: corn starch and Lysozyme protein [19] appear to resemble the overlapped peaks in Figure 4-4. The fourth pseudo-component showed peak decomposition around 600°C, which represents the passive pyrolysis weight loss.
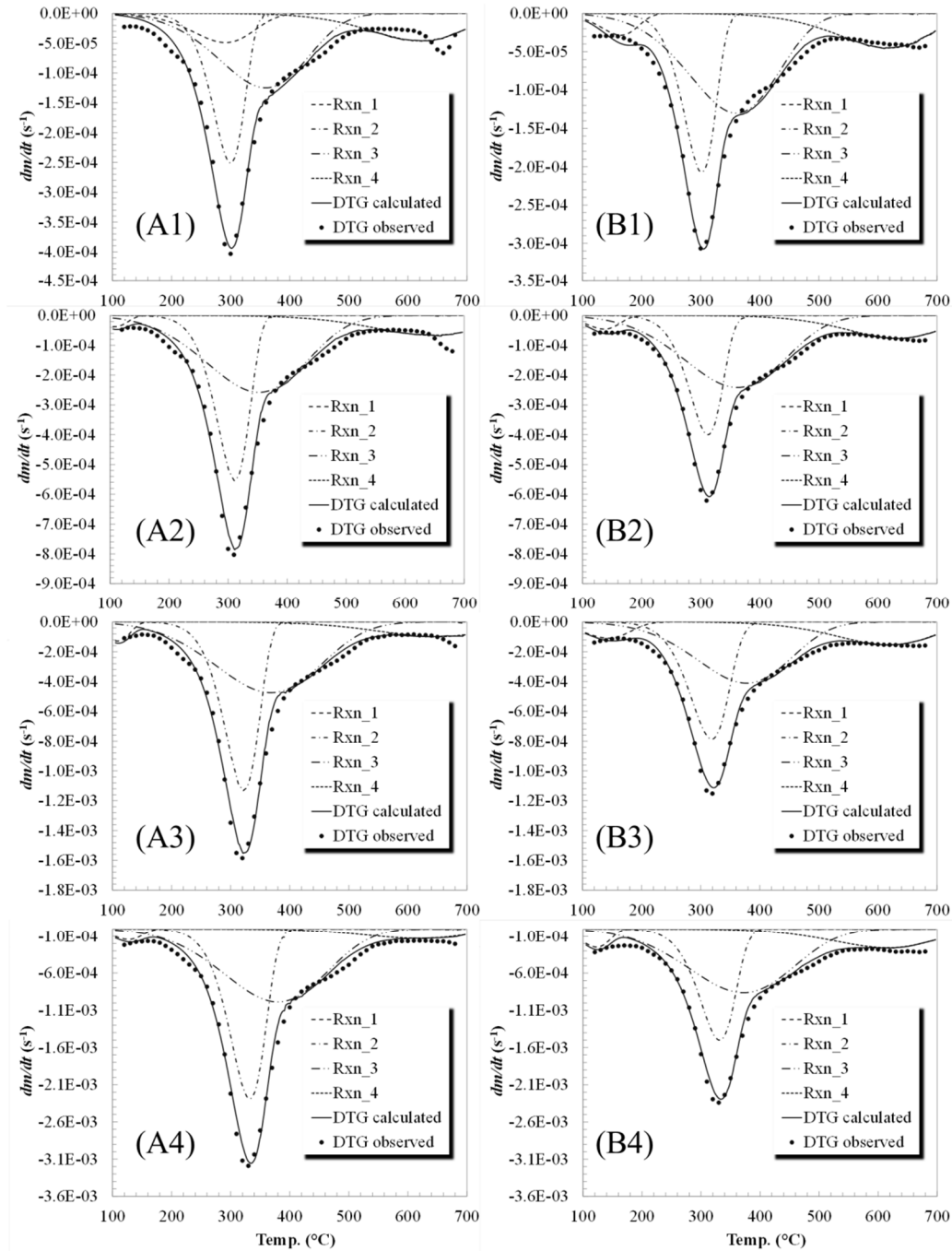
Figure 4-4 Comparison between observed weight loss (markers) and calculated weight loss (lines) using independent parallel reactions (IPR) model for Algae 1 (A) and Algae 2 (B) with the different heating rates, 5, 10, 20 and 40°C min⁻¹, represented by the numerals

Table 4-4 Pyrolysis kinetics of the two algae consortia as modeled using Independent parallel reactions (IPR) model

Reaction	Kinetics	Algae 1				Algae 2			
		5°C min^{-1}	10°C min^{-1}	20°C min^{-1}	40°C min^{-1}	5°C min^{-1}	10°C min^{-1}	20°C min^{-1}	40°C min^{-1}
1	w_1	0.11	0.01	0.02	0.02	0.04	0.03	0.05	0.03
	A_1 (s^{-1})	3.3E+01	3.8E+04	8.6E+04	5.4E+04	1.0E+03	4.3E+03	1.0E+02	9.0E+04
	E_{a1} (kJ mol^{-1})	47.00	49.17	49.65	48.57	47.06	46.20	32.89	49.63
2	w_2	0.31	0.36	0.39	0.42	0.29	0.30	0.35	0.31
	A_2 (s^{-1})	2.1E+06	3.1E+06	3.6E+06	5.3E+06	2.1E+06	2.3E+06	2.7E+05	4.1E+06
	E_{a2} (kJ mol^{-1})	97.09	97.66	97.03	97.24	97.36	96.35	84.23	95.86
3	w_3	0.41	0.49	0.49	0.50	0.49	0.52	0.43	0.51
	A_3 (s^{-1})	1.8E+00	1.1E+00	1.7E+00	4.9E+00	1.8E+00	1.2E+00	5.5E+00	3.6E+00
	E_{a3} (kJ mol^{-1})	39.59	33.60	33.26	35.77	39.59	34.42	39.42	33.87
4	w_4	0.16	0.14	0.11	0.07	0.18	0.15	0.17	0.15
	A_4 (s^{-1})	3.5E+01	1.4E+01	2.8E+01	8.1E+01	3.8E+01	8.6E+01	8.5E+01	8.1E+01
	E_{a4} (kJ mol^{-1})	78.06	69.37	69.35	69.28	78.03	80.49	74.27	69.10
QOF*	DTG (%)	3.31	2.89	2.80	2.76	2.78	2.09	2.54	3.03
	TG (%)	1.62	1.03	0.61	0.55	0.80	0.75	0.56	0.53

*Quality of fit

The differences observed between the apparent activation energies determined using isoconversional methods, and those determined using the independent parallel reactions (IPR) model are attributed in part to the reaction model used. While isoconversional methods determine an overall apparent activation energy without specifying a reaction model (model-free), modeling the pyrolysis kinetics necessitate the assumption of a reaction model with multiple activation energies for the different reactions involved. Damartzis et al. (2011) showed a similar contrast between the activation energies of cardoon pyrolysis determined using isoconversional methods and those using IPR model [5]. They suggested that isoconversional methods are most suited to qualitative evaluations of the pyrolysis process, whereas models such as IPR are more suitable quantitatively to study and model the pyrolysis process.

It is worth noting, however, that in terrestrial biomasses such as wood, and crop residues, the individual pseudo-components resulting from kinetic modelling, such as IPR, can be easily associated with original biomass ingredients, *i.e.*, cellulose, hemicellulose and lignin. However, given the species heterogeneity of the algal consortia investigated here, not to mention the complex structures in individual algal species, it is not possible to map the modeled pseudo-component to specific structural components or intermediate species. Nonetheless, coupling these pseudo-components to the evolved species, via spectral analysis, can offer better understanding of the original species undergoing decomposition.

5. Conclusions

1. The algae genus *Mougeotia* was the common genus in the Algae 1 harvest, while the genus *Cladophra* was predominant in the Algae 2 harvest.

2. In isoconversional methods, the apparent activation energies for pyrolysis of Algae 1 were lower than Algae 2 pyrolysis.

3. Friedman method activation energy values were within 12% of Kissinger-Akahira-Sunose (KAS) and Flynn-Wall-Ozawa (FWO) values.

4. The activation energy dependence on conversion suggests complex reaction schemes which should not be reduced to a single-step reaction.

5. The pyrolysis kinetics of each consortium was modeled using independent parallel reaction (IPR) model as a group of four parallel, independent, first-order reactions.

6. References

[1] Agrawal, A., Chakraborty, S., 2013. A kinetic study of pyrolysis and combustion of microalgae Chlorella vulgaris using thermo-gravimetric analysis, Bioresour. Technol. 128, 72-80.

[2] Blaine, R.L., Kissinger, H.E., 2012. Homer Kissinger and the Kissinger equation, Thermochimica Acta. 540, 1-6.

[3] Carrier, M., Loppinet-Serani, A., Denux, D., Lasnier, J., Ham-Pichavant, F., Cansell, F., Aymonier, C., 2011. Thermogravimetric analysis as a new method to determine the lignocellulosic composition of biomass, Biomass Bioenerg. 35, 298-307.

[4] Conley, D.J., Paerl, H.W., Howarth, R.W., Boesch, D.F., Seitzinger, S.P., Havens, K.E., Lancelot, C., Likens, G.E., 2009. Controlling eutrophication: nitrogen and phosphorus, Science. 323, 1014-1015.

[5] Damartzis, T., Vamvuka, D., Sfakiotakis, S., Zabaniotou, A., 2011. Thermal degradation studies and kinetic modeling of cardoon (C< i> ynara cardunculus) pyrolysis using thermogravimetric analysis (TGA), Bioresour. Technol. 102, 6230-6238.

[6] Demirbas, A., Fatih Demirbas, M., 2011. Importance of algae oil as a source of biodiesel, Energy convers manage. 52, 163-170.

[7] Doyle, C., 1962. Estimating isothermal life from thermogravimetric data, J Appl Polym Sci. 6, 639-642.

[8] Flynn, J.,H., Wall, L.,A., 1966. General Treatment of the Thermogravimetry of Polymers, Journal of Research of National Bureau of Standards- A. Physics and Chemistry. 70Z, 487-523.

[9] Friedman, H.L., 1965. Kinetics of thermal degradation of char-foaming plastics from thermogravimetry: application to a phenolic resin, Journal of Polymer Science. 6, 183-195.

[10] Gai, C., Zhang, Y., Chen, W., Zhang, P., Dong, Y., 2013. Thermogravimetric and kinetic analysis of thermal decomposition characteristics of low-lipid microalgae, Bioresour. Technol. 150, 139-148.

[11] García, R., Pizarro, C., Lavín, A.G., Bueno, J.L., 2013. Biomass proximate analysis using thermogravimetry, Bioresour. Technol. 139, 1-4.

[12] Gomez, C.J., Varhegyi, G., Puigjaner, L., 2005. Slow pyrolysis of woody residues and an herbaceous biomass crop: a kinetic study, Ind Eng Chem Res. 44, 6650-6660.

[13] Gómez, X., Cuetos, M.J., García, A.I., Morán, A., 2007. An evaluation of stability by thermogravimetric analysis of digestate obtained from different biowastes, J. Hazard. Mater. 149, 97-105.

[14] Heathwaite, A., 2010. Multiple stressors on water availability at global to catchment scales: understanding human impact on nutrient cycles to protect water quality and water availability in the long term, Freshwat. Biol. 55, 241-257.

[15] Higgins, S.N., Malkin, S.Y., Todd Howell, E., Guildford, S.J., Campbell, L., Hiriart-Baer, V., Hecky, R.E., 2008. An ecological review of *Cladophora glomerata* (Chlorophyta) in the Laurentian great lakes1, J. Phycol. 44, 839-854.

[16] Jenkins, B., Baxter, L., Miles Jr, T., Miles, T., 1998. Combustion properties of biomass, Fuel Process Technol. 54, 17-46.

[17] Jones, D.B., 1941. Factors for converting percentages of nitrogen in foods and feeds into percentages of proteins. US Department of Agriculture Washington, DC.

[18] Kebede-Westhead, E., Pizarro, C., Mulbry, W.W., 2006. Treatment of swine manure effluent using freshwater algae: production, nutrient recovery, and elemental composition of algal biomass at four effluent loading rates, J. Appl. Phycol. 18, 41-46.

[19] Maddi, B., Viamajala, S., Varanasi, S., 2011. Comparative study of pyrolysis of algal biomass from natural lake blooms with lignocellulosic biomass, Bioresour. Technol. 102, 11018-11026.

[20] Mani, T., Murugan, P., Abedi, J., Mahinpey, N., 2010. Pyrolysis of wheat straw in a thermogravimetric analyzer: Effect of particle size and heating rate on devolatilization and estimation of global kinetics, Chemical Engineering Research & Design: Transactions of the Institution of Chemical Engineers Part A. 88, 952-958.

[21] McCoy, B.J., 1999. Distribution kinetics for temperature-programmed pyrolysis, Ind Eng Chem Res. 38, 4531-4537.

[22] Morris, M.K., 1982. Effects of wastewater discharges on periphyton growth in Lake Mead, Nevada-Arizona,.

[23] Muller-Feuga, A., 2000. The role of microalgae in aquaculture: situation and trends, J. Appl. Phycol. 12, 527-534.

[24] Na, J., Lee, H.S., Oh, Y., Park, J., Ko, C.H., Lee, S., Yi, K.B., Chung, S.H., Jeon, S.G., 2011. Rapid estimation of triacylglycerol content of Chlorella sp. by thermogravimetric analysis, Biotechnol. Lett. 33, 957-960.

[25] Ozawa, T., 1965. A New Method of Analyzing Thermogravimetric Data, Bull. Chem. Soc. Jpn. 38, 1881-1886.

[26] Pittman, J.K., Dean, A.P., Osundeko, O., 2011. The potential of sustainable algal biofuel production using wastewater resources, Bioresour. Technol. 102, 17-25.

[27] Sanchez, M., Otero, M., Gomez, X., Moran, A., 2009. Thermogravimetric kinetic analysis of the combustion of biowastes, Renewable Energy. 34, 1622-1627.

[28] Sharara, M., Sadaka, S., 2014. Thermogravimetric Analysis of Swine Manure Solids Obtained from Farrowing, and Growing-Finishing Farms, Journal of Sustainable Bioenergy Systems. 4, 75-86.

[29] Skulberg, O.M., 2004. 30 Bioactive Chemicals in Microalgae, Handbook of Microalgal Culture: Biotechnology and Applied Phycology. 485.

[30] Starink, M., 2003. The determination of activation energy from linear heating rate experiments: a comparison of the accuracy of isoconversion methods, Thermochimica Acta. 404, 163-176.

[31] Teng, H., Wei, Y., 1998. Thermogravimetric studies on the kinetics of rice hull pyrolysis and the influence of water treatment, Ind Eng Chem Res. 37, 3806-3811.

[32] Vyazovkin, S., 1996. A unified approach to kinetic processing of nonisothermal data, Int J Chem Kinet. 28, 95-101.

[33] Xin, L., Hong-ying, H., Ke, G., Ying-xue, S., 2010. Effects of different nitrogen and phosphorus concentrations on the growth, nutrient uptake, and lipid accumulation of a freshwater microalga Scenedesmus sp. Bioresour. Technol. 101, 5494-5500.

[34] Yao, F., Wu, Q., Lei, Y., Guo, W., Xu, Y., 2008. Thermal decomposition kinetics of natural fibers: activation energy with dynamic thermogravimetric analysis, Polym. Degrad. Stab. 93, 90-98.

[35] Zhao, H., Yan, H., Dong, S., Zhang, Y., Sun, B., Zhang, C., Ai, Y., Chen, B., Liu, Q., Sui, T., 2013. Thermogravimetry study of the pyrolytic characteristics and kinetics of macro-algae Macrocystis pyrifera residue, Journal of thermal analysis and calorimetry. 111, 1685-1690.

Chapter 5 Combustion Kinetics of Swine Manure and Algal Solids

1. Abstract

In this study, combustion kinetics of swine manure, as well as algae grown using swine manure wastewater were investigated. Four heating rates (1, 5, 10, and 20°C min^{-1}) were used to determine combustion kinetics using thermogravimetry. Swine manure solids showed higher carbon concentration (10.6%) and hydrogen concentration (18.8%) as well as energy content (14.2%) than algal biomass solids. Each feedstock showed a distinct decomposition profile that increasingly shifted with increasing the heating rate. The combustion kinetics were determined using Kissinger method, Flynn-Wall-Ozawa (FWO), and Kissinger-Akahira-Sunose (KAS). Differences between FWO and KAS were below 2% throughout the entire conversion. Average activation energy for swine manure and algae, using FWO, were 172.6 kJ mol^{-1}, and 165.1 kJ mol^{-1}, respectively. Combustion of three blends of algae-swine manure solids were studied at 10°C min^{-1} with no synergistic effects observed.

2. Introduction

The objective of this study is evaluating the air combustion kinetics of both swine manure separated solids, and microalgae that were grown on swine wastewater slurries. The impetus behind this research is the significant contribution of livestock production to global Greenhouse gas (GHG) emissions, i.e., more than 18% [25]. A large proportion of these emissions is attributable to manure management practices, which include: manure open-pit storage, and manure application to cropland, resulting in CO_2, CH_4 and N_2O emissions. Expansions in swine production and increases in the number of animals per farm further have compounded the manure problem. Due to the large volumes of manure per farm, combined with the high cost of

its transportation, manure is occasionally applied to agricultural fields at rates beyond the assimilative capacity of the soil, resulting in over-application. In addition to increasing GHG emissions, over-application also results in nutrient runoff and in contamination of groundwater and surface-water reserves [4]. Many approaches are available to mitigate the challenges associated with swine manure management while also utilizing its energy content. A promising technique is liquid-solid separation of swine manure followed by thermochemical conversion of the manure solids, i.e., incineration, gasification or pyrolysis [28]. Sommer *et al.* (2009) evaluated various manure management scenarios and technologies with respect to their impact on GHG emissions [26]. They reported a reduction between 49% and 82% in emissions with the separation and incineration of manure as compared to the baseline scenario of outside storage then land application to grassland or arable soils.

Reducing the nutrient loading of swine manure slurry is among the main strategies to cope with the increasing manure reserves and declining arable lands for application. The treatment of wastewater by algae cultivation was shown to help reduce nitrogen, phosphorous, and heavy metals loading in the water effluent while also reducing its chemical oxygen demand (COD) [7, 27]. Kebede-westhead *et al.* (2003, 2006) investigated the efficacy of scrubber algal consortium in removing nutrients and heavy metals from dairy and swine manure effluents [8, 9]. Nutrient removal efficiencies were found to be dependent on the nutrient loading rates, temperature, and insolation. The low fatty acids content in the algae harvested from water remediation applications makes them unlikely feedstock for lipid-extraction or biofuel production [14]. Alternative uses of the harvested algal biomass include composting, direct land application, and incineration. The implementation of a creative manure management scenario could prove beneficial. As an example, solid-liquid separation of the manure, and the utilization

of the liquid fraction for algae cultivation, and finally harvesting the algae solids, and utilizing algae and manure solids for thermochemical conversion could be implemented. This scenario can potentially reduce the overall GHG emissions and the nutrients runoff while also generating two biomass streams (manure, and algal solids) with medium to high heating values (14 ~ 21 kJ g^{-1}) [24, 5].

The study of biomass thermal decomposition under a controlled environment is essential to the development of large-scale conversion platforms. Thermogravimetric analyses (TGA) facilitate the study of biomass decomposition in various gas environments under isothermal or non-isothermal conditions. An earlier study investigated the pyrolytic decomposition kinetics of two different swine manure solids, in nitrogen environments, using model-free kinetics methods [22]. Otero *et al.* (2011) investigated the kinetics of co-firing coal and swine manure biomass and determined the activation energies for their blends [16]. Similarly, several studies examined the pyrolysis of various micro- and macro-algal species and reported a varying range of activation energies [13, 1, 21]. Sanchez-Silva *et al.* (2013) investigated pyrolysis, oxidation, and gasification of *Nannochloropsis gaditana* alga species [19]. Very few studies reported on the combustion kinetics of swine manure solids, or algae consortia produced on a wastewater substrate. Also, to our knowledge, no studies investigated the combustion characteristics of blends of swine manure with algal solids.

The goal of this study was to investigate the combustion characteristics of swine manure solids, and microalgae biomass solids, both harvested from the same production system. Also, this study reported the combustion kinetics for both feedstocks using various model-fitting and model-free methods. Finally, the combustion of swine manure-algal consortia blends was investigated to characterize potential interaction between these two feedstocks.

3. Materials and Methods

3.1. Swine manure

In this study, swine manure was collected from a growing-finishing farm (Washington County, Arkansas), which houses 818 hogs. This farm is part of an Arkansas Agricultural experiment station, Division of Agriculture, at the University of Arkansas, Fayetteville. Since no mechanical solids separation was practiced on farm, the manure sludge was collected directly from the settling pond using a fine-meshed sampling bag. Pyrolysis kinetics of these manure solids have been previously reported [22].

3.2. Microalgae solids

The microalgae biomass used in this study was grown in a series of open channels, 3.0 m × 0.15 m, using diluted swine manure slurries collected from the same hog farm mentioned earlier. The dilution was performed to maintain the levels of dissolved ammonia (NH_3) in the slurry below 40 mg L^{-1}. Details of NH_3 loading influence will be discussed in a separate publication. The algae growth channels were lined with fibrous media to facilitate attachment. The algal growth system was open during production without control over the growing species. The microalgae harvest followed a 5-day cycle using rubber-bladed scrapers. An earlier study investigated the pyrolysis kinetics of these algal consortia [21].

3.3. Material preparation and analysis

After collection, swine manure and microalgae were stored separately in airtight plastic containers and kept at 4°C for at least 48 hours. Later, each feedstock was thawed at room temperature then oven-dried at 105°C for 24 h. Dried manure and microalgae were ground using a cutting mill to 1 mm particle size (Thomas Wiley® cutting mill- Model 3383L10, Swedesboro,

NJ). Samples were collected from the ground microalgae and swine manure solids to perform various analyses. A fraction of the ground, dried manure solids and microalgae was further ground to less than 200μm diameter (1 μm = 10^{-6} m) for use in thermogravimetric analyses using a cutting mill (Polymix PX-MFC 90 D, Kinematica AG, Switzerland).

The moisture in the dried, ground feedstock was quantified as the weight loss after drying for 24 h at 105°C, following procedure ASTM E871 – 82 (2006). The volatile matter and ash contents were determined according to standards: ASTM E872 – 82 (2006), and ASTM D2974-87 (2007), respectively, whereas the fixed carbon content (%) was determined by weight differences. Elemental analysis of each feedstock was performed in a diagnostic laboratory (Huffman Laboratories, Golden, CO, USA). The higher heating values (HHV) were determined using bomb calorimetry (Parr instruments, Model 1341, Moline, IL, USA) according to the standard method, ASTM D5865-12 (2012).

3.4. Thermogravimetric analysis

Oxidative decomposition of swine manure solids and microalgae biomass was investigated using a thermogravimetric analyzer (Model TGA 4000, PerkinElmer, Inc. Waltham, MA, USA). The samples were heated in air environments (50 mL min^{-1}) from 30°C to 800°C at 4 different linear heating rates: 1, 5, 10 and 20°C min^{-1}, where sample temperature and mass were recorded as a function of time. In each test, the data-sampling rate was 1 data point $second^{-1}$. Sample size was kept consistently at 1.0 ± 0.1 mg (1 mg= 10^{-6} kg) to minimize mass and heat transfer limitations relevant in gas-solid reactions such as combustion. The samples were heated in alumina crucibles (Al_2O_3), which were cleaned and ashed between tests. Also, thermogravimetric tests were performed using an empty clean crucible, under each heating rate

mentioned earlier, to quantify and subtract the crucible buoyancy effect from the thermogravimetric data.

3.5. Manure-algae blends

Representative samples from dry, ground algae and manure solids were used to create blends with different mixing ratios. Three blends of algae and swine manure were prepared with three mixing ratios: 1:3, 1:1, and 3:1, on a weight-basis. TGA tests of each of these blends were studied at one heating rate, 10°C min^{-1}.

3.6. Data processing

Temperature, time and weight data for each test were imported to the MATLAB software package (MATLAB R2014a, The Mathworks, Inc., Natick, MA, USA) then smoothed using a Gaussian filter routine (σ =7.0) [12]. Weight loss (TG) and weight loss derivatives (DTG) were generated using the smoothed data in each test. The following section details the theory and the corresponding mathematical expressions used to determine the combustion kinetics in swine manure solids and algal biomass.

3.7. Theory

The sample conversion (α) is represented by the change in the sample weight:

$$\alpha = \frac{W_o - W_t}{W_o - W_\infty} \tag{1}$$

Where W_o, W_∞, and W_t are the sample starting weight, final weight, and the weight at intermediate time t, respectively. The conversion temperature-derivative ($d\alpha/dT$) is presented in the following equation:

$$\frac{d\alpha}{dT} = \frac{A}{\beta} \exp\left(\frac{-E_a}{RT}\right) f(\alpha) \tag{2}$$

The reaction kinetic parameters, i.e., A, E_a, and $f(\alpha)$ define the sample decomposition rate. A is the frequency factor, E_a the activation energy, and $f(\alpha)$ is a conversion-dependent function. This

triplet depends on the sample nature, as well as on the reaction conditions. β, R and T represent the sample heating rate, the universal gas constant, and the sample absolute temperature, respectively. The integration of equation (2) yields:

$$g(\alpha) = \int_0^T \frac{A}{\beta} \exp\left(\frac{-E_a}{RT}\right) dT \tag{3}$$

where $g(\alpha)$ is the integral form of $f(\alpha)$. In this study, three different methods were used to determine the combustion kinetic parameters for swine manure and algal biomass, i.e., Kissinger, Kissinger-Akhaira-Sunose (KAS), and Flynn-Wall-Ozawa (FWO). Each of these methods requires at least 3 tests at different (β) in order to extract the kinetic parameters. These methods all belong to isoconversional methods, where the reaction rate parameters for conversion at different heating rates (β) are determined for points corresponding to the same degree of conversion (α).

Kissinger method

In this method, the conversion-dependent function, $f(\alpha)$, is assumed to be first-order, i.e., $f(\alpha) = (1 - \alpha)$. Also, the activation energy (E_a) and frequency factor (A) are determined at the peak decomposition rate, $(d\alpha/dt)_{max}$, using the corresponding temperatures, T_{max}, under different heating rates (β). Accordingly, the following linearized relationship (equation 4) is used to extract the reaction parameters from multiple thermogravimetric tests:

$$\ln\left(\frac{\beta}{T_{max}^2}\right) = \ln\left(\frac{AR}{E_a}\right) - \frac{E_a}{RT_{max}} \tag{4}$$

Plotting $\ln(\beta/T_{max}^2)$ versus ($1/T_{max}$) yields a straight line with the slope (E_a/R), and the intercept $\ln(AR/E_a)$, which are then used to determine the activation energy (E_a) and frequency factor (A) values.

Kissinger-Akahira-Sunose (KAS) method

In this modified Kissinger method, the assumption that the reaction is first-order is dropped and instead, *f(α)* is coupled with the intercept term as shown in equation (5) below. This method determines the reaction rate parameters over the entire decomposition range, not only at the peak decomposition points.

$$\ln\left(\frac{\beta}{T^2}\right) = \ln\left[\frac{AR}{E_a}\right] - \ln(g(\alpha)) - \frac{E_a}{RT} \qquad (5)$$

Equation (5) yields a family of straight-lines by plotting *ln* (β/T^2), and $1/T$ values corresponding to different conversion (α) degrees, at different *heating rates (β)*. The activation energy, E_a, at each (α) is determined from the slope term, while the combined intercept term represent the frequency factor, *A*, and the integral form of the decomposition model, *g(α)*.

Flynn-Wall-Ozawa (FWO) method

Similar to KAS, this method uses a linearized form of the integral expression in equation (3) to determine the kinetic triplet:

$$\ln\beta = \ln\left[\frac{AE_a}{Rg(\alpha)}\right] - 5.33 - 1.052\left(\frac{E_a}{RT}\right) \qquad (6)$$

(ln β) and *(1/T)* for each heating rate *(β)* are plotted at the different conversion degrees *(α)* then fitted to a straight line. The slope term, in each straight line, represents the apparent activation energy, (-1.052 E_a/R), while the intercept combines the reaction model in its integral form, *g(α)*, the apparent activation energy, E_a ,and the frequency factor, *A*.

4. Results and discussion

4.1. Proximate, elemental and heating value analyses

Table 5-1 shows the composition of manure solids and algal biomass solids used in this study. The volatile matter content in the swine manure solids, 70.95%, and the algal biomass, 71.40%, were not significantly different (t-test, *p*= 0.42).. The mean ash content of the algal

biomass was significantly higher than that in the swine manure solids (t-test, $p<0.0001$). This difference is can be attributed to the type of microalgae grown, the amount of salt and minerals in the growth substrate, and the amount of salt absorbed with intercellular water in the algae. Both values, however, were appreciably higher than those reported for wood and perennial grasses, i.e., <10% [18]

Table 5-1 Proximate, elemental and heating value analyses of algae and swine manure

		Algae	Swine Manure
Proximate analysis (db%*)			
	Volatile matter	71.40	70.95
	Fixed carbon**	10.41	18.15
	Ash	18.19	10.90
Ultimate analysis (db %)			
	C	41.5	46.4
	H	5.6	6.9
	N	5.4	1.8
	S	0.51	0.6
	O**	27.0	33.4
HHV $_{bomb\ calorimetry}$*** (kJ g^{-1})		16.62	19.39
HHV$_{[21]}$ (kJ g^{-1})		16.59	19.16

*dry weight basis
**by difference
***Higher heating value per unit dry weight

In addition to the ash differences, the organic matter composition showed variability between both feedstocks as evidenced by the C, H, N, and O contents. The higher C and H contents in the swine manure and low ash content, as compared to algal biomass, may account for the difference in the higher heating values. Elevated levels of carbon and hydrogen indicate the presence of unoxygenated hydrocarbons, which resulted in high combustion enthalpies. In addition to bomb calorimetry determination, a predictive correlation developed by Sheng and Azevedo (2005) was used to estimate the heating value of both feedstocks from their elemental composition [23]. Although the latter correlation was developed by regression of data obtained from lignocellulosic biomass, the model showed good agreement with calorimetery values, i.e., 0.24%, and 1.17% below the calorimetrically determined values. The heating values of algae and swine manure solids were sensitive to the ash content, and consequently, to their production conditions. When grown under nitrogen-limited conditions, the alga species *Chlorella vulgaris* was shown to store high amounts of lipid and, consequently, exhibited a higher calorific content, 28 kJ g^{-1} [20]. The composition of manure solids was reported to depend on the age and storage conditions [17]. Biological decomposition of manure, whether aerobic or anaerobic, resulted in a loss of organic matter and, correspondingly, a loss of stored chemical energy.

4.2. Thermogravimetric decomposition

Figure 5-1 shows the weight loss (TG), and weight loss derivative (ash-free basis) (DTG) during air combustion of algal and swine manure solids under different heating rates. Increasing in the heating rate (β) resulted in a delay in the weight loss towards higher temperatures. Only marginalweight loss occurred below 200°C in both feedstocks, mostly due to moisture evaporation. Above 200°C, however, the weight loss proceeded in two consecutive stages, i.e., devolatilization, and char oxidation, as indicated by the weight loss derivative plots. Similar

weight loss profiles were observed in oxidative tests of miscanthus, poplar and rice husks [11].
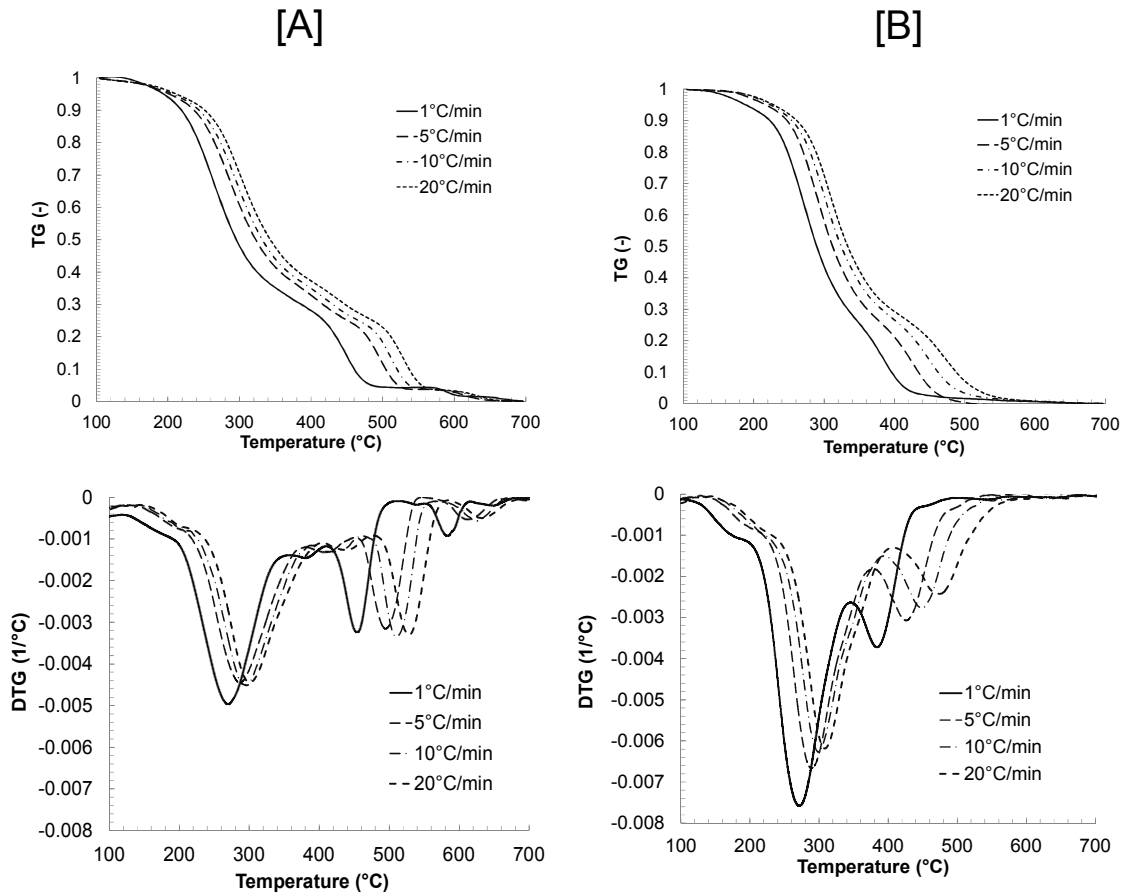
Figure 5-1 Thermogravimetric weight loss (TG) (ash-free basis) and its derivative (DTG) for [A] algae and [B] swine manure samples, at heating rates (β) = 1, 5, 10, and 20°C min^{-1}

The first stage, below 350°C, marked the destruction and devolatilization of labile

organic species, such as hemicellulose (starch), through pyrolytic reactions. Comparisons

between peak weight loss temperatures for swine manure and algae solids, during this stage,

show algae peak decomposition to precede swine manure decomposition peaks (Table 5-2).

However, decomposition peaks for swine manure solids during this stage were between 40% and

50% higher than those observed during algae decomposition. This step typically involves

autocatalytic, solid-phase reactions, which are also observed under inert (oxygen-free)

conditions.

117

Table 5-2 Combustion characteristics for algae and swine manure samples under different heating rates

Feedstock	Heating rate	Devolatilization stage		Char Oxidation stage	
		$-(dW/dT)_p$	T_p	$-(dW/dT)_p$	T_p
	($°C\ min^{-1}$)	(% $°C^{-1}$)	(°C)	(% $°C^{-1}$)	(°C)
Algae					
	1	0.497	269.6	0.324	454.3
	5	0.446	287.1	0.316	494.7
	10	0.451	296.0	0.334	509.7
	20	0.444	300.5	0.330	528.1
Swine Manure					
	1	0.758	270.7	0.372	383.9
	5	0.667	289.3	0.318	426.2
	10	0.627	299.0	0.307	448.6
	20	0.618	308.1	0.277	474.4

In an earlier study of inert thermal decomposition (pyrolysis) for the same algal consortia, initial decomposition peaks where observed at 298.6, 308.0, and 315.7°C for the heating rates 5, 10, and 20°C min^{-1}, respectively [21]. Comparing these values with the ones obtained under air conditions in the current study (Table 5-2) delineates the fact that oxidative conditions expedited the initial decomposition stage as evidenced by the shift in maximum decomposition rate point, between 12 and 15°C. This shift is attributed to a mild oxidative effect, which contributes to decomposition through low-temperature oxidation of labile species. In a study of thermal decomposition of pinewood waste, the increase in oxygen concentration also resulted in a shift of the first decomposition peak towards lower temperatures [3]. These observations indicate that oxidation and thermal devolatilization both occur in parallel at low temperatures. However, in a thermogravimetric study of dairy manure decomposition under inert and oxidative conditions,

the first major peak under inert conditions occurred earlier, at 290°C, than under oxidative

conditions, at 300°C [29].

The char oxidation stage began in both feedstocks above 350°C. In algae, char oxidation

proceeded over a wider temperature range and encompassed multiple decomposition peaks, as

illustrated in Figure 5-1. During char oxidation stage, maximum weight loss rate in algae

occurred between at 50 to 70°C higher than that of swine manure. Magnitude of char oxidation

rate (derivative) in both feedstocks, however, did not vary greatly (Table 5-2). The observed

gradual shift in the shape of char oxidation peaks with increases in the heating rate, i.e., spread of

the peak at the base, for both biomass illustrated the mass-transfer limiting nature of the

oxidation process. Since char oxidation is a solid-gas reaction, its progress depends primarily on

the diffusion of the oxidizing agent within the sample matrix. Increasing the heating rate resulted

in less available time for sample oxidation at each temperature point, resulting in a spread of the

decomposition step over a wider temperature range.

4.3. Oxidation kinetics

Kinetics of decomposition over the two stages, pyrolysis, and oxidation, were calculated

at the respective peak decomposition points using Kissinger method (Table 5-3). The goodness-

of-fit, R^2, and p-values for the linear regression in both stages in each feedstock indicated a good

fit. In the algal and swine manure solids, the activation energy corresponding to the pyrolytic

decomposition, the first peak, was higher than that associated with the char decomposition peak.

This observation could be explained by the differences, outlined earlier, in the nature of pyrolysis

and oxidation reactions; mainly that the pyrolytic decomposition stage could be temperature-

sensitive than char oxidation. The activation energy associated with pyrolytic decomposition of algal biomass, 236.8 kJ mol^{-1}, exceeded that for swine manure, 198.9 kJ mol^{-1}. In an earlier study, the mean activation energy using Kissinger method for the same algal biomass in a nitrogen atmosphere was 213.4 kJ mol^{-1} [21], which is below the value observed in this work for the first stage of decomposition under oxidative conditions.

Table 5-3 Combustion kinetics in algae and swine manure using Kissinger method

Decomposition kinetics	Algae	Swine Manure
Stage I (Devolatilization)		
E_a, kJ mol^{-1}	236.8	198.7
A, s^{-1}	9.28E+19	1.60E+16
R^2	0.9993	0.9993
Stage II (Char Oxidation)		
E_a, kJ mol^{-1}	184.17	124.21
A, s^{-1}	5.1E+5	3.0E+2
R^2	0.998	0.998

The activation energies using isoconversional methods, i.e., Flynn-Wall-Ozawa (FWO) and Kissinger-Akahira-Sunose (KAS) are shown in Figure 5-2, and also in Table 5-4. Activation energy, and corresponding standard errors, obtained by fitting the experimental data to equations (5) and (6) at $\Delta\alpha$= 0.01 intervals are presented in Figure 5-2. The standard errors, corresponding to each fitted E_a value, were consistently below 10% of the activation energy value, and the R^2 values were over 0.98, indicating a good fit. In manure and algal solids, differences in activation energy (E_a) values between isoconversional methods, i.e., FWO and KAS, for the same feedstock were below 2% throughout the entire conversion.
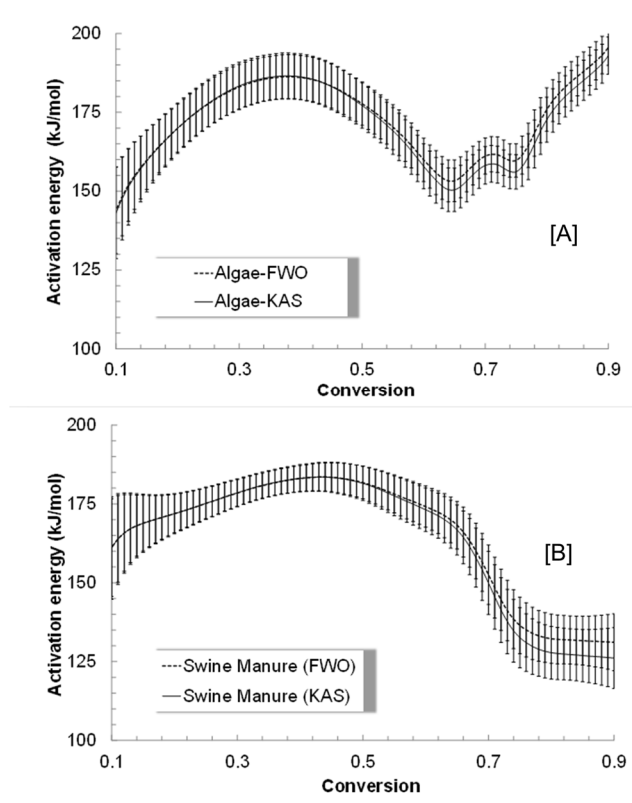
Figure 5-2 Activation energy (Ea) of [A] algae and [B] swine manure solids as a function of the conversion (α) using isoconversional methods: Kissinger-Akahira-Sunose (KAS) and Flynn-Wall-Ozawa (FWO)

E_a increases with conversion (α) up to $\alpha = 0.4$, where the activation energies for algal and swine manure solids were 186.1 and 183.1 kJ mol^{-1}, respectively. As the conversion progressed further, however, each feedstock showed a distinctly different relationship of E_a as a function of α. In swine manure solids, the activation energy gradually decreased between $\alpha = 0.4$ and 0.6. As the conversion continued, $\alpha > 0.7$, however, the activation energy dropped more precipitously to reach 126.1 kJ mol^{-1} at $\alpha = 0.9$. Algal solids, on the other hand, showed two increases in the activation energy values, at $\alpha > 0.7$. It is apparent that algal solids oxidation involves multiple steps that take place over a wider temperature range, when compared to combustion of swine

manure solids. Despite these differences, averaged values of the activation energy over the entire conversion range, i.e., $0.1 \leq \alpha \leq 0.9$, were similar. The average activation energy for algae and swine manure solids using FWO method, were 172.6 ± 12.4 kJ mol^{-1} and 165.1 ± 18.8 kJ mol^{-1}, respectively. Similarly, the average activation energy for algae and swine manure solids using KAS method were 171.3 ± 13.0 kJ mol^{-1}, and 163.1 ± 20.6 kJ mol^{-1}, respectively. A recent study of oxidation kinetics for algae species *Nannochloropsis oculta* and *Chlorella vulgaris* reported average activation energy values using FWO to be 151.8 and 213.4 kJ mol^{-1}, respectively [2]. In a study investigating combustion characteristics of swine manure solids-coal blends, the average activation energy for the combustion of swine manure solids, using FWO method, was 119.6 kJ mol^{-1} [16].

Table 5-4 Combustion kinetics in algae and swine manure using Flynn-Wall-Ozawa (FWO), and Kissinger-Akahira-Sunose (KAS) methods

	(α)	Flynn-Wall-Ozawa (FWO)			Kissinger-Akahira-Sunose (KAS)		
		E_a (kJ mol^{-1})	Ln z (s^{-1})	R^2	E_a (kJ mol^{-1})	Ln z (s^{-1})	R^2
Algae	0.1	144.0	33.5	0.982	143.1	19.0	0.980
	0.2	170.0	37.6	0.996	169.9	23.0	0.996
	0.3	183.1	39.2	0.997	183.4	24.6	0.997
	0.4	186.1	38.6	0.997	186.2	23.9	0.997
	0.5	177.7	35.4	0.997	177.2	20.6	0.997
	0.6	159.9	29.7	0.996	157.9	14.9	0.996
	0.7	161.1	27.2	0.997	158.2	12.1	0.997
	0.8	175.9	27.2	0.997	172.7	12.0	0.997
	0.9	195.6	29.4	0.998	193.0	14.1	0.998
Swine manure	0.1	161.2	36.9	0.982	161.0	22.5	0.980
	0.2	171.9	37.6	0.997	171.9	23.0	0.997
	0.3	178.5	38.0	0.999	178.5	23.4	0.999
	0.4	183.1	38.1	0.999	183.1	23.4	0.999
	0.5	181.8	36.8	0.998	181.5	22.1	0.998
	0.6	174.1	33.9	0.997	173.2	19.1	0.997
	0.7	152.5	27.8	0.992	149.9	12.9	0.991
	0.8	132.2	22.1	0.993	127.8	7.0	0.992
	0.9	131.1	20.8	0.991	126.1	5.7	0.989

4.4. Combustion of Algae-swine manure blends

Weight-loss and weight-loss derivatives, at 10°C min^{-1}, for the oxidation of algae and swine manure solids, and their blends are shown in Figure 5-3. The three algae to manure blending ratios: 1:3, 1:1, and 3:1, all exhibited intermediate profiles between those of pure algae or of swine manure. The DTG curves illustrate the transition in the decomposition rate with the change in the blending ratio. Increasing the share of swine manure in the blends reduced the temperature range associated with the weight loss, and increased the devolatilization stage

weight loss, height of first DTG peak. Similarly, temperature corresponding to the devolatilization peak (stage 1) increased with the increase in the ratio of swine manure solids in the blends (Table 5-5).
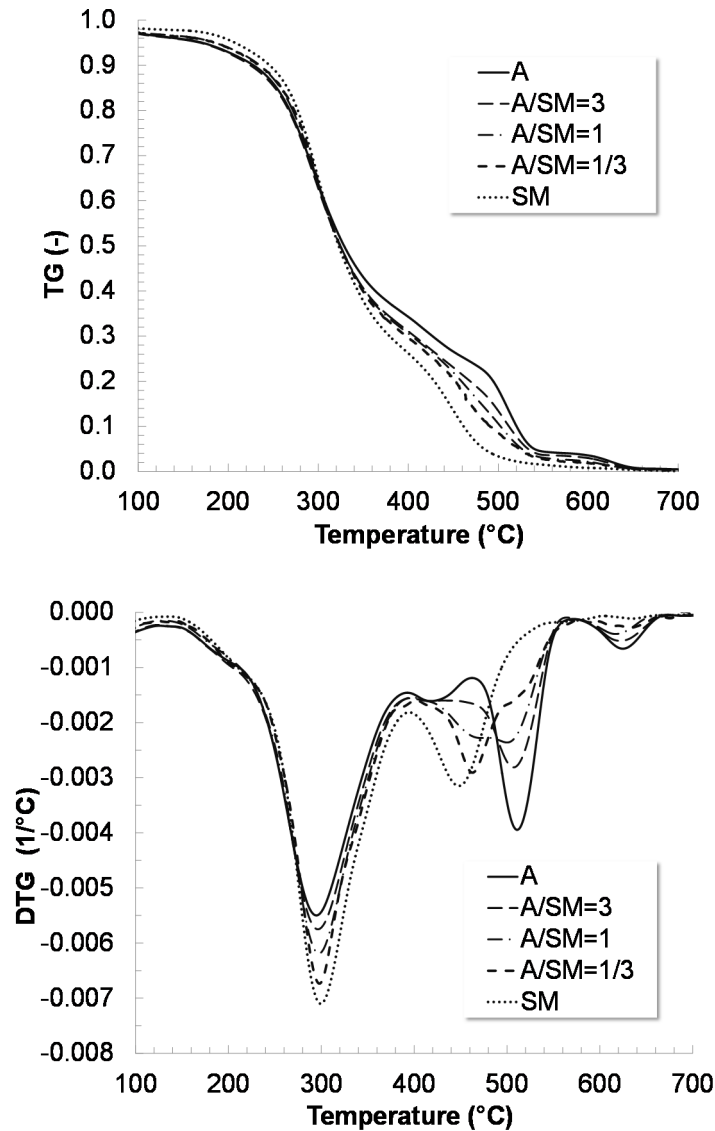
Figure 5-3 The influence of the mixing ratios of algae (A) and swine manure (SM) on the weight loss (TG) (ash-free basis) and temperature derivative of weight loss (DTG) of mixtures at heating rate (β)=10°C min^{-1}

The transitions of the TG and DTG curves, as well as the decomposition rate maxima values, suggested a summative effect of blending. To quantify these observations, the normalized root-

mean-square deviation (*NRMSD*) was calculated in each blend between the experimental data
and the corresponding weighted average calculated using data from pure algae and swine manure
oxidation. The *NRMSD* (%) was calculated for both the TG and DTG data of the 3 blends using
the following equation:

$$NRMSD \ (\%) = 100 * \frac{\sqrt{\frac{1}{p}\sum_{n=1}^{p}(Y_n - \widehat{Y_n})^2}}{Y_{max} - Y_{min}}$$
(7)

Where *p* represents the number of weight-loss observations in each test (4,166 points at this
heating rate), *Y* represents *TG* (or *DTG*) data at each observation, and $\widehat{Y}$ represents the weighted
mean value corresponding to each *Y*. *Y*$_{max}$ and *Y*$_{min}$ represent the maximum and minimum *TG* (or
DTG) values, respectively. The *NRMSD* (%) values for the *TG* data in the three blends, i.e.,
algae: swine manure = 3:1, 1: 1, and 1: 3 were 1.5, 0.6, and 1.2%, respectively. For the DTG
data, the *NRMSD* (%) values were 1.7, 2.4, and 7.3%, respectively.

Table 5-5 Combustion characteristics for algae and swine manure blends at 10°C min^{-1}

Feedstock	Devolatilization stage		Char Oxidation stage	
	$-(dW/dT)_p$	T_p	$-(dW/dT)_p$	T_p
	(% °C^{-1})	(°C)	(% °C^{-1})	(°C)
Algae (A)	0.451	296.0	0.334	509.7
A: SM= 3:1	0.499	296.3	0.246	507.7
A: SM =1:1	0.535	297.6	0.203	498.2
A: SM =1:3	0.570	299.6	0.240	459.6
Swine Manure (SM)	0.627	299.0	0.277	448.6

The low values of deviation between weighted mean and experimental data suggested a
mainly additive (non-synergetic) effect in firing algae and swine manure solid mixtures. Non-
synergetic behavior was reported in the pyrolysis of algae-coal blends [10] as well as in the co-
firing (combustion) of torrefied biomass-coal blends [6] and coal-sewage sludge blends [15]. In
the current study, both biomass were shown to have comparable activation energy values and an

additive decomposition behavior in a combustion context. Given that both feedstocks, i.e., swine manure solids, and algal biomass grown on swine manure wastewater, originate in the livestock production facility, understanding their individual, as well combined, thermal decomposition behavior is crucial to properly design thermochemical utilization of these materials. Similarly, given the variability in yields and collection intervals between algae and swine manure, the likelihood of highly variable reserves of each biomass type is quite high. Accordingly, understanding and predicting the decomposition behavior of their blends adds flexibility to the operation of any thermal conversion unit. Further research on this subject may examine the behavior of the ash fraction, i.e., agglomeration and fusion tendencies, in each biomass, as well as for their blends.

5. **Conclusions**

- Swine manure solids showed a higher carbon concentration and larger Higher Heating Value than algal biomass solids
- Weight loss in swine manure solids took place over a narrower temperature range compared to that of algal biomass
- In both feedstocks, combustion weight loss proceeded in two stages: devolatilization and char oxidation.
- Activation energy, using Kissinger method was higher during first weight loss stage in both feedstocks.
- Average activation energy for algae and swine manure solids, using isoconversional methods, was comparable.
- Co-combustion of swine manure and algal solids was found to be additive, with behavior similar to weighted mean computed from individual feedstocks.

6. References

[1] Agrawal, A., Chakraborty, S., 2013. A kinetic study of pyrolysis and combustion of microalgae Chlorella vulgaris using thermo-gravimetric analysis, Bioresour. Technol. 128, 72-80.

[2] Ali, S.A.M., Razzak, S.A., Hossain, M.M., 2014. Apparent kinetics of high temperature oxidative decomposition of microalgal biomass, Bioresour. Technol.

[3] Amutio, M., Lopez, G., Aguado, R., Artetxe, M., Bilbao, J., Olazar, M., 2012. Kinetic study of lignocellulosic biomass oxidative pyrolysis, Fuel. 95, 305-311.

[4] Bernet, N., Béline, F., 2009. Challenges and innovations on biological treatment of livestock effluents, Bioresour. Technol. 100, 5431-5436.

[5] Biller, P., Ross, A.B., 2011. Potential yields and properties of oil from the hydrothermal liquefaction of microalgae with different biochemical content, Bioresour. Technol. 102, 215-225.

[6] Goldfarb, J.L., Liu, C., 2013. Impact of blend ratio on the co-firing of a commercial torrefied biomass and coal via analysis of oxidation kinetics, Bioresour. Technol. 149, 208-215.

[7] Hoffmann, J.P., 1998. Wastewater treatment with suspended and nonsuspended algae, J. Phycol. 34, 757-763.

[8] Kebede-westhead, E., Pizarro, C., Mulbry, W.W., Wilkie, A.C., 2003. Production and Nutrient Removal by Periphyton Grown Under Different Loading Rates of Anaerobically Digested Flushed Dairy Manure, J. Phycol. 39, 1275-1282.

[9] Kebede-Westhead, E., Pizarro, C., Mulbry, W.W., 2006. Treatment of swine manure effluent using freshwater algae: production, nutrient recovery, and elemental composition of algal biomass at four effluent loading rates, J. Appl. Phycol. 18, 41-46.

[10] Kirtania, K., Bhattacharya, S., 2013. Pyrolysis kinetics and reactivity of algae–coal blends, Biomass Bioenerg. 55, 291-298.

[11] Kok, M.V., Özgür, E., 2013. Thermal analysis and kinetics of biomass samples, Fuel Process Technol. 106, 739-743.

[12] Liu, N., Chen, H., Shu, L., Zong, R., Yao, B., Statheropoulos, M., 2004. Gaussian smoothing strategy of thermogravimetric data of biomass materials in an air atmosphere, Ind Eng Chem Res. 43, 4087-4096.

[13] Maddi, B., Viamajala, S., Varanasi, S., 2011. Comparative study of pyrolysis of algal biomass from natural lake blooms with lignocellulosic biomass, Bioresour. Technol. 102, 11018-11026.

[14] Mulbry, W., Kondrad, S., Buyer, J., 2008. Treatment of dairy and swine manure effluents using freshwater algae: fatty acid content and composition of algal biomass at different manure loading rates, J. Appl. Phycol. 20, 1079-1085.

[15] Otero, M., Sanchez, M., García, A., Morán, A., 2006. Simultaneous thermogravimetric-mass spectrometric study on the co-combustion of coal and sewage sludges, J therm anal calorim 86, 489-495.

[16] Otero, M., Sánchez, M.E., Gómez, X., 2011. Co-firing of coal and manure biomass: A TG–MS approach, Bioresour. Technol. 102, 8304-8309.

[17] Sanchez-Silva, L., López-González, D., Garcia-Minguillan, A., Valverde, J., 2013. Pyrolysis, combustion and gasification characteristics of *Nannochloropsis gaditana* microalgae, Bioresour. Technol. 130, 321-331.

[18] Scragg, A., Illman, A., Carden, A., Shales, S., 2002. Growth of microalgae with increased calorific values in a tubular bioreactor, Biomass Bioenerg 23, 67-73.

[19] Sharara, M.A., Holeman, N., Sadaka, S.S., Costello, T.A., 2014. Pyrolysis kinetics of algal consortia grown using swine manure wastewater, Bioresour. Technol. 169, 658-666.

[20] Sharara, M., Sadaka, S., 2014. Thermogravimetric Analysis of Swine Manure Solids Obtained from Farrowing, and Growing-Finishing Farms, Journal of Sustainable Bioenergy Systems 4 (1), 75-86.

[21] Sheng, C., Azevedo, J., 2005. Estimating the higher heating value of biomass fuels from basic analysis data, Biomass Bioenerg. 28, 499-507.

[22] Shuping, Z., Yulong, W., Mingde, Y., Chun, L., Junmao, T., 2010. Pyrolysis characteristics and kinetics of the marine microalgae *Dunaliella tertiolecta* using thermogravimetric analyzer, Bioresour. Technol. 101, 359-365.

[23] Smith, P., Martino, D., Cai, Z., Gwary, D., Janzen, H., Kumar, P., McCarl, B., Ogle, S., O'Mara, F., Rice, C., Scholes, B., Sirotenko, O., Howden, M., McAllister, T., Pan, G., Romanenkov, V., Schneider, U., Towprayoon, S., Wattenbach, M., Smith, J., 2008. Greenhouse gas mitigation in agriculture, Philos. Trans. R. Soc. Lond. B. Biol. Sci. 363, 789-813.

[24] Sommer, S.G., Olesen, J.E., Petersen, S.O., Weisbjerg, M.R., Valli, L., Rodhe, L., Béline, F., 2009. Region-specific assessment of greenhouse gas mitigation with different manure management strategies in four agroecological zones, Global Change Biol. 15, 2825-2837.

[25] Wang, L., Min, M., Li, Y., Chen, P., Chen, Y., Liu, Y., Wang, Y., Ruan, R., 2010. Cultivation of green algae Chlorella sp. in different wastewaters from municipal wastewater treatment plant, Appl. Biochem. Biotechnol. 162, 1174-1186.

[26] Wnetrzak, R., Kwapinski, W., Peters, K., Sommer, S., Jensen, L., Leahy, J., 2013. The influence of the pig manure separation system on the energy production potentials, Bioresour. Technol. 136, 502-508.

[27] Wu, H., Hanna, M.A., Jones, D.D., 2012. Thermogravimetric characterization of dairy manure as pyrolysis and combustion feedstocks, Waste Manag. Res. 30, 1066-1071.

Chapter 6 Gasification of Phycoremediation Algal Biomass

Citation

1. Sharara, M. and Sadaka, S. 2012. Auger Gasification of Algal Blooms Produced in a Waste
    Water Treatment Facility. *In* ASABE Annual International Meeting. Dallas, Texas- July
    2012.

2. Sharara, M. and Sadaka, S. xxxx. Gasification of Phycoremediation Algal Biomass.
    BioResources [submitted December 2014, under review]

1. Abstract

Microalgae have been utilized in wastewater treatment strategies in various contexts.
Uncontrolled algal species are a cheap and effective remediation strategy. This study investigates
the thermochemical potential of wastewater treatment algae (phycoremediation) as means to
produce renewable fuel streams and bio-products. Three gasification temperature levels: 760,
860 and 960°C were investigated in an auger gasification platform. Temperature increases
resulted in corresponding increases in CO, and H_2 concentrations in the producer gas from 12.8%
and 4.7% at 760°C to 16.9% and 11.4% at 960°C, respectively. Condensables yields ranged
between 15.0% and 16.6% whereas char yields fell between 46% and 51%. The high ash content
(40% dry basis) is the main reason behind the elevated char yields. On the other hand, the
relatively high yields of condensables, and a high C concentration in the char are attributed to the
low conversion efficiency in this gasification platform. Combustion kinetics of raw algae, in a
thermogravimetric analyzer (TGA), showed three consecutive stages of weight loss, i.e., drying,
devolatilization and char oxidation. Increasing the algae gasification temperature led to increases

in the temperature of peak char oxidation. Future studies will further investigate improvements to the performance of the auger gasification.

2. Introduction

Microalgae are attracting wide interest as a renewable feedstock given their short life cycle, high photosynthetic efficiency, in addition to the full range of products and services they furnish. Historically, macro and microalgae have been utilized in the production of nutritional supplements, feed, cosmetics, and pharmaceuticals [3, 6]. Increased awareness of the consequences of fossil fuels overuse, and the resulting emissions, prompted the interest in algae as a renewable energy resource. Algae cultivation, as means for both carbon sequestration and fuel production, is among the exciting technologies in this regard [34, 35, 4]. Another service provided by algae, which is receiving renewed attention, is wastewater treatment, typically referred to as "phycoremediation". Discharges of enriched effluents to rivers and lakes from sewage treatment plants and livestock farms were shown to result in eutrophication and hypoxic conditions [18, 36]. Since phosphorous (P) and nitrogen (N) are typically the limiting factors to algal blooms in balanced aquatic environment, introducing untreated (nutrient-rich) effluents instigates their growth. Various studies successfully demonstrated microalgae potential as a treatment option for livestock production effluents [40, 16], and municipal wastewater treatment plants [1]. The N and P uptake by periphytic algal communities grown in an algal turf scrubber system (ATS) were evaluated as a treatment option for a nutrients-rich creek in Northwest Arkansas [31]. A mixed algal culture (green, blue-green, diatoms and flagellates) has been evaluated as scrubbers of absorbable xenobiotic (AOX) as reported by Dilek *et al.* 1999 [9]. They also used this mixture to control color in industrial pulp and paper plant effluents. Immobilized microalgae and bacteria in polymer matrices (natural and synthesized polymers)

also received attention as another approach that facilitates the assimilation of nutrients and metals while protecting the selected algal strains from invasive ones [13, 5].

The quality of wastewater-grown algal biomass was investigated to evaluate its potential use as a source of high-value chemicals, fuel, and feed. Despite their high protein content, in excess of 40% on dry mass basis, the high levels of heavy metals in wastewater algae can exceed the maximum dietary levels tolerated in livestock thus reducing the value of wastewater algae as a feed source [40]. Similarly, the increased nitrogen concentration in growth substrate was found to reduce the lipid accumulation in algae cellular structures [21]. Consequently, the low content of fatty acids in wastewater treatment algae makes them a poor candidate for lipids extraction. Another algal biomass utilization route is biological digestion. Under mesophilic conditions (35°C), algae were found to exhibit slow, incomplete degradation and low gas production rates compared to sewage sludge [11]. Relative improvement in algae digestibility, reported under thermophilic conditions, 50 to 55°C, was attributed the partial destruction of cell walls, which improved accessibility to bacteria. Later investigations showed that 40% of the organic fraction in algae was not biodegradable [15]. Yen and Brune (2007) proposed blending waste paper with algal sludge to adjust the C: N ratio to become $20 \sim 25$, and also to minimize ammonia (NH_3) release during decomposition [45]. Significant increase in methane productivity was observed after blending, compared to unblended algal biomass; 1170 ml $L^{-1}d^{-1}$ compared to 573 ml $L^{-1}d^{-1}$. Algal cell walls resistance to bacterial degradation, combined with the low C: N ratio in algae, between 6 to 9, are often cited as causes behind low algae digestibility.

Thermochemical processes, whether under aqueous or dry conditions, offer the flexibility to produce gaseous, liquid, and solid value-products from algal biomass without the need for metabolic degradation. Combustion, gasification, pyrolysis, and hydrothermal liquefaction

processes have been rigorously investigated on a wide variety of feedstock ranging from wood and crop residues [32, 37, 30] to industrial and municipal wastes [20, 42] and livestock manures [12, 27, 46]. Bio-crude produced from the hydrothermal liquefaction of *Spirulina* algae has been characterized and compared with swine manure and digested sludge bio-crudes [38]. Few investigations, however, were carried out to examine atmospheric pyrolysis, gasification, and combustion of microalgae feedstock. This can be attributed to the high drying overhead, which diminishes the benefit of thermochemical conversion. Another problem associated with microalgae combustion is the high ash and mineral contents which results in slagging and fouling. Co-firing microalgae with coal or natural gas has been considered as an environmentally sound investment, with the exhaust CO_2 being utilized to grow the algal biomass culture [10, 22]. Ross et al. (2008) studied the thermochemical behavior of a group of marine macroalgae species; *Fucus vesiculosus*, *Chorda filum*, *Laminaria digitata*, *Fucus serratus*, *Laminaria hyperborea*, and *Macrocystis pyrifera* [28]. Ash contents for these species varied between 9% and 18%, which would complicate combustion and gasification. Demirbas (2009) reported the optimal temperature range for pyrolysis oil production in two mosses (*Polytrichum commune* and *Thuidium tamarascinum*) and two algae (*Cladophora fracta* and *Chlorella protothecoid*) to be 350 ~ 450°C [7]. This is mainly because higher temperatures favor further cracking and, consequently, more gaseous products. In another study, steam gasification of char recovered from fast pyrolysis of cyanobacterial blooms was investigated [44]. They reported the particle size to have no effect on gas composition, while the residence time was significant in the gasification process yields. They reported a maximum gas yield (1.84 Nm^3 kg^{-1}), and carbon conversion (98.8%) at 850°C, 15 minute residence, and 0.45- 0.90 mm particle size.

There appears to be a need for further investigation of the quality of char produced from aquatic biomass gasification predominantly in an auger reactor. The objectives of this investigation are the investigation of wastewater microalgae as a feedstock for the gasification process, and studying the quality of the char products under various temperatures.

3. Materials and Methods

3.1. Biomass Collection and Characterization

In this study, Algal biomass was harvested from a pilot-scale shallow raceway at Noland wastewater treatment plant (Fayetteville, AR). The algal species grown in that system and investigated in this study are essentially mixtures of indigenous uncontrolled aquatic species (algae and diatoms). Harvesting was accomplished manually by scraping the raceway carpeted bedding then straining the harvested biomass on a large screen to remove free water. Aquatic biomass was collected in plastic airtight containers and stored at 0°C prior to preparation and analyses. The algal biomass used here was compiled from harvests during June, July and August 2011. The biomass was oven-dried at 80°C, as opposed to 105°C, until weight loss was minimal to avoid significant losses of volatile matter. Dried biomass was then pulverized using a 1.5 hp (1.1 kW) grinder (Model No.3, Wiley Mill, Swedesboro, NJ). Proximate analyses were performed according to standard procedures, i.e., moisture content (ASTM E871-82 (2006)), volatile matter (ASTM E82-82 (2006), and ash content (ASM D2974-8 (2007)). Fixed carbon, on the other hand, was determined by subtraction. The elemental analysis was performed in a specialized diagnostic laboratory (Huffman laboratories Inc., Golden, Colorado). Higher heating value (HHV) of algae samples was determined using oxygen bomb calorimetry (model 1241, Parr Instruments) (ASTM D5865-12 (2012)). Chemical oxygen demand (COD) of the dried raw algal biomass, and the gasification chars was determined by first diluting each solid sample with

deionized water (100 g water: 1 g solids). The suspensions were then thoroughly homogenized

and left to settle for 30 minutes. The suspension was then filtered, and a 2-mL aliquot of the

filtrate was added to COD digestion vial (0-15,000 ppm range). A digital reactor Block

(DRB200, HACH Company, Loveland, CO) was used to digest each sample at 150°C for 2

hours. After cooling the samples to below 120°C, the COD was determined using a portable

spectrophotometer (DR 2700, HACH Company, Loveland, CO).

3.2. Auger Gasification System

Atmospheric, air gasification tests were conducted in an auger gasification/pyrolysis

system. This system was designed, and constructed in the bioenergy laboratory at the Rice

Research and Extension Center (Stuttgart, AR), Figure 6-1 shows schematic diagram of the

gasification system used. Preliminary results of this investigation were reported by the authors

[33]. The reactor is essentially an externally heated cylindrical reactor that uses motorized augers

to move the feedstock, and also uses a three-zone electrical heater (Model HTF55347C,

Lindberg/Blue M. Ashville, NC) to heat the reactor. The feeding rate was controlled by adjusting

the rotational speed of the injection (metering) auger, as shown in Figure 6-1. Multiple

calibrations were performed using the ground algal biomass prior to actual gasification tests to

accurately adjust biomass feed rate, and also to determine the biomass fullness ratio (α), which

represents the percentage of the auger cross-section area occupied by the biomass. Table 6-1 lists

a summary of the parameters of the three gasification tests reported in this study.

135

Table 6-1 Parameters of algae gasification tests

Test	1	2	3
Furnace Temperature (°C)	760	860	960
Auger speed (RPM)	6.02	6.20	6.32
Biomass feed rate (g min^{-1})	34.7	36.1	40.9
Air flow rate (LPM)	20.0	20.0	18.1

All tests were initiated after furnace temperature, as well as the temperatures inside the reactor, became constant. Each test lasted 15 minutes during which gas was sampled for 10 minutes after 5 minutes of initiating the feeding. Tar and char produced after each test were collected, weighed, and stored for further analyses. After exiting the tar collection unit, the producer gas was cooled and cleaned using a tar trap lined with glass wool. Flow rate of cleaned producer gas was then measured using a 5 VDC volumetric air flowmeter (OMEGA- FLR1000 series). Producer gas composition was determined using a 5-gas analyzer (O_2, CO, CO_2, H_2 and CH_4) (Model 7905AQ, NOVA Analytical Systems). In this study, however, the methane concentration was not reported due to interference from other produced hydrocarbons that significantly influenced methane readings.

3.3. Thermogravimetric Analysis

The oxidation behavior of the raw algal biomass, as well as the algae gasification chars, was investigated using thermogravimetry. The dry samples were first milled and sieved to generate a sub-sample with a particle size less than 0.2 mm. A thermogravimtric analyzer (Model TGA 4000, PerkinElmer, Inc. Waltham, MA, USA) was used to determine the temperature-weight loss relationships for the different samples under oxidizing conditions. Simulated air was used as the purge gas (50 mL min), at a heating rate of 5°C min^{-1}. The sample weight was maintained at 5 mg (+/- 0.1 mg) in all the TGA tests. Both the particle size and the sample size were kept sufficiently small to ensure that the decomposition is kinetically controlled, and not

diffusion-controlled. Each sample was placed in a clean, inert alumina crucible (Al_2O_3). A blank

test was conducted, with an empty crucible, under the regular test conditions to quantify the

buoyancy of the crucible. The experimental data was then corrected by subtracting the blank test

results.
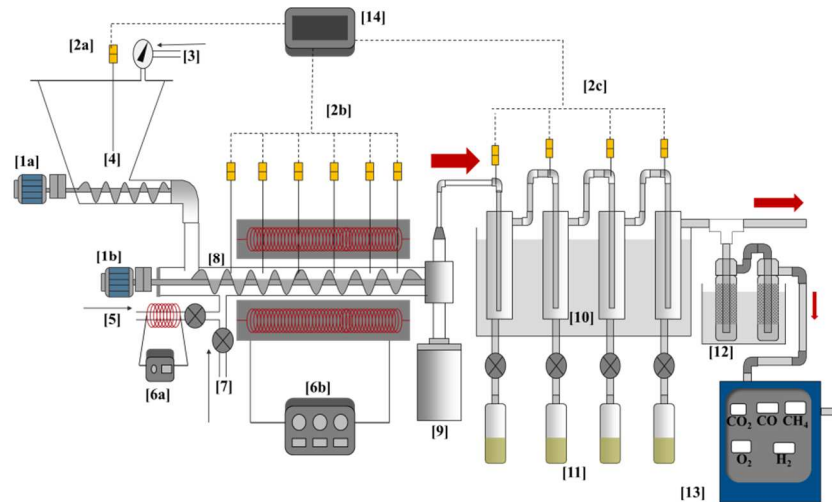
[1 a, b]:Controllable DC motors   [6 a, b]:Controllable heaters   [11]:Tar collection bottles
[2 a, b, c]:Type-K Thermocouples   [7]:Oxidant feed (air)   [12]:Gas wash bottles
[3]: Nitrogen purge   [8]:Auger reactor   [13] Permanent gases analyzer
[4]: Injection/metering auger   [9]:Char collector   [14]:Data logging unit
[5]:Auxiliary steam feed   [10]:Condensers assembly

Figure 6-1 Auger gasification/pyrolysis reactor

4. Results and Discussions

4.1. Temperature Profile

In addition to the thermocouples controlling the furnace temperature, based on the

reactor's external temperature, five thermocouples were installed to measure the biomass

temperature inside the reactor. In the three gasification tests, a shift in the temperature profile

was observed after biomass feeding was initiated. The first half of the externally heated auger

reactor, i.e., L<0.6 m, underwent gradual drop in temperatures, as shown in Figure 6-2, while

temperatures in the further section of the reactor showed a gradual increase. Nominal gasification temperatures, i.e., 760, 860 and 960°C, were maintained in the reactor section directly surrounded by the heating element. Before biomass feeding, the temperature profile is determined primarily by the set temperature of the heating element, proximity to the heating element, and the heat transfer affected by the gasifying agent. After feeding, however, typical gasification stages take place along the reactor length consecutively: drying, devolatilization (pyrolysis), oxidation and partial oxidation. Both drying and devolatilization, which are endothermic reactions, take place at the first part of the reactor, while oxidation and partial oxidation, both exothermic reactions, take place towards the end of the reactor. This sequence of stages might explain the observed temperature profile changes. Similar thermal stratification was observed in fixed-bed gasification reactors, i.e., up draft and downdraft reactors [47]. Fixed-bed reactors are known for their ease of operation, but they typically result in higher tar yields than fluidized-bed gasifiers [23, 39].

4.2. Producer Gas and Condensable Yields

Figure 6-3 below lists the average concentration of CO, CO_2 and H_2 in the producer gas under the three temperatures levels studied. Concentrations of both CO and H_2 increased with temperature increase from 12.8% and 4.7%, respectively, at 760°C, to 16.9% and 11.4% at 960°C, respectively. The CO_2 concentration, on the other hand, dropped with increasing reaction temperatures, from 14% at 760°C to 11.6% at 960°C. At atmospheric pressure, the volumetric energy density of H_2 and CO is 12.8, and 12.5 MJ m^3, respectively. Accordingly, the higher heating value (HHV) of the produced gas, without considering the CH_4, varies from 2.20 MJ m^{-3} at 760°C to 3.57 MJ m^{-3} at 960°C. CO, CO_2, and H_2 concentration trends are in agreement with char gasification reactions, i.e., Boudouard and the water-gas

reactions. Both reactions are endothermic and move forward, to yield more CO and H_2 and less H_2O and CO_2, with the increase in temperatures.
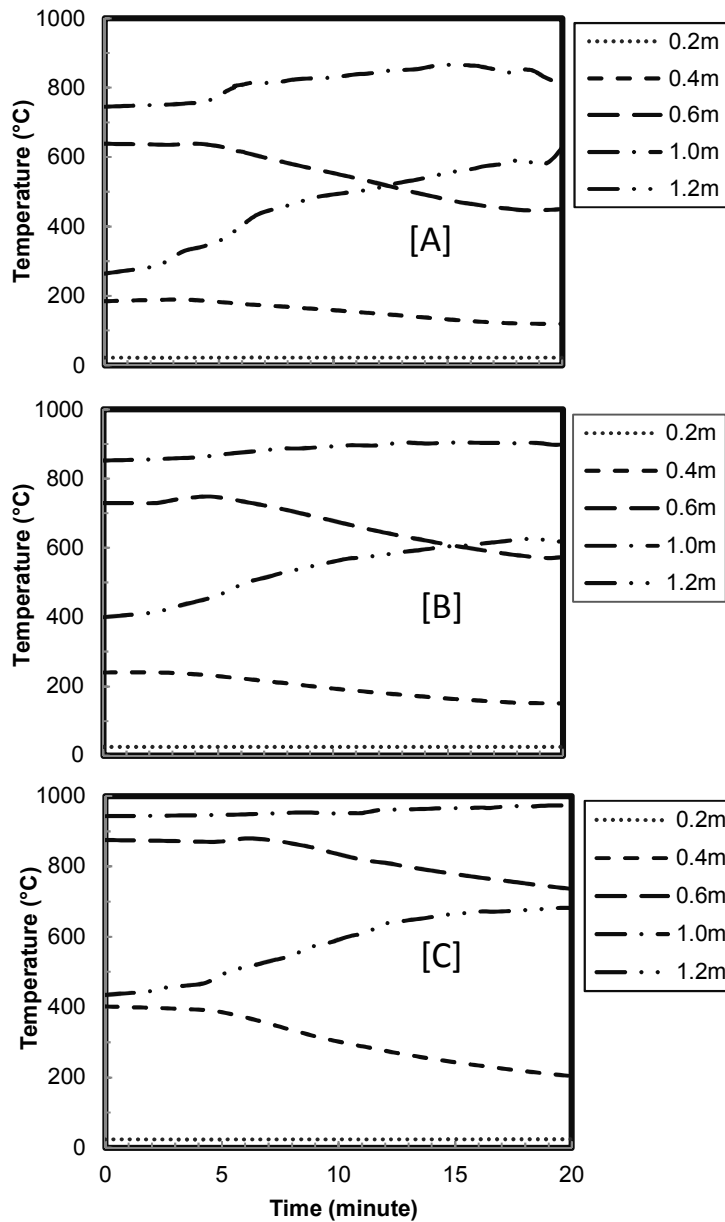
Figure 6-2 Temperature profiles in auger gasification at [A] 760°C [B] 860°C [C] 960°C

$C + CO_2 = 2\ CO\ (159.9\ kJ.mol^{-1})$ [Boudouard reaction]

$C + H_2O\ (g) = CO + H_2\ (131.3\ kJ.mol^{-1})$ [Water-gas reaction]
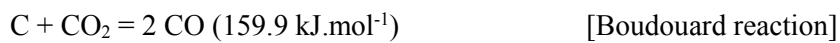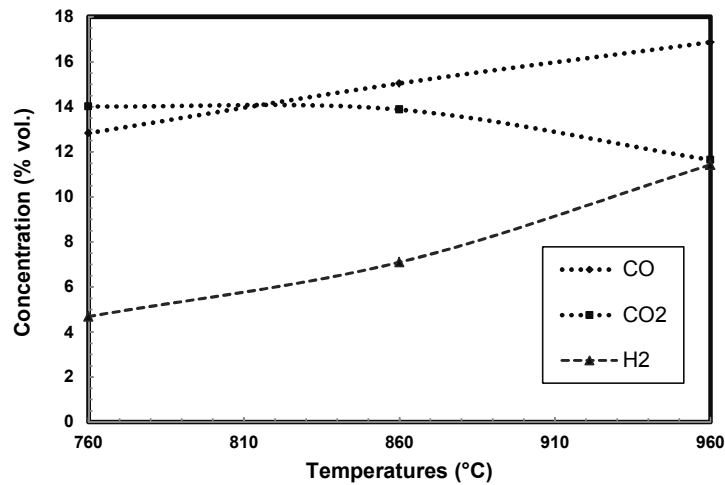
Figure 6-3 Concentration of some product gases under different temperature levels

However, concentrations of H_2 and CO, the energy-positive gas species, were still considerably low, i.e., 10% and 16%, respectively, at the highest temperature. This could be attributed to the low C and H concentrations in the starting material (Table 6-2), as well as the low heat transfer coefficient in indirectly heated reactors (Brown and Brown, 2012). It is worth noting that most studies that utilized auger reactors in biomass conversion have been primarily for pyrolysis tests [14, 26]. In the context of gasification, however, increasing the biomass temperature and residence time could improve the conversion efficiency in auger reactors, thus maximize H_2 and CO production.

The yield of producer gas varied within a relatively small range, from 0.59 m^3 to 0.80 m^3 per 1 kg of dry algae. These rates are significantly lower than those reported for traditional biomass such as pine wood sawdust, i.e., more than 2.0 m^3 per 1 kg of dry, ash-free biomass [25]. The low producer gas yield could be attributed to the high mineral content of algal biomass (> 40%). Using the dry, ash-free mass (DAF) as the basis, the producer gas yields in algae gasification tests become 1.02 to 1.38m^3 kg^{-1} DAF. The difference between these dry, ash-free yields and

140

those attributed to lignocellulosic biomass, over $2m^3 \ kg^{-1}_{DAF}$, can be attributed to auger reactor performance.
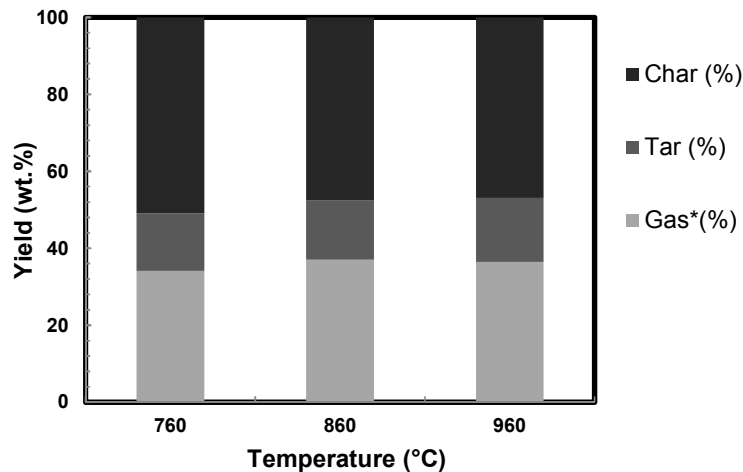
Figure 6-4 Products distribution under different gasification temperatures

The high yield of condensables, 16.6% at 960°C, further underlines the low gas conversion efficiency even at such high temperatures (Figure 6-4). In downdraft gasification, the yield of condensables (tar and water) was shown to typically fall below 1% of the original biomass [43]. By contrast, countercurrent (updraft) gasifiers were reported to yield condensables between 12.7% and 37.2% of fed biomass, which vary according to the type of feedstock and the operational parameters [8]. Earlier studies [29, 30], which utilized the auger gasification platform used in current study, reported yields of condensables that varied from 18% to 34%. The auger gasifier, therefore, could be considered an intermediate platform between downdraft (concurrent) and updraft (countercurrent) gasifiers in terms of the yield of condensables.

4.3. Char Yields and Characteristics

Given the high ash content (minerals) of the algal biomass investigated, the char yields were around 50% of the algae fed into the system, as shown in Figure 6-4. The decrease in char yields

141

with increasing the gasification temperatures, from 50.9% at 760°C to 46.9% at 960°C, is

explained by the increased reaction severity, which increases char reactivity and, thus, the yields

of producer gas and condensables. Despite the high minerals present in the algal biomass, and

the high temperatures used here, no large aggregates were observed during or after the tests.

Mechanical feeding (screw conveyor) might have been advantageous, in this case, in avoiding

stagnant zones where potential hot spots typically occur, facilitating the formation of clinkers.

The high concentration of silica (SiO_2) in the algae ash fraction, 71.8% (Table 6-2), could be

attributed to the presence of diatoms, which utilize Si in building cellular walls and structures

(Kroger *et al.* 2000).

The elemental analysis of the ash in the original biomass could assist in predicting the

thermal behavior of the mineral oxides, and their sintering potential. The following indices

(Mettanant *et al.* 2009) were devised to determine the sintering potential based on the higher

heating value (HHV) of the feedstock, and the relative amounts of sodium, potassium and silica.

$$\frac{(K_2O + Na_2O)}{SiO_2} > 1; and\ \frac{(K_2O + Na_2O)}{HHV} > 0.34$$

For the phycoremediation algae in this study, the values of both indices: 0.035, and

0.238, respectively, are below those associated with increased sintering tendency. This

observation could help in using this feedstock as an added fuel in co-firing of coal or

lignocellulosic biomass without risking an increased sintering potential.

The elemental composition of the chars could be used to further understand the carbon

conversion efficiency. The concentration of carbon progressively dropped from 28.3% in the raw

algae to 17.7, 15.6, and 14.1% in the chars with increasing the conversion temperature. Using the

char yield in each test, the percentages of carbon retained in the biochar and that released in gas

or liquid form could be computed using equations 1 and 2, respectively.

Table 6-2 Characterization of raw algae and product chars

Temperature (°C)		25	760	860	960
Proximate analysis (%)					
	Moisture content (wb*)	13.8	2.2	2.1	2.2
	Volatile matter (db**)	42.2	6.8	6.9	5.7
	Fixed carbon [†] (db)	15.9	18.1	12.6	12.6
	Ash content (db)	41.9	75.1	80.5	81.8
Ultimate analysis (%)					
	C	28.26	17.71	15.59	14.07
	H	3.63	0.58	0.41	0.70
	N	2.83	0.98	0.71	0.48
	O[†]	23.06	8.84	6.78	2.14
	S	0.57	0.64	0.66	0.74
Ash analysis (%)					
	Al_2O_3	3.55	3.33	3.38	3.36
	CaO	9.75	10.38	10.93	10.45
	Fe_2O_3	3.00	2.53	2.73	2.57
	MgO	1.20	1.22	1.21	1.20
	MnO	1.39	1.51	1.49	1.50
	P_2O_5	3.77	3.83	3.70	3.66
	K_2O	1.96	2.02	2.00	2.00
	SiO_2	71.8	72.30	70.76	71.54
	Na_2O	0.55	0.50	0.52	0.49
Higher heating value (MJ kg^{-1})		10.55	5.67	4.71	4.46
Chemical Oxygen Demand (COD) (mg/L)		10,190	330	320	480

*Wet, mass-basis

**Dry, mass-basis

[†] By difference

$$Carbon\ retained\ in\ biochar\ (\%) = \frac{Char\ yield(\%) * Carbon\ Conc.\ in\ char\ (\%)}{Carbon\ Conc.\ in\ original\ feedstock\ (\%)} \quad (1)$$

$$Carbon\ released\ (\%) = 100 - Carbon\ retained\ in\ biochar\ (\%) \qquad (2)$$

Using equation 1, the carbon retained in the biochar decreases with the increase in gasification temperature from 31.9% of the original biomass C at 760°C to 23.4% at 960°C. This pattern is in agreement with the observed increases in gas yield upon increasing the conversion temperature. On the other hand, the carbon released (equation 2) was 68.1, 73.8, and 76.6% of the original carbon at gasification temperatures: 760, 860, and 960°C, respectively. In gasification literature, the carbon conversion efficiency, which relates the amount of carbon released in the producer gas to that in the original biomass, typically falls between 70% and 90% [41]. In the current study, if the condensables were re-injected into the gasification chamber and utilized to produce more energy-positive gases, the released carbon (%) could be considered a proxy for the carbon conversion efficiency. Despite the application of relatively high gasification temperatures, i.e., 860 ~ 960°C, carbon conversion in this study is still noticeably lower than the typical values reported in biomass gasification literature. Since the reaction severity is a function of both reaction temperature and time, it is clear the residence time was insufficient to facilitate complete conversion. The high yield of condensables and high C concentration in the char indicate that both the residence times for the solids and the devolatilized species were not sufficient. Either increasing the length of the heated reactor, or reducing the rotational speed of the auger would increase the solids residence time, and thus, the reaction severity. On the other hand, the volatile fraction (gas, and condensables) needs longer residence time at high temperatures to facilitate tar cracking and the water-gas reaction. Increasing the volatiles residence time could be accomplished as an added step, i.e., using a heated coiled pipe that approximates the freeboard section in fluidized-bed gasifiers. Accordingly, the design of this

added section (diameter, length, and temperature) could be informed by reported values of gas velocity and reactor height in fluidized-bed gasification studies.

4.4. TGA Characterization of Raw Algae and Biochar

Figure 6-5 [A] shows the combustion weight-loss against temperature for the raw algae, as well as the gasification chars produced under different temperatures. The weight-loss derivative curves (DTG), Figure 6-5 [B], further elucidate the different combustion stages. In the raw algae, the weight loss proceeded in three consecutive stages: drying, devolatilization, and char oxidation. The first stage, i.e., drying, took place below 100°C as the first weight-loss peak indicates (Figure 6-5 [B]). The volatile matter loss, the second stage, took place between 150 and 400°C. The third stage, char oxidation, preceded between 400 and 600°C. These observations indicate that under extremely high heat transfer conditions, full conversion is achievable at, or below, a particle temperature of 600°C.

For the gasification chars, no drying peaks were detectable. Similarly, no weight loss took place below 300°C. This is attributed to the gasification weight loss, which involves the loss of moisture, as well as, the devolatilization of the bulk of the volatile matter. Two weight loss peaks were detected during the combustion of the algae chars. The temperatures corresponding to decomposition peaks in each stage, as compared to those for raw algae, are listed in Table 6-3. In the algae chars, the temperature corresponding to the first oxidation peak increased from 433.5°C to 472.8°C with the increase in gasification temperature from 760 to 960°C, respectively. Earlier study on the combustion of biomass pyrolysis chars reported peak decomposition to occur at 378°C for olive kernels, 412°C for cotton residue, and 509°C for wood (Kastanaki and Vamvuka 2006). It is worth noting that, in the current study, the third decomposition stage for the raw algae, i.e., char oxidation, took place at a higher temperature,

515.7°C than those for the gasification chars. This observation could be attributed to the fact that under gasification, or any thermal treatment, the original biomass matrix is transformed into a new one (biochar) that has its one thermal and oxidative properties.
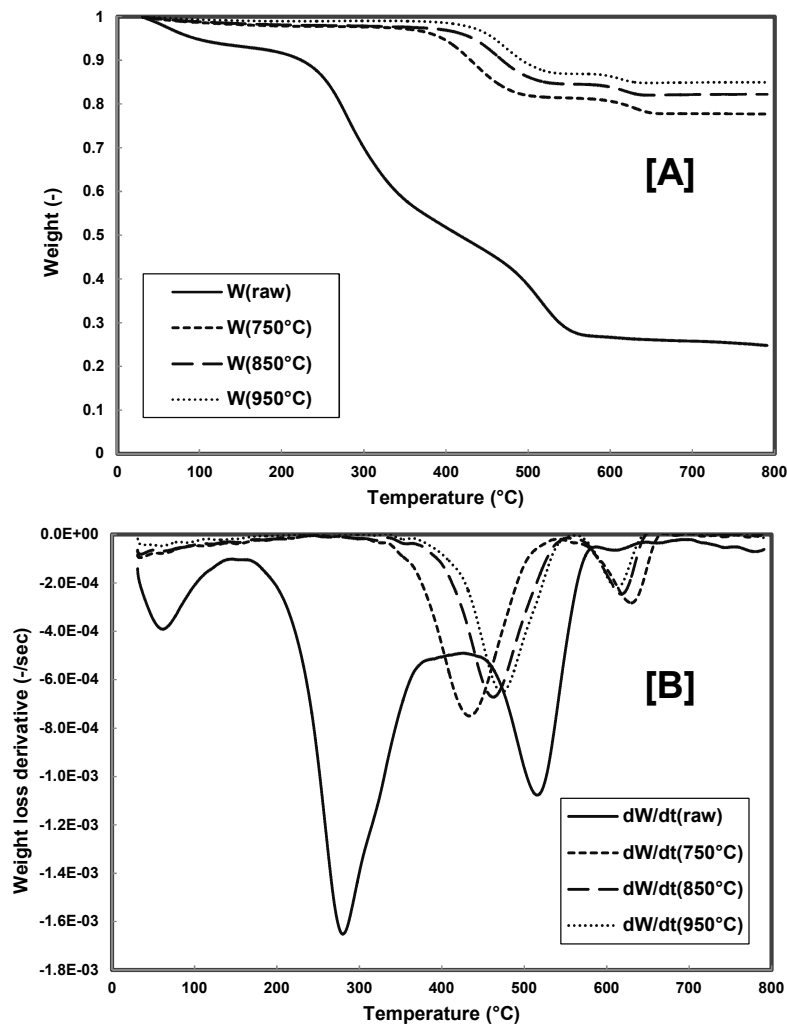

Figure 6-5 Oxidation profile of raw algae and gasification chars at 5°C min^{-1}: [A] weight loss profiles [B] derivative of weight loss

Table 6-3 Characteristics of oxidation thermogram for raw and charred algal biomass at a heating rate of 5°C min-1

Temperature(°C)	25	760	860	960
T_{p1} (°C)	279.8	433.5	462.1	472.8
$(dW/dt)_{p1}$ (mg s^{-1})	-1.65E-03	-7.50E-04	-6.72E-04	-6.52E-04
T_{p2} (°C)	515.7	629.5	617.8	611.6
$(dW/dt)_{p2}$ (mg s^{-1})	-1.08E-03	-2.83E-04	-2.46E-04	-2.22E-04

4.5. Implications of Results

With the proliferation of phycoremediation applications in industrial, agricultural and municipal contexts, the yields of algal biomass harvests are expected to increase. Given their composition and unique biological structures, algal biomasses are not readily accessible to composting and anaerobic digestion. Similarly, thermochemical conversion of algal biomass faces various complications, mainly the high moisture and ash contents, and the low energy density. In addition to retrieving a fraction of the algae energy, however, thermochemical conversion processes could be thought of as a densification step for the algae minerals in a carbon-rich form (biochar). These biochars could be blended with lignocellulosic chars and land applied, which would enhance the P content of the blend. Alternatively, these chars could be activated to produce a filtration medium. This alternative will work, in tandem, with the phycoremediation scrubbers to minimize further the leaching and run-off of problematic minerals and metals.

5. Conclusions

- The development of temperature profiles during auger gasification indicated formation of different reaction zones, similar to those observed in fixed-bed systems.

- Increasing the gasification temperature decreased the CO_2 yield, but increased the yield of CO, H_2, and, consequently the gas heating value.

- Char yields decreased from 50% to 46% with increasing the gasification temperature from 760°C to 960°C, respectively.

- The high ash concentrations in the raw algae biomass resulted in low gas yields, and high char yields.

- High condensables yields and high carbon concentrations in the char indicate low conversion efficiencies, even at the highest temperature tested.

- The chars retained 27.8%, 21.2%, and 19.8% of the energy contained in unit mass of raw algae with gasification temperatures 760°C, 860°C, and 960°C, respectively.

- Concentrations of C, P, and K oxides in the algae chars were between 140~177 g kg^{-1}, 2.8~3.0 g kg^{-1}, and 1.5~1.6 mg kg^{-1}, respectively.

- TGA combustion analysis showed an influence of the gasification temperatures on the char oxidation kinetics.

6. References

[1] Åkerström, A.M., Mortensen, L.M., Rusten, B., Gislerød, H.R. (2014). Biomass production and nutrient removal by Chlorella sp. as affected by sludge liquor concentration, J. Environ. Manage. 144, 118-124.

[2] Brown, J., Brown, R. (2012). Process optimization of an auger pyrolyzer with heat carrier using response surface methodology, Bioresour. Technol. 103, 405-414.

[3] Brown, M.R. (2002). Nutritional value and use of microalgae in aquaculture, Avances en Nutrición Acuícola VI.Memorias del VI Simposium Internacional de Nutrición Acuícola. 3, 281-292.

[4] Chisti, Y. (2007). Biodiesel from microalgae, Biotechnol. Adv. 25, 294-306.

[5] de-Bashan, L.E., Bashan, Y. (2010). Immobilized microalgae for removing pollutants: review of practical aspects, Bioresour. Technol. 101, 1611-1627.

[6] Del Campo, J.A., García-González, M., Guerrero, M.G. (2007). Outdoor cultivation of microalgae for carotenoid production: current state and perspectives, Appl Microbiol Biotechnol 74, 1163-1174.

[7] Demirbas, A. (2009). Thermochemical conversion of mosses and algae to gaseous products, Energy Sources, Part A. 31, 746-753.

[8] Di Blasi, C., Signorelli, G., Portoricco, G. (1999). Countercurrent fixed-bed gasification of biomass at laboratory scale, Ind Eng Chem Res. 38, 2571-2581.

[9] Dilek, F., Taplamacioglu, H., Tarlan, E. (1999). Colour and AOX removal from pulping effluents by algae, Appl. Microbiol. Biotechnol. 52, 585-591.

[10] Doucha, J., Straka, F., Lívanský, K. (2005). Utilization of flue gas for cultivation of microalgae Chlorella sp.) in an outdoor open thin-layer photobioreactor, J. Appl. Phycol. 17, 403-412.

[11] Golueke, C.G., Oswald, W.J., Gotaas, H.B. (1957). Anaerobic digestion of Algae, Appl. Microbiol. 5, 47-55.

[12] He, B., Zhang, Y., Funk, T., Riskowski, G., Yin, Y. (2000). Thermochemical conversion of swine manure: an alternative process for waste treatment and renewable energy production, Trans. ASAE. 43, 1827-1834.

[13] Hernandez, J., de-Bashan, L.E., Bashan, Y. (2006). Starvation enhances phosphorus removal from wastewater by the microalga *Chlorella sp.* co-immobilized with *Azospirillum brasilense*, Enzyme Microb. Technol. 38, 190-198.

[14] Ingram, L., Mohan, D., Bricka, M., Steele, P., Strobel, D., Crocker, D., Mitchell, B., Mohammad, J., Cantrell, K., Pittman Jr, C.U. (2007). Pyrolysis of wood and bark in an auger reactor: physical properties and chemical analysis of the produced bio-oils, Energy Fuels. 22, 614-625.

[15] Jewell, W.J., McCarty, P.L. (1971). Aerobic decomposition of algae, Environ. Sci. Technol. 5, 1023-1031.

[16] Ji, M., Kim, H., Sapireddy, V.R., Yun, H., Abou-Shanab, R.A., Choi, J., Lee, W., Timmes, T.C., Jeon, B. (2013). Simultaneous nutrient removal and lipid production from pretreated piggery wastewater by Chlorella vulgaris YSW-04, Appl. Microbiol. Biotechnol. 97, 2701-2710.

[17] Kastanaki, E., Vamvuka, D. (2006). A comparative reactivity and kinetic study on the combustion of coal–biomass char blends, Fuel. 85, 1186-1193.

[18] Kemp, W., Boynton, W., Twilley, R., Means, J., Stevenson, J. (1983). The decline of submerged vascular plants in upper Chesapeake Bay: summary of results concerning possible causes [Aquatic vegetation, factors as runoff of agricultural herbicides, erosional inputs of sediments, nutrient enrichment and associated algal growth], Marine Technology Society Journal (USA).

[19] Kroger, N., Deutzmann, R., Bergsdorf, C., Sumper, M. (2000). Species-specific polyamines from diatoms control silica morphology, Proc. Natl. Acad. Sci. U. S. A. 97, 14133-14138.

[20] Larson, E.D., Consonni, S., Kreutz, T.G. (2000). Preliminary economics of black liquor gasifier/gas turbine cogeneration at pulp and paper mills, Journal of Engineering for gas turbines and power. 122, 255-261.

[21] Li, Y., Horsman, M., Wang, B., Wu, N., Lan, C.Q. (2008). Effects of nitrogen sources on cell growth and lipid accumulation of green alga Neochloris oleoabundans, Appl. Microbiol. Biotechnol. 81, 629-636.

[22] Ma, J., Hemmers, O. (2010). Thermo–economic analysis of microalgae co-firing process for fossil fuel-fired power plants,.

[23] McKendry, P. (2002). Energy production from biomass (part 3): gasification technologies, Bioresour. Technol. 83, 55-63.

[24] Mettanant, V., Basu, P., Butler, J. (2009). Agglomeration of biomass fired fluidized bed gasifier and combustor, The Canadian Journal of Chemical Engineering. 87, 656-684.

[25] Narvaez, I., Orio, A., Aznar, M.P., Corella, J. (1996). Biomass gasification with air in an atmospheric bubbling fluidized bed. Effect of six operational variables on the quality of the produced raw gas, Ind Eng Chem Res. 35, 2110-2120.

[26] Pittman Jr, C.U., Mohan, D., Eseyin, A., Li, Q., Ingram, L., Hassan, E.M., Mitchell, B., Guo, H., Steele, P.H. (2012). Characterization of bio-oils produced from fast pyrolysis of corn stalks in an auger reactor, Energy Fuels. 26, 3816-3825.

[27] Priyadarsan, S., Annamalai, K., Sweeten, J., Mukhtar, S., Holtzapple, M. (2004). Fixed-bed gasification of feedlot manure and poultry litter biomass. Trans. ASAE. 47, 1689-1696.

[28] Ross, A., Jones, J., Kubacki, M., Bridgeman, T. (2008). Classification of macroalgae as fuel and its thermochemical behaviour, Bioresour. Technol. 99, 6494-6504.

[29] Sadaka, S., Sharara, M., Ubhi, G. (2014). Performance Assessment of an Allothermal Auger Gasification System for On-Farm Grain Drying, Journal of Sustainable Bioenergy Systems. 4, 19-32. doi: 10.4236/jsbs.2014.41003.

[30] Sadaka, S. (2013). Gasification of raw and torrefied cotton gin wastes in an auger system. Appl. Eng. Agric. 29, 405-414.

[31] Sandefur, H.N., Matlock, M.D., Costello, T.A. (2011). Seasonal productivity of a periphytic algal community for biofuel feedstock generation and nutrient treatment, Ecol. Eng. 37, 1476-1480.

[32] Scott, D.S., Piskorz, J., Radlein, D. (1985). Liquid products from the continuous flash pyrolysis of biomass, Ind Eng Chem Proc DD. 24, 581-588.

[33] Sharara, M.A., Sadaka, S. (2012). Auger Reactor Gasification of Algal Blooms Produced in a Waste Water Treatment Facility. Paper No. 12-1337915. Presented at 2012 ASABE Annual International Meeting, Dallas, Texas July 29-August 1, 2012.

[34] Sheehan, J., Dunahay, T., Benemann, J., Roessler, P. (1998). A look back at the US Department of Energy's aquatic species program: biodiesel from algae. National Renewable Energy Laboratory Golden.

[35] Stewart, C., Hessami, M. (2005). A study of methods of carbon dioxide capture and sequestration—the sustainability of a photosynthetic bioreactor approach, Energy convers manage. 46, 403-420.

[36] Valiela, I., McClelland, J., Hauxwell, J., Behr, P.J., Hersh, D., Foreman, K. (1997). Macroalgal blooms in shallow estuaries: controls and ecophysiological and ecosystem consequences, Limnol. Oceanogr. 42, 1105-1118.

[37] Van der Drift, A., Van Doorn, J., Vermeulen, J. (2001). Ten residual biomass fuels for circulating fluidized-bed gasification, Biomass Bioenerg. 20, 45-56.

[38] Vardon, D.R., Sharma, B., Scott, J., Yu, G., Wang, Z., Schideman, L., Zhang, Y., Strathmann, T.J. (2011). Chemical properties of biocrude oil from the hydrothermal liquefaction of< i> Spirulina algae, swine manure, and digested anaerobic sludge, Bioresour. Technol. 102, 8295-8303.

[39] Warnecke, R. (2000). Gasification of biomass: comparison of fixed bed and fluidized bed gasifier, Biomass Bioenerg. 18, 489-497.

[40] Wilkie, A.C., Mulbry, W.W. (2002). Recovery of dairy manure nutrients by benthic freshwater algae, Bioresour. Technol. 84, 81-91.

[41] Worley, M., Yale, J. (2012). Biomass Gasification Technology Assessment: Consolidated Report.

[42] Xu, X., Antal, M.J. (1998). Gasification of sewage sludge and other biomass for hydrogen production in supercritical water, Environ. Prog. 17, 215-220.

[43] Yamazaki, T., Kozu, H., Yamagata, S., Murao, N., Ohta, S., Shiya, S., Ohba, T. (2005). Effect of superficial velocity on tar from downdraft gasification of biomass, Energy Fuels. 19, 1186-1191.

[44] Yan, F., Luo, S., Hu, Z., Xiao, B., Cheng, G. (2010). Hydrogen-rich gas production by steam gasification of char from biomass fast pyrolysis in a fixed-bed reactor: influence of temperature and steam on hydrogen yield and syngas composition, Bioresour. Technol. 101, 5633-5637.

[45] Yen, H., Brune, D.E. (2007). Anaerobic co-digestion of algal sludge and waste paper to produce methane, Bioresour. Technol. 98, 130-134.

[46] Young, L., Pian, C.C. (2003). High-temperature, air-blown gasification of dairy-farm wastes for energy production, Energy. 28, 655-672.

[47] Zainal, Z., Rifau, A., Quadir, G., Seetharamu, K. (2002). Experimental investigation of a downdraft biomass gasifier, Biomass Bioenerg. 23, 283-289.

Chapter 7 Life Cycle Assessment of Swine Manure Management through Thermochemical Conversion

1. Abstract

Proper swine manure management is crucial to reducing the impacts of swine production on the surrounding ecosystems. Existing swine manure management practices are responsible for a large share of greenhouse gas (GHG) emissions, and eutrophying conditions in aquatic systems. The aim of this study was to utilize life cycle assessment (LCA) to investigate the gasification of swine manure solids as a manure management strategy. This study details a proposed scenario that encompasses manure drying and gasification within the different stages in swine manure management, starting with the swine houses and ending with land application. A complete analysis of the various stages was performed to identify the changes and burdens associated with each. The assessment showed that liquid storage of manure is credited with the highest GHG emissions burden. Solid-liquid separation decreased GHG emissions in the manure liquid fraction. Liquid fraction management stages are credited with the highest fossil fuel energy use. Land application of manure slurry mixed with biochar residue is the only stage that mitigated GHG emissions, because of the avoided use of synthetic fertilizers. Similarly, land application was credited with the largest savings in fossil fuel energy use due to the avoided energy associated with synthetic fertilizers production. Increasing thermochemical conversion efficiency was shown to greatly affect the scenario's overall energy use. Improvements in drying technology can favor this scenario as a manure management strategy.

2. Introduction

The agriculture sector is credited with a major contribution to global climate change and ecosystems degradation [1]. Local, regional, and global agreements are increasingly mandating regulations to restrict these emissions in order to minimize the short- and long-term environmental degradation. Livestock production, in particular, has been recognized as a major source of greenhouse gas (GHG) emissions, eutrophication drivers: nitrogen (N), and phosphorous (P), and fossil fuel use [2, 3]. The vulnerability of livestock production, and the agriculture sector as a whole, to climate change further incentivizes the search and the adoption of sustainable agriculture practices [4].

Manure management is the major source of nitrous oxide (N_2O), methane (CH_4), and carbon dioxide (CO_2) emissions in livestock production [5]. Liquid manure management systems, relevant to swine production, further increase the adverse effects of manure. Liquid storage promotes anaerobic conditions, which transform organic matter to methane (CH_4) and ammonia (NH_3). Furthermore, uncontrolled anaerobic and aerobic conditions initiate nitrification-denitrification process, which converts a part of manure nitrogen (N) to N_2O. Solid-liquid separation of swine manure was recognized as an emission mitigation strategy. However, increased N_2O and CH_4 emissions were reported during storage of manure separated solids [6]. Transforming the separated solids into a gas fuel (syngas) and a stable nutrient-rich co-product (biochar), via gasification, can potentially reduce the emissions associated with manure separated solids.

Evaluation of the emissions and impacts associated with this conversion strategy, i.e., gasification of swine manure solids, expands the set of technologies available to livestock producers for manure management. Life cycle assessment (LCA) is an important tool to assist in

decision making through evaluating the environmental performance of proposed strategies. According to ISO standard 14040 (2007), LCA assessment takes into account the various inputs and output flows, and the corresponding environmental burdens, resulting from production or disposal decisions.

The goal of this study is to evaluate a manure management scenario that utilizes gasification of swine manure solids as a disposal/energy retrieval strategy using LCA tool.

3. Materials and Methods

3.1. LCA goal and scope

The goal of this LCA is to determine the impacts associated with swine manure management, using gasification as a manure solids treatment option. Figure 7-1 shows a schematic diagram of the proposed swine manure management (SMM) scenario. The scope of this life cycle assessment covers manure management stages for 1,000 kg of flushed swine manures at 5% dry matter content, without accounting for animal maintenance (feed, drinking water, climate control), until the land application of both the liquid fraction (slurry) and the gasification co-product (biochar). The functional unit (FU) is the disposal of 1 metric ton (1,000 kg) of swine manure slurry, at 5% DM, via gasification and land application.

The excreted manure (urine, and feces) are flushed from the shallow pits under the house, using manure slurry from storage. The flushed manure is stored in a holding tank, and stirred, before being pumped into the separation stage. Manure separation is accomplished using a screw press separator. This class of size-separators utilizes a tapered screw and a fine-mesh screen (0.75-3 mm) to fractionate the manure into solids-rich and liquids-rich fractions. The solid fraction is transported to a thermochemical conversion facility that contains: a dryer, a gasifier,

155

and a gas boiler. The manure gasification is accomplished in an atmospheric, fluidized-bed gasifier to produce syngas, which is fired (burnt) in a gas boiler for heat, in addition to biochar. Part of the generated steam, in the gas boiler, is recycled to provide the heat necessary for drying. On the other hand, biochar is transported to the field for land application.
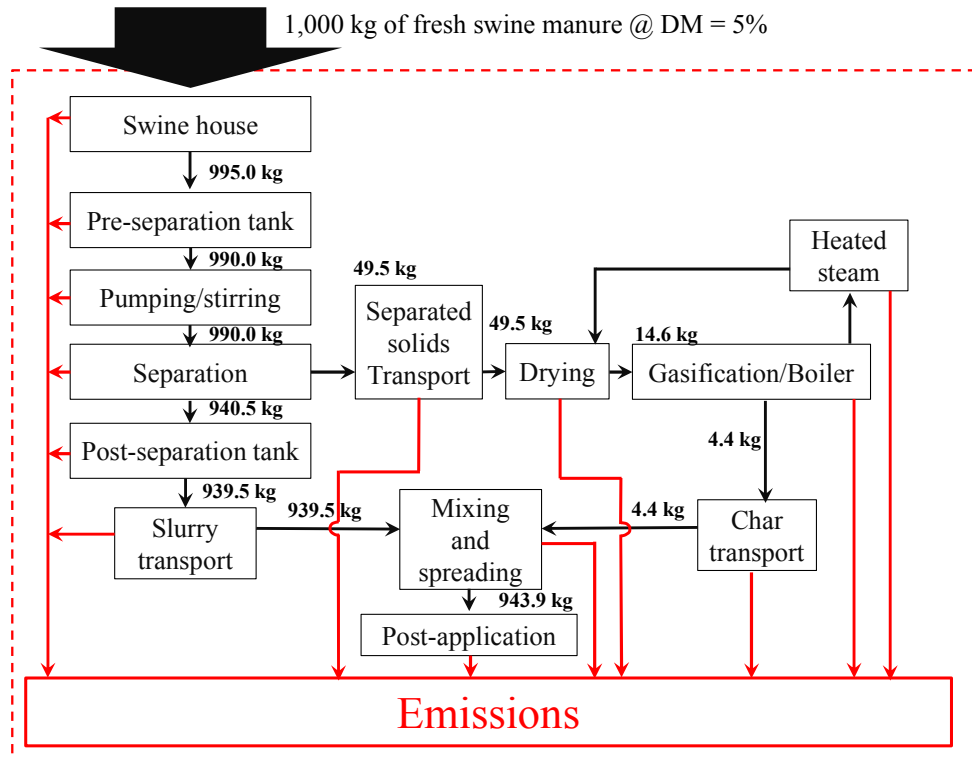
Figure 7-1 The scope of proposed swine manure management scenario (black arrows represent main product flow, red arrows represent emissions)

On the other hand, the liquid-fraction (slurry) is stored then transported to an agricultural field for land application. In this model, the emissions associated with the land application of char and slurry will be presented in detail separately first, then combined to present the total impacts of char-slurry land application. The total impacts represent the summation of the impacts for each substrate without any synergistic effects. Inventory of mass, energy and emission flows in each stage is presented in the following sections.

3.2. Inventory

3.2.1. Swine House

According to manure characteristics standard (ASABE D384.2, 2005), the amount of total solids in as-excreted swine manure is around 13% by weight. However, in farms where swine manure is handled in a slurry form, the manure is diluted using flushing water, which is recirculated manure slurry, to ensure proper manure removal. The concentration of manure solids, therefore, drops from 13% in as-excreted manure to around 5%. In this study, composition of swine manure solids was taken from first-hand analyses of manure solids sampled from flushed slurry in a feeder-finisher farm in Washington County, Arkansas.

The diluted manure is flushed, every 2 weeks by gravity drainage using a pull-plug system (i.e., no energy or mechanical power is needed for drainage). During the 2-week storage, various biogenic emissions, namely, CO_2, CH_4, NH_3, and N_2O are released due to aerobic and anaerobic activities in the manure substrate.

Table 7-1 Characteristics of swine manure solids

Characteristics	Swine Manure
Dry Matter (DM), %	5.0
Volatile matter (% DM)	81.6
Ash (% DM)	18.4
C (% DM)	50.8
Total-N (% DM)	4.3
O (%DM)	21.0
H (%DM)	6.9
S (%DM)	1.3
P (%Ash)	20.9
K (%Ash)	21.1
Na (%Ash)	10.3
Ca (%Ash)	20.5
Mg (%Ash)	12.1
Cu (%Ash)	0.01
Zn(%Ash)	0.04

Ammonia emissions (NH_3) in swine house

Kai *et al.* (2008) reported emissions of 0.43 kg NH_3-N per pig for untreated manure slurry, and 0.14 kg NH_3-N per pig for acidified slurry [7]. In the same study, the excreted N per pig was reported to be 3.15 kg N per pig. Accordingly, the amount of ammonia emissions per unit mass of N can be computed as follows:

NH_3 emissions % of total N= $100*(0.43$ kg $_{NH3-N}$ pig^{-1}/3.15 kg $_N$ pig^{-1} = 13.7 %

In another study which evaluated Greehouse gas (GHG) emissions in Danish agriculture, NH_3 emissions factor (EF) for pig houses (fully-slated floors) was estimated to be 16% [8]. The conservative EF value, 16%, will be used in this study.

NH_3 emissions = Total manure * DM (%) * N (%) * NH_3-EF (%)

$$= 1{,}000 * (5/100) * (4.3/100) *(16/100) = 0.344 \text{ kg }_{NH3\text{-}N}$$

NH_3 emissions = 0.344 kg $_{NH3-N}$ * (17/14) = <u>0.418 kg $_{NH_3}$</u>

Nitrous oxide emissions (N_2O) in swine house

Using the N_2O emissions factor reported in IPCC (2006) for liquid slurry systems with a natural crust cover (EF_{N2O} = 0.005 kg$_{N2O-N}$ kg$_N$$^{-1}$, Table 10.21 [9]), the total N_2O emitted can be calculated

N_2O emissions = $1{,}000*(5/100) * (4.3/100) *0.005 * (44/28)$ = <u>0.017 kg $_{N_2O}$</u>

Methane emissions (CH_4) in swine house

The IPPC guidelines (2006) were used to calculate CH_4 emissions using the volatile solids (VS) fraction in the manure according to the following formula:

CH4 (kg) = VS (kg) * B_o* 0.67 * MCF

Where,

B_o is the maximum CH_4 producing capacity for manure, m^3_{CH4} kg^{-1}_{VS}, MCF is the methane conversion factor, while 0.67 is the methane density at standard pressure and temperature (kg m^{-3}). B_o here corresponds to market swine (B_o=0.48 m^3_{CH4} kg^{-1}_{VS}). MCF is selected based on the average annual temperature, and the manure management system. In this study, the average annual temperature in Arkansas was taken from national climatic data center for the National Oceanic and Atmospheric Administration (NOAA) to be 16°C. Correspondingly, the MCF value for the slurry/liquid manure system, with natural crust cover, was 18%.

CH4 emissions (kg) = VS (kg) * B_o* 0.67 * MCF

=1,000 * (5/100) * (81.6/100) * 0.48 * 0.67 * (18/100) = <u>2.36 kg $_{CH4}$</u>

Carbon dioxide (CO_2) emissions

Carbon dioxide emissions were calculated indirectly as the difference between total C loss, and the CH_4 emissions. Since the dry matter loss during temporary storage under house was reported to be 10% [10], and since carbon represents 50% of the dry matter weight, the same loss percentage is taken to represent carbon loss during storage. Accordingly, the total C-loss can be calculated as follows:

C-loss (kg) = 1,000 * (5/100) * (50.8/100) * (10/100) = 2.54 kg $_C$

C-loss as CH_4 = 2.36 kg $_{CH4}$ * (12/16) = 1.77 kg $_C$ as CH_4

C-loss as CO_2 can be calculated as follows:

C-loss as CO_2 = 2.54 – 1.77 =0.77 kg $_C$ as CO_2

CO_2 emissions = 0.77 * (44/12) = 2.82 kg $_{CO2}$

3.2.2. External storage (pre-separation) tank

The emissions associated with the storage tank (covered with natural crust cover) will be roughly equivalent to those calculated for in-house emissions, except for NH_3 emissions. According to Poulsen *et al.* (2001), the amount of NH_3 devolatilized during open storage is estimated to be 2% of the total N in fresh manure [11]. Accordingly, the ammonia emissions can be calculated as follows:

NH_3 emissions = Total manure * DM (%) * N (%) * NH_3-EF (%) *(17/14)

=1,000*(5/100)*(4.3/100) * (2/100) * (17/14) = 0.418 kg $_{NH3}$

3.2.3. Pumping and mixing

In this step, swine manure slurry is stirred then pumped to the mechanical separation stage. Therefore, the separation unit capacity has to be first selected in order to properly size the slurry pump. A SEPCOM$^©$ model with 15 m^3 h^{-1} capacity (power requirement is 5.5 kW, supplied by a 3-phase electrical engine) [12]. In this study, the separator will operate on 75% of its full capacity to minimize stoppages or interruption (capacity = 15 * 0.75 = 11.25 m^3 h^{-1}). The manure slurry density was assumed to equal that for water given that the solids concentration is less than 5%. The pumping head is assumed to be 10 meters. Accordingly, the following formula can be used to compute the pumping power requirements:

$$P(kW) = \frac{Q\left(m^3/h\right) * \rho\left(kg/m^3\right) * g\left(m/s^2\right) * h(m)}{3600(s\ h^{-1}) * 1000(W\ kW^{-1})}$$

P_{pump} (kW) = 11.25* 1,000 *9.81*10 / (3,600*1,000) = 0.307 kW

Assuming 60% pump efficiency, the shaft power requirement is:

P_{shaft} (kW) = 0.307/ (60/100) = 0.511 kW

For 1,000 kg of swine manure slurry (equivalent to 1 m^3 of slurry assuming the same density as water), the time required for pumping can be calculated:

t_{pump} (h) = 1/11.25 = 0.089 h, and the energy requirement for pumping is

E_{shaft} (kWh) = 0.511 kW * 0.089 h = 0.045 kWh

In similar studies [11, 13], however, the energy requirements for pumping and stirring 1,000 kg of manure slurry were taken to be 0.5 kWh and 1.2 kWh, respectively. Thus, the total energy consumption associated with this stage (stirring and pumping) will be taken to be:

$E_{pumping/mixing}$ (kWh) = 0.5 + 1.2 = <u>1.7 kWh</u>

3.2.4. Mechanical separation

The mechanical separator discussed earlier, 5.5 kWh and 15 $m^3\ h^{-1}$ capacity, can be used to model the liquid-solid separation energy requirements. Assuming that the unit will operate at 75% capacity, the energy requirements per 1,000 kg slurry can be calculated.

$E_{Separation}$ (kWh) = Slurry amount (kg) * P (kW) / (Q ($m^3\ h^{-1}$) * ρ (kg m^{-3}))

$$= 1,000\ (kg) * 5.5\ (kW) / (11.25\ (m^3\ h^{-1}) * 1,000\ (kg\ m^{-3}))$$

$$= \underline{0.489 \text{ kWh}}$$

In another study, the power requirement for a mechanical screen press separator was reported to be 0.50 kWh tonne^{-1} (1 tonne = 1,000 kg) [14]. Therefore the energy requirement for separation will be modeled as 0.5 kWh. A local U.S. electricity mix was used to model the impacts of power utilization. No air emissions or water contamination are associated with manure during this stage.

The separation indices reported for screw presses in the review by Hjorth *et al.* (2010) were used here to determine the size and composition of both fractions [15]. In that study, the solids content in the original slurry varied from 1.8% to 6.3%. In Table 7-2, the separation index (%) is defined as the mass of a given compound in the solid fraction to the mass of that compound in the original (unseparated) slurry. The mass of the separated solids fraction (containing both solids and slurry) ranges between 5% and 7.3% [14], the lower value (5%) will be used in this study.

3.2.5. Solids Transportation (solid-fraction)

Before drying, the wet solids produced from the liquid-solid separation stage are transported to the drying/conversion facility. An assumption of the transportation distance was based on observations of swine farms with separation and composting facilities. A typical distance between unit operations, which will be used in this study, is 500 meters. The transportation units can be calculated.

Ton-Kilometers (tkm) =

Solids fraction (kg) * Distance (m) / (1000 (kg ton^{-1}) * 1000 (m km^{-1})) =

49.5 (kg) * 500 (m)/ (1000 (kg ton^{-1}) * 1000 (m km^{-1})) = <u>0.025 tkm</u>

Table 7-2 Separation indices for mechanical screw press separation [15]

Raw pig slurry	Separation index (%)			
DM (%)	Volume	Dry matter	N-total	P-total
5.7	7	28	7	15
6.3	-	64	-	46
5.7	5	28	6	12
5.3	4	27	7	7
1.8	-	51	31	42
1.8	-	26	11	7
6.3	7	21	4	13
Mean	5.75	35	11	20.3
(S.D.)	(1.50)	(16)	(10)	(16.5)

3.2.6. Drying (solid-fraction)

The solids fraction is dried to further reduce the moisture to levels acceptable for gasification, i.e., <15%. Generally speaking, drying could be accomplished passively by relying on sun exposure and natural air circulation, or through active methods where air is heated and circulated through the wet mixture (using blowers), and the material is moved inside the dryer to ensure quick, and uniform dryness. Given that exposed swine manure sludge is malodorous and easily-degradable, active drying techniques will be implemented in this model. In a 100% efficiency dryer, the thermal energy required to remove 1 kg of moisture from manure was reported to be 2.3 MJ [16]. Hospido *et al.* (2005) evaluated different scenarios for utilizing solid sludge from urban wastewater treatment plants (WWTP). In their study, the electricity and heat consumption associated with 1 ton (1,000 kg) of dried sludge were 118 kWh and 1,638 kWh, respectively. The plant also utilizes steam as the heat carrier, with 15.2 m$^3{}_{water}$ ton $_{DM}{}^{-1}$.

Consequently, these values can be used to compute the energy requirements and emissions associated with manure drying:

Electricity required =

(DM in solid fraction (kg) * Electricity req. to dry 1 ton of sludge)/1000 (kg ton^{-1})

= (14.6 (kg) * 118 (kWh ton^{-1})) / 1000 (kg ton^{-1}) = <u>1.72 kWh</u>

Similarly,

Heat required = (14.6 (kg) * 1,638 (kWh ton^{-1})) / 1000 (kg ton^{-1}) = <u>23.91 kWh</u>

Water consumption (kg) = 14.6 (kg) * 15.2 (m^3 ton $_{DM}$ $^{-1}$)* / 1000 (kg ton $^{-1}$)

= 0.222 m^3 $_{H_2O}$

During drying, as much as 20% of the manure-N was reported to devolatilize, often as NH_3 [17]. Also, C loss during drying was reported to be around 4%. In the municipal sludge drying process model, 44.3 g of volatile organic compounds (VOC) emissions were reported per 1 ton of sludge dried. The same emissions level will be used to model the manure emissions in this study.

VOC emissions = (14.6 (kg) * 44.3 (g ton^{-1})) / 1000 (kg ton^{-1}) = <u>0.647 g $_{VOC}$</u>

NH_3 emissions = Dry manure-N (kg) * (20/100) * (17/14) = <u>0.042 kg $_{NH3}$</u>

3.2.7. Gasification

In this thermochemical conversion process, the dry manure solids are transformed, at elevated temperatures (600-800°C) to gas (referred to as producer gas, or syngas) in addition to ash-rich solid char (biochar), and a small amount of condensables (tar). Gasification utilizes air, or other oxidizing agent, to partially oxidize the biomass C into CO and CO_2. However, given the dearth of data on the gasification of swine manure solids, the dataset used in this study (Table 7-3) was compiled from available studies on swine manure solids and feedstock, such as, poultry litter, sewage sludge, cattle feedlot manure, that have similar characteristics (high ash, high N_2, etc.). The main product, syngas, is burnt in a steam boiler to generate steam that is used to satisfy heating needs on farm, e.g., the drying manure solids, and heating the farrowing crates. The syngas heat will displace natural gas demand and, consequently, the energy and emissions associated with natural gas production.

Table 7-4 shows the different emissions associated with the pyrolysis-gasification technology for municipal solid wastes (MSW) [18], which will be used in the current study to represent the emissions associated with the gasification facility for the swine manure solids.

Table 7-3 Gasification process model for 1 kg of dry swine manure solids

Parameters	Values	Source
Air requirements (kg_{air} kg^{-1})	2.54	Calculated from composition, ER=0.20
Manure solids HHV (MJ kg^{-1})	19-20	[19, 20]
Cold-gas efficiency (%)	50-80	[21]
Boiler thermal efficiency (%)	78	[22]
Char yield (g kg^{-1})	300-490	[20, 23, 24]
Electricity req. (kWh kg^{-1})	0.339	[18]
Thermal energy req. (MJ kg^{-1})	0.8-1.6	[25]

The cold-gas efficiency translates as the chemical energy retained in the syngas as a share of the total chemical energy in the feedstock, without considering the gas sensible heat. In this case, however, since the syngas will be used to replace a heat source (natural gas), both the

sensible and chemical energy in the syngas will be considered. Accordingly, the conversion efficiency value will increase, with hot gas efficiency (HGE) taken to be between 60% and 90%. A 70% HGE was used in this model. Accordingly, the amount of heat generated (MJ) due to gasification can be calculated after subtracting the thermal energy required for the process (calculated using the pyrolysis enthalpy in Table 7-3, taken here to be 1.0 MJ kg^{-1}).

Generated heat (MJ) =

DM (kg) * [HHV (MJ kg^{-1}) * HGE (%) * Boiler efficiency (%) – h $_{pyrolysis}$ (MJ kg^{-1})]

= 14.6 (kg) * [19.5 (MJ kg^{-1}) * 0.70 * 0.78 – 1.0(MJ kg^{-1})] = <u>140.71 MJ</u>

Since the thermal energy requirement for drying, 23.91 kWh (or 86.08 MJ), is met using a portion of this heat product, the credit for avoided natural gas use (MJ) becomes:

Displaced natural gas (MJ) = 140.71 – 86.08 = <u>54.63 MJ</u>

This amount of thermal energy is diverted to additional uses on farm, i.e., heating.

In addition to heat production, gasification yields a char fraction which will be utilized as a soil amendment. The char is assumed to be N-free since all nitrogen typically devolatilizes during gasification as N-species. On the other hand, P and K were assumed to be sequestered fully in the char fraction.

Char produced (kg) = DM (kg) * Char yield (%) = 13.9 (kg) * (300 g kg^{-1})/1000 (g kg^{-1})

=14.59 (kg) * 0.3 = 4.38 kg $_{Char}$

Given that the gasification/boiler stage generates two products, i.e., heated steam, and biochar, the impacts associated with this stage need to be divided (allocated) between both

products. Economic allocation was selected given that the products are incompatible, energy and mass, making the mass allocation inapplicable.

The economic value of the heat generated in the gasification/boiler stage can be determined using the price and energy content for natural gas. The price and energy content of 1 cubic foot of natural gas were 0.0132$ and 1030 British thermal units (Btu), respectively. Since 1 MJ equals 947.817 Btu, the economic value of the heat generated can be determined.

The economic value for the heat energy ($) =

$$140.71 \ (MJ) * (0.0132 \ (\$ \ cu.ft^{-1})/ \ 1030 \ (Btu \ cu.ft^{-1})) *947.817 \ (Btu \ MJ^{-1}) = \$ \ 1.70$$

Similarly, the economic value of the biochar can be estimated from the prices of P and K fertilizers, in addition to the price of sequestered CO_2 in the form of recalcitrant C. Price of 1 kg of P_2O_5, K_2O fertilizers and 1 kg of CO_2e sequestered were taken to be $1.98, $1.02, and $0.02, respectively [26]. Amounts of P_2O_5 and K_2O in the biochar will be determined by neglecting any P or K losses to the gaseous species during gasification.

P_2O_5 in biochar = 0.39 (kg $_{P, \ char}$) * 4.58 (kg $_{P2O5}$ kg $_P$ $^{-1}$) = 1.78 kg $_{P2O5}$

K_2O in biochar = 0.68 (kg $_{K, \ char}$) * 2.41 (kg $_{K2O}$ kg $_K$ $^{-1}$) = 1.64 kg $_{K2O}$

The char C represents 28% of the char weight, and the recalcitrant C, which will be considered for the sequestration benefit, is 75% of the char C [27]. Accordingly:

CO_2 sequestered = 1.25 (kg $_{C, \ char}$) * 0.75 * (44/12) (kg $_{CO2}$ kg $_C$ $^{-1}$) = 3.43 kg $_{CO2}$

Using these yields, the economic value of the produced biochar can be calculated.

The economic value for the biochar ($) =

167

$$=1.78 \text{ (kg}_{P2O5}) *1.98 \text{ ($ kg}_{P2O5}{}^{-1}) +1.02 \text{ (kg}_{K2O}) *1.98 \text{ ($ kg}_{K2O}{}^{-1}) +$$

$$3.43 \text{ (kg CO}_2\text{e)} *0.02 \text{ ($ kg CO}_2\text{e}^{-1}) = \$5.27$$

Economic allocation for the generated heat = $100*(1.70/(5.27+1.70)) = 24.4\%$

Economic allocation for the biochar = $100*(5.27/(5.27+1.70)) = 75.6\%$

Table 7-4 Emissions to the air resulting from the gasification process (per 1 kg of feedstock) [18]

Substance	Gasification (milligram $kg_{DM}{}^{-1}$)
CO_2	1,000,000
NOx	780
CO	100
SO_2	52
HCl	32
PM	12
VOCs	11
HF	0.34
Hg	0.069
As	0.06
Ni	0.04
Cd	0.0069

3.2.8. Biochar transportation

In this step, the impacts of biochar transportation to the field as well as the biochar land incorporation will be considered. The transportation (in ton-kilometer units) can be determined from the biochar yield shown in Table 7-3. The transportation distance here will also be assumed to be 10 km.

$$\text{Ton-kilometer} = \text{DM (kg)} * \text{char yield (kg kg}_{DM}{}^{-1}) * \text{Distance (km)}$$

$$=14.59 \text{ (kg)} * 0.3 \text{ (kg}_{char} \text{ kg}_{DM}{}^{-1}) * 10 \text{ (km)} = \underline{0.044 \text{ tkm}}$$

3.2.9. <u>Post-land application for the char (solid fraction)</u>

Char land application was shown to be beneficial both as a fertilizer/soil conditioner, and also as a carbon sequestration option. In this study, the benefits of biochar application to the soil will be determined as the avoided synthetic fertilizers due to the presence of P and K in the char, and also as avoided biogenic CO_2 in the form of char recalcitrant C. Additional benefits of char application include improved water holding capacity, and reduced N_2O emissions. However, due to the scarcity of quantifiable data on these benefits, and the strong dependency on crop, soil and climate conditions, these additional benefits will not be considered in this study. The amount of avoided P_2O_5 and K_2O fertilizers, and sequestered CO_2 were determined, in section 3.2.7, to be 1.78 kg $_{P_2O_5}$, 1.64 kg $_{K_2O}$, and 3.43 kg $_{CO_2}$.

3.2.10. <u>Liquid-fraction post-separation tank</u>

The separated slurry is stored in an exposed tank until it is transported to field for application. During storage, the organic fraction of this slurry undergoes transformation resulting in GHG emissions. The following section lists the computations for the various emissions.

CH_4 emissions

The IPCC (2006) equation used earlier to compute CH_4 emissions in the swine house and the pre-separation tank was also used here to calculate the emissions during post-separation storage of the liquid slurry.

CH_4 emissions (kg) = VS (kg) * B_o* 0.67 * MCF

The volatile solids loading (VS) in this storage step was much lower than in the pre-separation tank, i.e., 21.5 kg compared to 33.1 kg.

$$CH_4 \text{ emissions (kg)} = 21.5 \text{ (kg)} * 0.48 * 0.67 * (18/100) = \underline{1.24 \text{ kg }_{CH4}}$$

CO_2 emissions

Hamelin *et al.* (2010) modeled the anaerobic decomposition of manure volatile solids to determine the ratio of CO_2 to CH_4 in the devolatilized species [28]. They reported a molar ratio for CO_2/CH_4 of 0.52. Consequently, the mass ratio for CO_2/CH_4 can be computed.

$$CO_2/ CH_{4 \, mass} = 0.52 * (MW_{CO2} \ MW_{CH4}^{-1}) = 0.52 * (44/16) = 1.43 \text{ kg }_{CO2} \text{ kg }_{CH4}^{-1}$$

$$CO_2 \text{ emissions} = 1.24 \text{ kg }_{CH4} * 1.43 \text{ (kg }_{CO2} \text{ kg }_{CH4}^{-1}) = \underline{1.78 \text{ kg }_{CO2}}$$

NH_3 emissions

The same assumption used earlier to determine NH_3 emissions, i.e., 2% of total-N, will be used here as well.

$$NH_3 \text{ emissions} = 1.4 \text{ (kg }_N) * (2/100) * (17/14) = 0.034 \text{ kg }_{NH3}$$

N_2O emissions

The same emissions factor used earlier, $EF_{N2O} = 0.005 \text{ kg }_{N2O} \text{ kg }_N^{-1}$, was used to calculate the total N_2O emitted during post-separation storage.

$$N_2O \text{ emissions} = \text{Total-N (kg)} * 0.005 * (44/28) = 0.011 \text{ kg }_{N2O}$$

3.2.11. <u>Slurry transportation (liquid-fraction)</u>

The distance between the post-separation tank and the fields where the slurry is land-applied is assumed to be 10 km (6.2 miles). This distance has been used before in a similar study to model the impacts of dairy cow slurry digestion and land application [29].

$$\text{Ton-kilometer transported} = \text{Slurry (kg)} * \text{distance (km)} / 1{,}000 \text{ (kg ton}^{-1})$$

$$= 939.5 \text{ (kg)} * 10 \text{ (km)} / 1{,}000 \text{ (kg ton}^{-1}) = \underline{9.395 \text{ tkm}}$$

The following section will outline the emissions associated with mixing and land application of the char and liquid slurry.

3.2.12. Mixing and application (liquid and solid fractions)

The energy requirement for slurry and char mixing (kWh electricity) is 1.2 kWh ton^{-1} [11] and the land application energy requirements and emissions were modeled using the vacuum spreader model available in U.S. EI database. The impacts of slurry application (without the char) are presented in the following section.

3.2.13. Post-land application for the slurry (liquid-fraction)

NH$_3$ emissions

NH$_3$ devolatilization resulting from manure land application is among the main sources of N emissions in the agricultural sector [30]. Rates of NH$_3$ emissions vary greatly with the variability in manure slurry characteristics, soil type, and weather conditions. Misselbrook *et al.* (2005) studied the influence of manure type (cattle, and pig manure), and land type (arable, and grassland) on NH$_3$ emissions. They reported NH$_3$ emissions between 6.0 and

21.5% of the total ammonical nitrogen (TAN) in the pig manure. Sommer and Hutchings (2001) reported NH_3 emissions to be 5% of total NH_4 in applied slurry with trail hose application, and 8-10% of total NH_4 under broadspreading [31]. According to literature, an estimated 39% of TAN in swine slurry devolatilizes as NH_3 during spring season land application [32]. In this study, NH_3 devolatilization was modeled as 20% of TAN in the slurry. Ratio of TAN was taken from Buckley et $al.$ (2010) to be 75% of the total N in the swine manure slurry (S.D. = 17%)[33].

NH3 emissions = N (kg) * (TAN Total N^{-1}) * NH_3-EF

$$= 1.36 \text{ (kg}_N) * (75/100) * (20/100) = 0.204 \text{ kg}_{NH3}$$

N_2O emissions

According to the IPCC report (2006), the emission factor value for N_2O resulting from organic amendments application ($EF_{N_2O\text{-}N}$) is 0.01 kg $_{N2O\text{-}N}$ kg_N^{-1}. Thus, the amount of N_2O emissions resulting from the field application of the liquid-fraction can be calculated.

N_2O emissions = 1.36 (kg$_N$) * 0.01 (kg $_{N2O\text{-}N}$ kg $_N^{-1}$) * (44/28) = 0.021 kg $_{N2O}$

CO_2 emissions

Rochette et $al.$ (2004) estimated the cumulative C loss (as CO_2) due to swine slurry application to spring maize plots to be 63% of the original slurry C [34]. This value will be used here to estimate the total CO_2 emissions due to land application.

CO_2 emissions = Total C (kg) * (63/100) * (44/12) = 11.79 * (63/100) * (44/12)

$$= \underline{27.2 \text{ kg }_{CO_2}}$$

Fertilizers displaced by liquid-fraction application

Land application of swine slurry is advantageous, both economically and environmentally, since it provides a share of the plant nutritional needs, and offsets an amount of the mineral fertilizers (N, P, and K) typically needed. The amount of avoided mineral fertilizer could be thought of as savings in energy and emissions associated with processing, producing and transporting these fertilizers. The nutritional value of the swine slurry is typically expressed as mineral fertilizer equivalent (MFE), which is a ratio representing the unit mass of mineral fertilizer avoided (NPK) per unit mass of manure. In this study, the MFE values for N, P_2O_5 and K_2O were 65%, 95%, and 100%, respectively [35].

Accordingly, the avoided N, P, and K fertilizers could be calculated as follows:

Avoided N fertilizer = Slurry N (kg) * MFE-N = 1.177 * (65/100) = $\underline{0.765 \text{ kg }_N}$

Avoided P fertilizer = Slurry P (kg) * MFE-P * 4.6 (kg $_P$ kg $_{P2O5}^{-1}$)

$$= 1.5 * (95/100) * 4.6 = \underline{6.7 \text{ kg }_{P2O5}}$$

Avoided K fertilizer = Slurry K (kg) * MFE-K * 2.4 (kg $_K$ kg $_{K2O}^{-1}$)

$$= 1.177 \text{ kg N} * (100/100) = \underline{3.0 \text{ kg }_{K2O}}.$$

NO_3 and P leaching

In this study, the N and P leaching will be assumed to follow the same trends reported by Wesnæs *et al.* (2009) [11]. In their study, 35% and 10% of the manure N and P were assumed to be leached out of the soil. Accordingly:

NO_3 leached (kg) = Slurry N (kg_N) * (35/100) * 4.43 (kg_{NO_3} $kg N^{-1}$)

$$= 1.36 * 0.35 * 4.43 = 1.8 \ kg_{NO_3}$$

P leached (kg) = Slurry P (kg_P) * (10/100)

$$= 1.53 * 0.10 = 0.15 \ kg_P$$

Table 7-5 Mass balance during manure utilization scenario for 1 functional unit

Fresh excreted manure in house (kg)	1,000.0
Ex. House (kg)	995.0
Ex. Tank (kg)	990.5
Ex. Separation (liquid fraction) (kg)	940.5
Ex. Separation (Solid fraction) (kg)	49.5
Ex. Drying (solid fraction) (kg)	14.6
Ex. Gasification (char) (kg)	4.4
Ex. Storage (liquid fraction) (kg)	939.5
Ex. Mixing (solid and liquid fractions) (kg)	943.9

Simapro© 8.0.4 software (PRé Consultants, The Netherlands, 2014) was used to model this scenario. Details of emissions associated with material, fuel and energy were provided by a modified edition of ecoinvent database, which accounts for U.S. electricity makeup [36]

Table 7-6 Summary of emissions and energy requirements for one functional unit

1. Swine house	
NH_3 emissions (kg)	0.418
N_2O emissions (kg)	0.017
CO_2 emissions (kg)	2.818
CH_4 emissions (kg)	2.362
2. Pre-separation storage tank	
NH_3 emissions (kg)	0.418
N_2O emissions (kg)	0.017
CO_2 emissions (kg)	2.818
CH_4 emissions (kg)	2.362
3. Stirring and pumping	

Electrical power requirements (kWh)	1.70
4. Mechanical separation	
Electrical power requirement (kWh)	0.50
5. Solids transportation	
Transportation (tkm)	0.025
6. Drying (solid fraction)	
Heat requirements (MJ)	83.59
Electricity requirements (kWh)	1.72
Water requirement (m^3)	0.222
VOC emissions (kg)	0.00064
NH$_3$ emissions (kg)	0.042
7. Gasification-Boiler (solid fraction)	
Electricity requirements (kWh)	4.94
Air needed (kg)	37.05
Generated heat (MJ)	140.71
CO$_2$ emissions (g)	14,585.4
NO$_x$ emissions (g)	11.38
CO emissions (g)	1.46
SO$_2$ emissions (g)	0.76
HCl emissions (g)	0.47
PM emissions (g)	0.18
VOCs emissions (g)	0.16
HF emissions (g)	0.0050
Hg emissions (g)	0.0010
As emissions (g)	0.0009
Ni emissions (g)	0.0006
Cd emissions (g)	0.00010
8. Char transportation (solid fraction)	
Transportation (tkm)	0.044
9. Post-land application for the char (solid fraction)	
Avoided P$_2$O$_5$ (kg)	1.78
Avoided K$_2$O (kg)	1.64
Avoided CO$_2$ (kg)	3.43
P leaching (kg)	0.039
10. Post-separation storage tank (liquid fraction)	
NH$_3$ emissions (kg)	0.028
N$_2$O emissions (kg)	0.011
CO$_2$ emissions (kg)	1.78
CH$_4$ emissions (kg)	1.24
11. Slurry transportation (liquid fraction)	
Transportation (tkm)	9.395
12. Mixing and land application (solid and liquid fractions)	
Mixing (kWh)	1.2
12. Post-land application for the slurry (liquid fraction)	
NH$_3$ emissions	0.204
N$_2$O emissions	0.021
CO$_2$ emissions	27.2
Avoided N fertilizer (kg)	0.77
Avoided P$_2$O$_5$ (kg)	6.7
Avoided K$_2$O (kg)	3.0
NO$_3$ leaching (kg)	1.8
P leaching (kg)	0.15

4. Results and Discussions

4.1. Impact assessment

Table 7-7 below presents cumulative values representing impacts of the manure

management scenario according to selected categories. These categories include two inventory

categories: water depletion, and non-renewable fossil fuel demand, and three impact categories: climate change (IPCC GWP100), freshwater and marine eutrophication (ReCiPe midpoint) [37]. Positive impact characterization values indicate an added environmental burden, while negative values represent avoided burden.

4.1.1. Global Warming potential (GWP)

The proposed manure management scenario had a net positive impact on global warming, with a 168.5 kg CO_2e emitted throughout the entire scenario. This value encompasses the different released emissions, such as, CO_2, CH_4, and N_2O, during the manure processing stages, using conversion factors. A detailed representation of the contribution of each stage to the cumulative GWP emissions is shown in Figure 7-2. In an LCA of swine manure management in Denmark, three management scenarios were compared: standard management (reference), pelletization of separated solids for incineration, or pelletization of separated solids for use as solid fertilizer. The reference scenario was credited with a GWP 100 burden of 257 kg CO_2e, while the pelletization for energy and for fertilizer scenarios had a GWP 100 burden of 263 and 248 kg CO_2e, respectively [11].

Table 7-7 Characterization of impacts for proposed swine manure management scenario

Impact category	Unit	Proposed swine manure management
Global Warming (GWP100)	kg CO_2e	168.465
Non-renewable, fossil	MJ	-353.832
Water depletion	m^3	-0.793
Marine eutrophication	kg N eq	0.512
Freshwater eutrophication	kg P eq	0.173

Emissions during manure storage under slatted floors in the house and during external storage represented majority of the greenhouse gas (GHG) emissions, with each stage contributing 36.7% of the total emissions.

This big contribution is attributed to the high levels of N_2O and CH_4 emissions during these two steps, with both gases having a significantly larger impact on global warming potential, as seen in Table 7-8. Similarly, the third largest contributing stage to GHG emissions is post-separation storage, i.e., 19.5% of scenario's GWP.

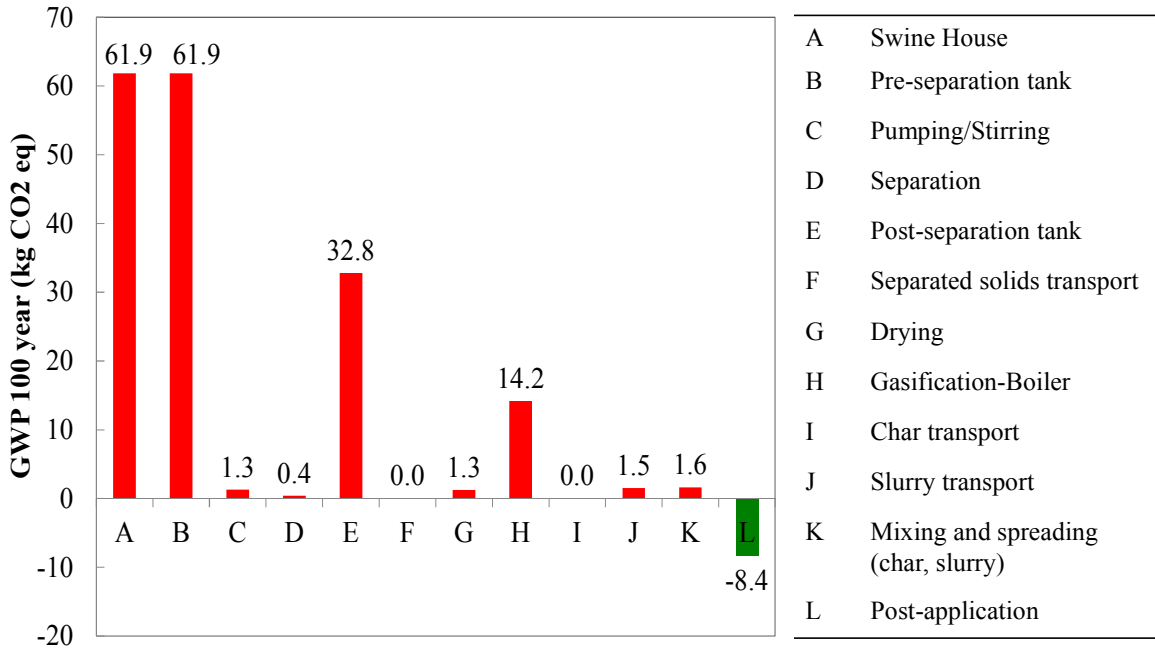|	
A	Swine House
B	Pre-separation tank
C	Pumping/Stirring
D	Separation
E	Post-separation tank
F	Separated solids transport
G	Drying
H	Gasification-Boiler
I	Char transport
J	Slurry transport
K	Mixing and spreading (char, slurry)
L	Post-application

Figure 7-2 Net contribution of each stage to the cumulative global warming potential over a 100 year period (GWP100) in units of kgCO₂ equivalent (kgCO₂e)

Manure solids gasification and syngas firing (in a boiler) are represented as one coupled process (step H in Figure 7-2) credited with 8.4% of the total GWP. Net positive contribution here indicates the avoided GHG emissions by firing (burning) syngas, instead of natural gas, did not completely offset the combined emissions from syngas firing, and those associated with gasifier

electricity consumption. The low hot gas efficiency used in this model, 70%, and the low boiler efficiency, 78%, contributed to an overall low ratio of avoided natural gas to GHG emitted from manure syngas firing, and thus a net positive GWP.

GWP for Drying manure solids, 1.3 $kgCO_{2e}$, represented 0.8% of overall GWP emissions. Despite being an energy-intensive process, the low GWP contribution here for drying is attributed to the fact that the process heat is recycled from the gasification-boiler output heat, which reduces the overall drying impact.

Table 7-8 CO$_2$ Equivalence factors for a 100 year period [1]

Substance	CO$_2$ equivalence factors
1 kg CO_2	1 kg CO_2e
1 kg CH_4	25 kg CO_2e
1 kg N_2O	298 kg CO_2e

The following stages: pumping, mixing, separation, transportation, and land application all represented 2.9% of the total GHG emissions. The negative emissions found in this scenario (savings) are attributed to the last stage, i.e., consequences of char-slurry land application. Here, negative emissions translate to emissions avoided due to the overall impact of land application. Despite the N_2O and CO_2 emissions arising from slurry land application, the emissions avoided by applying organic fertilizers: N, P, and K, instead of synthetic fertilizers outweighed these positive emissions. The GHG emissions resulting from producing 1 kg from each of the N, P, and K fertilizers, i.e., urea as N, P_2O_5, and K_2O are 3.19, 2.63, and 1.58 kg CO_2e, respectively [34].

4.1.2. Fossil fuel use

Cumulative fossil fuel use in this scenario was -353.8 MJ, which indicates fossil fuel savings. Figure 7-3 details the individual contribution of manure management stages to overall saving. Manure storage steps, from an energy perspective, were all passive and therefore had no fossil fuel expenditure or saving. The maximum energy burden was credited to the slurry transportation stage which represented 28.2% of total fossil fuel energy input, followed by the slurry-char spreading stage which represented 27.2% of total fossil fuel energy input.

The gasification-boiler stage was credited with an energy saving of 28.1 MJ, through offsetting natural gas firing to produce the same amount of thermal energy. This energy saving is additional to the recycled heat which was utilized in the drying stage. The energy demand for the drying process, 14.9 MJ, represents the electricity demand in the dryer, which cannot be met through the gasification-boiler stage. The main energy saving in this scenario, -403.5 MJ, was attributed to the consequences of slurry-char land application. This saving stems from the avoided synthetic fertilizers, and in consequence, the fossil fuel energy used in their production. For illustration, production of 1 kg N fertilizer (urea) requires 60.8 MJ of energy. Similarly, production of 1 kg of P_2O_5 and K_2O translate to 33.3 and 15.9 MJ of fossil fuel energy expenditure.

4.1.3. Water depletion

This category indicates the total water use from different water sources: lakes, rivers, and wells. In this study, total water depletion was a process credit, i.e., avoided water depletion of 0.793 m^3. This credit is an indirect water saving resulting from the last step by displacing synthetic fertilizers with the slurry-char mixture. Difference between land application impacts on water depletion, -0.815 m^3, and total impact, -0.793 m^3, is attributed to all the energy-positive

stages in the scenario. However, the savings accrued by land application vastly outweighed the combined water depletion potential for these stages.
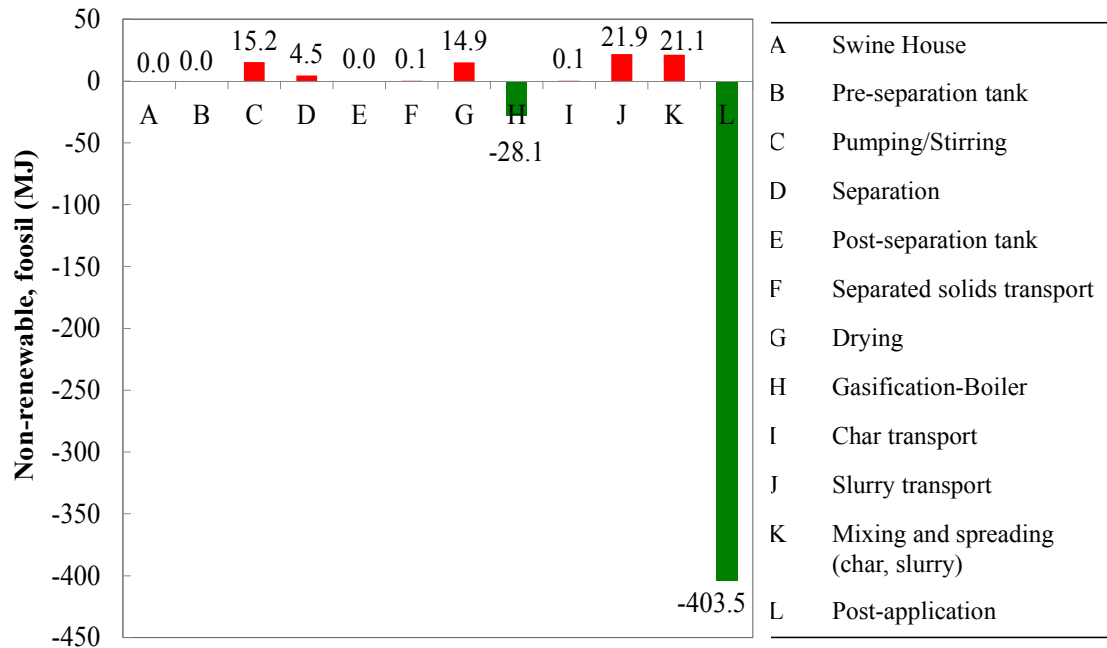

Figure 7-3 Net contribution of each stage to the cumulative fossil fuel energy use (MJ)

4.1.4. <u>Marine eutrophication</u>

This mid-point impact category expresses the amounts of nutrients emitted throughout the scenario, expressed in units of kg N equivalent, which reach marine water causing eutrophic conditions. The studied scenario had a net positive (a burden) of marine eutrophication, 83.1% of which is attributed to the slurry-char land application consequences. This could be explained by the nitrate (NO_3) leaching, and NH_3 emissions resulting from slurry land application. Throughout the entire scenario, 80% of eutrophication potential is attributed to NO_3 leaching, while the remainder is due to NH_3 emissions. The eutrophying effect of NH_3 occurs through forming acid rains that deposit back in water bodies causing N enrichment. Swine houses and pre-separation

storage are each responsible for 7.5% of total eutrophication potential due to their NH_3 emissions.

4.1.5. <u>Freshwater eutrophication</u>

Given that P is the limiting factor for most freshwater bodies, introducing P to rivers and lakes result in eutrophying conditions. In this study, 98% of total freshwater eutrophication potential is attributed to the last step, i.e., impacts of slurry-char application. The leaching of 10% of P in both the char, and the slurry are responsible for this impact.

4.2. Model sensitivity to thermochemical conversion parameters

In order to better understand the implications of the proposed thermochemical conversion system (drying-gasification-boiler) on the overall scenario, the conversion parameters, i.e., hot-gas efficiency (HGE) and boiler efficiency were altered to represent two additional scenarios. The first represents low-efficiency conditions: HGE and boiler efficiencies at 60% and 68%, respectively. The second, a high efficiency scenario, shows HGE and boiler efficiency at 80% and 88%, respectively. Figure 7-4 and Table 7-9 show the impacts of these performance levels on the gasification-boiler stage, and on the entire scenario. A 10% point increase in the performance of both the gasifier and the boiler yielded a decrease in the GWP for this stage by 3.5 kg CO_2e (24.6% decrease), and a corresponding increase in fossil fuel energy saving by 59.9MJ (213.5% increase). A 10% drop corresponded to a 21.5% increase in GWP, from 14.2 to 17.2 kg CO_2e, and a change from a fossil fuel energy saving of 28.1 MJ to an energy expenditure of 24.3 MJ. The sensitivity of the fossil fuel use to conversion efficiencies (gasifier, and boiler) indicate the tight balance between the energy demand for the drying process and the energy

181

released during conversion. The non-linear response in the efficiency scenarios is due to the fact that the overall efficiency for the gasification-boiler is the product of the conversion and the boiler efficiencies. No noticeable changes were observed in the other impact categories with changes in efficiencies.

For the entire scenario, increasing the thermochemical conversion efficiency yielded a 2.0% decrease in GWP and a 17.0% increase in fossil fuel savings. These findings suggest that the proposed thermal conversion alternative has a marginal impact on the GWP for the entire management scenario. It is worth noting, however, that the combined GWP for the separation, drying and gasification-boiler stages, 15.5 kgCO$_2$e, are lower than the difference in GWP between pre-separation storage, 61.9 kgCO$_2$e, and post-separation storage, 32.8 kgCO$_2$e. Put differently, the separation-drying-gasification-boiler combination can be considered an emission reduction measure through which manure storage emissions are minimized.
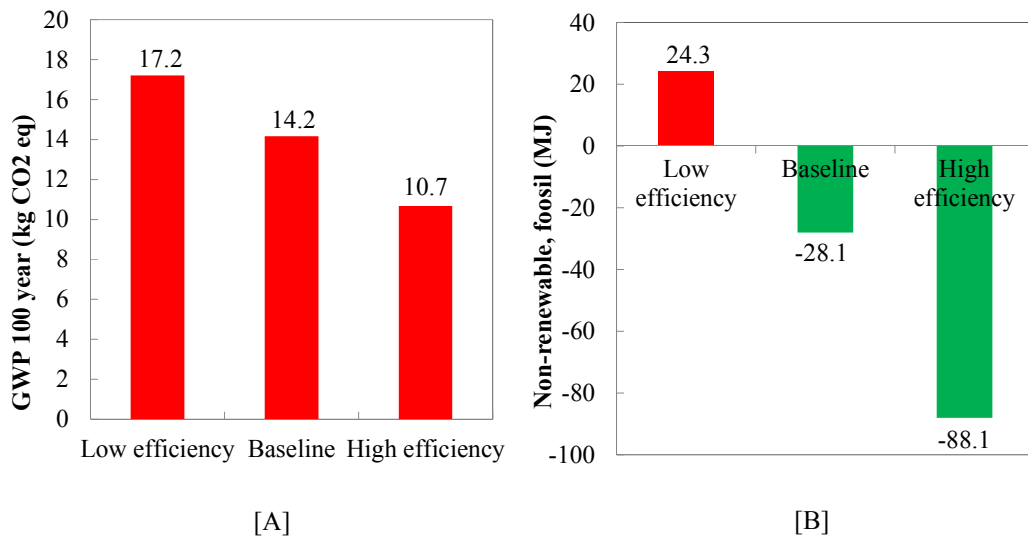

Figure 7-4 Impacts of gasification-boiler performance on: [A] global warming potential (GWP 100), and [B] Fossil fuel energy use (MJ)

From an energy perspective, however, the gasification system has a significant impact on the total energy use in manure management, even with the exorbitant energy requirements for drying. Improvements to thermal conversion efficiency (gasification, and syngas firing) combined with improvements to the drying technology can significantly improve the overall impacts for swine manure management via thermochemical conversion.

Table 7-9 Impacts of thermochemical conversion performance on swine manure management scenario

Impact category	Unit	Low efficiency Gasification-Boiler	Baseline	High efficiency Gasification-Boiler
Global Warming (GWP100)	kg CO_2e	171.512	168.465	164.976
Non-renewable, fossil	MJ	-301.444	-353.832	-413.814
Water Depletion	m^3	-0.793	-0.793	-0.794
Marine eutrophication	kg N eq	0.512	0.512	0.512
Freshwater eutrophication	kg P eq	0.173	0.173	0.173

4.3. Implications of this study

The findings in this investigation contribute to the ongoing discussion on manure management best practices. Given the swine manure composition, and the management practiced on farm, thermochemical conversion is less favorable than wet disposal technologies, i.e., anaerobic digestion. Comparative LCA for gasification and anaerobic digestion can further outline the benefits and shortcomings associated with each as swine manure management tool.

From GHG emissions and energy use perspectives, land application of swine manure appears beneficial. However, in regions of intensive swine production where unfertilized arable lands are scarce, thermochemical conversion can be regarded more as an auxiliary approach for nutrient/emission management than as an energy production venture. Adopting innovative sludge

drying technologies in regions of intensive production can greatly reduce the drying energy demand, and consequently, the GHG emissions. Also, better understanding of biochar agronomic value could potentially incentivize thermochemical conversion of manure solids.

5. Conclusions

- Swine manure liquid storage (before, and after solid-liquid separation) contributed 88.2% of the GHG emissions for the entire proposed manure management scenario.

- Solid-liquid separation reduced the GHG emissions associated with open tank manure storage, by 47.0%

- Despite the high energy demand associated with manure drying, thermochemical conversion can supply the drying thermal energy.

- Land application of slurry-biochar mixture is credited with 8.4 kgCO$_2$e in avoided GHG emissions, and 403.5 MJ of avoided fossil fuel energy use resulting from avoided synthetic fertilizer production.

- Improvements to drying, and thermochemical conversion efficiency can greatly reduce fossil fuel use in manure management.

6. References

[1] Intergovernmental Panel on Climate Change (IPCC). Fourth Assessment Report (AR4) 2007. Available online at: http://www.ipcc.ch/publications_and_data/ar4/syr/en/contents.html [Last accessed: January 27, 2015].

[2] Reddy PP. Agriculture as a Source of GHGs. In: Climate Resilient Agriculture for Ensuring Food Security: Springer; 2015, p. 27-42.

[3] Bockstaller C, Vertès F, Fiorelli J, Rochette P, Aarts H. Tools for evaluating and regulating nitrogen impacts in livestock farming systems. Advances in Animal Biosciences 2014; 5: 49-54.

[4] Kurukulasuriya, P., & Rosenthal, S. 2013. Climate change and agriculture: a review of impacts and adaptations. The World Bank Environmental Department. Paper No. 91. Available online at: https://openknowledge.worldbank.org/handle/10986/16616 [Last accessed: January 27, 2015].

[5] Environmental Protection Agency (EPA). Inventory of U.S. Greenhouse Gas Emissions and Sinks: 1990- 2012 2014; EPA 430-R-14-003.

[6] Fangueiro D, Coutinho J, Chadwick D, Moreira N, Trindade H. Effect of cattle slurry separation on greenhouse gas and ammonia emissions during storage. J Environ Qual 2008; 37: 2322-31.

[7] Kai P, Pedersen P, Jensen J, Hansen MN, Sommer SG. A whole-farm assessment of the efficacy of slurry acidification in reducing ammonia emissions. Eur J Agron 2008; 28: 148-54.

[8] Mikkelsen M, Gyldenkærne S, Poulsen H, Olesen J, Sommer S. Emissions of ammonia, nitrous oxide and methane from Danish Agriculture 1985-2002: Methodology and Estimates. National Environmental Reserach Institute (NERI), Ministry of Environment, Denmark 2006; no. 231.

[9] Dong H, Mangino J, McAllister T, Have D. Emissions from livestock and manure management. IPCC Guidelines for National Greenhouse Gas Inventories-Volume 4 2006; 10.

[10] Jensen LS, Sommer SG. Manure Organic Matter–Characteristics and Microbial Transformations. Animal Manure Recycling: Treatment and Management 2013: 67-90.

[11] Wesnæs M, Wenzel H, Petersen BM. Life cycle assessment of slurry management technologies. Danish Ministry of the Environment/Danish Environmental Protection Agency 2009.

[12] Dinuccio E, Paschetta E, Gioelli F, Balsari P. Efficiency of mechanical separation of digested and not digested slurry 2010: 13-5. Online at: http://www.ramiran.net/ramiran2010/docs/Ramiran2010_0229_final.pdf [Last accessed: January 27, 2015].

[13] Nguyen TLT, Hermansen JE, Mogensen L. Fossil energy and GHG saving potentials of pig farming in the EU. Energy Policy 2010; 38: 2561-71.

[14] Møller HB, Lund I, Sommer SG. Solid–liquid separation of livestock slurry: efficiency and cost. Bioresour Technol 2000; 74: 223-9.

[15] Hjorth M, Christensen KV, Christensen ML, Sommer SG. Solid–liquid separation of animal slurry in theory and practice. A review. Agron Sustain Dev 2010; 30: 153-80.

[16] Day D, Funk T, Hatfield J, Stewart B. Processing manure: physical, chemical and biological treatment, in Animal waste utilization: effective use of manure as a soil resource. CRC Press 1998.

[17] Jensen LS. Animal Manure Residue Upgrading and Nutrient Recovery in Biofertilisers. In: Animal Manure Recycling: John Wiley & Sons, Ltd; 2013, p. 271-294.

[18] Zaman A. Life cycle assessment of pyrolysis–gasification as an emerging municipal solid waste treatment technology. Int J Environ Sci Technol 2013; 10: 1029-38.

[19] Ro KS, Cantrell KB, Hunt PG. High-temperature pyrolysis of blended animal manures for producing renewable energy and value-added biochar. Ind Eng Chem Res 2010; 49: 10125-31.

[20] Wnetrzak R, Kwapinski W, Peters K, Sommer S, Jensen L, Leahy J. The influence of the pig manure separation system on the energy production potentials. Bioresour Technol 2013; 136: 502-8.

[21] Arena U. Process and technological aspects of municipal solid waste gasification. A review. Waste Manage 2012; 32: 625-39.

[22] Pa A, Bi XT, Sokhansanj S. A life cycle evaluation of wood pellet gasification for district heating in British Columbia. Bioresour Technol 2011; 102: 6167-77.

[23] Lima IM, Boateng AA, Klasson KT. Pyrolysis of Broiler Manure: Char and Product Gas Characterization. Ind Eng Chem Res 2008; 48: 1292-7.

[24] Ro KS, Cantrell KB, Hunt PG. High-temperature pyrolysis of blended animal manures for producing renewable energy and value-added biochar. Ind Eng Chem Res 2010; 49: 10125-31.

[25] Daugaard DE, Brown RC. Enthalpy for pyrolysis for several types of biomass. Energy Fuels 2003; 17: 934-9.

[26] Roberts, K. G., Gloy, B. A., Joseph, S., Scott, N. R., & Lehmann, J. (2009). Life cycle assessment of biochar systems: Estimating the energetic, economic, and climate change potential. Environ Sci Technol, 44(2), 827-833.

[27] Wu H, Hanna MA, Jones DD. Life cycle assessment of greenhouse gas emissions of feedlot manure management practices: Land application versus gasification. Biomass Bioenerg 2013; 54: 260-6.

[28] Hamelin, L., Wesnæs, M., Wenzel, H., & Petersen, B. M. (2010). Life cycle assessment of biogas from separated slurry. Danish Ministry of the Environment/Danish Environmental Protection Agency.

[29] Pehme S. Life Cycle Inventory & Assessment Report: Dairy cow slurry biogas with grass as an external C source, Estonia. Baltic Manure report. 2013.

[30] Smith K, Jackson D, Misselbrook T, Pain B, Johnson R. PA—Precision agriculture: reduction of ammonia emission by slurry application techniques. J Agric Eng Res 2000; 77: 277-87.

[31] Sommer SG, Hutchings N. Ammonia emission from field applied manure and its reduction—invited paper. Eur J Agron 2001; 15: 1-15.

[32] Hutchings NJ, ten Hoeve M, Jensen R, Bruun S, Søtoft LF. Modelling the potential of slurry management technologies to reduce the constraints of environmental legislation on pig production. J Environ Manage 2013; 130: 447-56.

[33] Buckley K, Mohr R, Therrien M. Yield and quality of oat in response to varying rates of swine slurry. C J Plant Sci 2010; 90: 645-53.

[34] Rochette P, Angers DA, Chantigny MH, Bertrand N, Côté D. Carbon dioxide and nitrous oxide emissions following fall and spring applications of pig slurry to an agricultural soil. Soil Sci Soc Am J 2004; 68: 1410-20.

[35] Lopez-Ridaura S, Werf Hvd, Paillat JM, Le Bris B. Environmental evaluation of transfer and treatment of excess pig slurry by life cycle assessment. J Environ Manage 2009; 90: 1296-304.

[36] EarthShfit. US-EI Database, Huntington, VT, USA 2012.

[37] Kim D, Thoma G, Nutter D, Milani F, Ulrich R, Norris G. Life cycle assessment of cheese and whey production in the USA. Int J Life Cycle Ass2013; 18: 1019-35.

Chapter 8 Conclusions

1. Survey of the literature on the subject of manure management and conversion showed the following:

   a. Increases in scale and the aggregation of swine production farms, while economically advantageous, have resulted in manure accumulation problems in high production regions.

   b. Various manure management technologies, i.e., biological, and thermal, are in practice to utilize swine manure while mitigating its negative impacts on surrounding ecosystems.

   c. Thermochemical conversion technologies are mature, stable and modular but, so far, underutilized in manure management.

2. Swine manure solids from two farms, i.e., farrowing and growing-finishing, were successfully characterized. The main findings were:

   a. The type of farm influenced the composition and the higher heating value (HHV) of swine manure solids.

   b. Compositional differences between swine manure types translated to variability in the weight loss rates, and the shape of decomposition peaks.

   c. The activation energy during pyrolysis of swine manure solids (T $\leq 420°C$) showed a gradual increase corresponding with the devolatilization of the sample ingredients (hemicellulose, cellulose, in addition to the keratin and lipid).

3. Algal consortia were successfully grown and harvested on a substrate of swine manure slurry to reduce the nutrient loading for the slurry. Characterization and thermogravimetric analysis of two algae harvests showed the following main findings:

   a. The algae genus *Mougeotia* was the common genus in the Algae 1 harvest, while the genus *Cladophra* was predominant in the Algae 2 harvest.

   b. In isoconversional methods, the apparent activation energies for pyrolysis of Algae 1 were lower than Algae 2 pyrolysis.

   c. The pyrolysis kinetics of each consortium was modeled using independent parallel reaction (IPR) model as a group of four parallel, independent, first-order reactions.

4. The combustion kinetics was studied for swine manure solids, algal biomass, and their blends. The main findings were:

   a. Swine manure solids showed a higher carbon concentration and larger Higher Heating Value than algal biomass solids

   b. Weight loss in swine manure solids took place over a narrower temperature range compared to that of algal biomass

   c. Average activation energy for algae and swine manure solids, using isoconversional methods, was comparable.

   d. Co-combustion of swine manure and algal solids was found to be additive, with behavior similar to weighted mean computed from individual feedstocks.

5. The gasification of wastewater treatment algae (phycoremediation) was studied in an auger gasification platform. Three temperature levels: 760, 860 and 960°C were investigated. The main findings were:

   a. The development of temperature profiles during auger gasification indicated formation of different reaction zones, similar to those observed in fixed-bed systems.

   b. Increasing the gasification temperature decreased the CO_2 yield, but increased the yield of CO, H_2, and, consequently the gas heating value.

   c. The high ash concentrations in the raw algae biomass resulted in low gas yields, and high char yields.

   d. High condensables yields and high carbon concentrations in the char indicate low conversion efficiencies, even at the highest temperature tested.

   e. Concentrations of C, P, and K oxides in the algae chars were between 140~177 g kg^{-1}, 2.8~3.0 g kg^{-1}, and 1.5~1.6 mg kg^{-1}, respectively.

6. Life cycle assessment (LCA) was used to investigate the gasification of swine manure solids as a manure management strategy. This study details a proposed scenario for manure management (1,000 kg of fresh manure at 5% dry matter) that includes: drying, gasification, and syngas burning in a boiler. The main findings in this study were:

a. Swine manure liquid storage (before, and after solid-liquid separation) contributed 88.2% of the GHG emissions for the entire proposed manure management scenario.

b. Solid-liquid separation reduced the GHG emissions associated with open tank manure storage, by 47.0%

c. Despite the high energy demand associated with manure drying, thermochemical conversion can supply the drying thermal energy.

d. Land application of slurry-biochar mixture is credited with 8.4 $kgCO_2e$ in avoided GHG emissions, and 403.5 MJ of avoided fossil fuel energy use resulting from avoided synthetic fertilizer production.

e. Improvements to drying, and thermochemical conversion efficiency can greatly reduce fossil fuel use in manure management.